

IV

Astronomical applications

1. Introduction

There are logically two parts to the astronomical applications: (A) the elucidation of the theoretical implications for observable quantities; (B) the comparison of the theoretical predictions with actual observations.

Part A is contained in the following three sections of this chapter; these explore the following theoretical relationships, from the standpoint of the present theory and its comparison with the expanding-universe theory:

- (1) the redshift-magnitude relation for a single luminosity class;
- (2) the redshift distribution for a single luminosity class of uniform spatial distribution;
- (3) the Schmidt luminosity-volume ratio for apparent-luminosity-limited samples of uniform spatial distribution;
- (4) the magnitude-aperture relation for galaxies, and its implications for cosmological tests based on (1) and (2) above;
- (5) the $\log N - \log S$ relation for radio sources of given luminosity function and spectral index;
- (6) the metric angular diameter-redshift relation for a uniform class of objects uniformly distributed in space.

While some further independent tests may be envisaged, the data presently available are for the most part totally inadequate for statistically significant studies.

The theoretical treatment is illustrated in Part A by reference to actual observations; however, the detailed description of the comparison between the best available data and the predictions of Part A is given in Sections 5–20 constituting Part B. There are separate sections on galaxies and quasars. Emphasis is on statistically controlled data and the utilization of standard statistical tests; however, extensive runs of data, even when of uncertain statistical homogeneity, are also discussed. In the last section, predictions and observations are compared for cases in which statistical levels of significance are uncertain and theoretical values, such as intrinsic simplicity, or economy in the use of parameters or energy, are involved in the comparisons. Examples of such cases include: the apparent near cutoff in the number of quasars above redshift 3; the energy output of quasars in comparison with that of galaxies; apparent superlight velocities; apparent rarity of quasars in identifications of optically very faint radio sources.

2. The redshift–magnitude relation

With the notation of Chapter III, consider a luminous object at a distance ρ in natural units from the point O of observation, which we take as origin. The redshift z is then $\tan^2(\rho/2)$, according to Chapter III. By the inverse square law of luminosity decrease with distance, and spherical geometry, the luminosity I , as a function of ρ , varies as $(\sin \rho)^{-2}$, apart from redshift effects. If at the source the spectral function is $f(v)$ and if observation is made in a frequency range $v_1 < v < v_2$, then the energy at the source contributing to this range is $\int_{v_1(1+z)}^{v_2(1+z)} f(v) dv$. This energy is not only diffused according to the inverse square law but also redshifted, or diminished by the factor $1 + z$ as observed. Consequently the observed luminosity L_{obs} varies as

$$\frac{1}{\sin^2 \rho} \frac{1}{1+z} \int_{v_1(1+z)}^{v_2(1+z)} f(v) dv.$$

Assuming that $f(v) \propto 1/v^\alpha$, it follows from this equation and trigonometry that

$$L_{\text{obs}} \propto \frac{(1+z)^{2-\alpha}}{z},$$

or in term of magnitudes,

$$m = 2.5 \log z - 2.5(2-\alpha) \log(1+z) + C.$$

For $\alpha \geq 1$, m is then a monotone increasing function of z , which if $\alpha = 1$ attains the finite limiting value C as $z \rightarrow \infty$. It attains this limiting value

relatively rapidly; at $z = \frac{2}{3}$, the brightness is within one magnitude of the limiting value. The finiteness of this limit is of course purely theoretical; any actual physical source, having finite energy, cannot have a constant spatial index $\alpha \leq 1$, since otherwise the integral $\int^{\infty} f(v) dv$ representing the total energy would be divergent; indeed, in actuality $f(v) = 0$ for sufficiently large v . However, at present, there is little evidence to suggest that variation in the spectral index is a significant factor over the presently observable redshift range, as regards the $m-z$ relation for quasars, and as in most treatments of the $m-z$ relation it will be neglected.

In any event, over a redshift range such as $0.4 < z < 2.5$, the chronometric theory predicts a dimming in apparent magnitude of < 1 mag for objects such as quasars of spectral index ~ 1 , while the Hubble model† (or Friedmann models having reasonable parameters) predicts a dimming of ~ 4 mag. Thus, barring extreme observational difficulties with the larger redshift ranges, the difference between the chronometric and expansion theories redshift predictions should not be difficult to detect. It will be found that, indeed, quasar observations are in quite satisfactory agreement with the chronometric prediction, but reject the Hubble law, at a high level of certainty. The latter result may be regarded as a form of demonstration of very strong evolutionary effects, within the expansion theory framework, as will be discussed later.

The theories also differ markedly for small z ; according to the chronometric theory,

$$m \sim 2.5 \log z + \text{const}, \quad 0 < z \leq 0.1.$$

There is thus a difference of 2.5 mag between the chronometric and expansion theories' predictions over either of the ranges, $0.001 \leq z \leq 0.01$ and $0.01 \leq z < 0.1$. Unfortunately, there are observational difficulties in these ranges, which may be less significant for quasar observations; these have been stressed for a long time by workers in the field. They are primarily: (a) the relatively greater difficulty of observing "standard candles" (in particular, "selection effects"); (b) the aperture effect; (c) the intrinsic velocities of the luminous objects; and, secondarily, (d) the "K-effect," and (e) galactic absorption, which is relatively small for the magnitude differences

† For brevity and in conformity with general usage, the term Hubble model (or theory) is used in the present work to indicate the Doppler model in which space is Euclidean and the redshift is proportional to distance. Historically, however, the term is a considerable oversimplification. On several occasions, partly with collaborators, Hubble expressed clear reservations about the Doppler theory of the redshift, but stated the opinion that the only likely theoretical alternative was a new fundamental physical development. Moreover, the redshift-distance relation was initially reported as "roughly linear" and later as involving additionally a definitely positive quadratic term; see Hubble (1936a).

involved. (Correction for galactic evolution is required only in the expansion theory.) As emphasized by Humason *et al.* (1956), the aperture effect is strongly z -dependent, and must be properly corrected for, in order to have a valid basis for comparison between theory and observation. On the other hand, as is clear from recent work of Sandage (1972a), the aperture correction is in practice model-dependent. As a consequence, for objects and redshift ranges in which the aperture effect is significant, the redshift-magnitude relation must be of a quite detailed nature as regards the surface brightness profile of galaxies, etc., in order to be testable. The data on bright cluster galaxies are such that each theory fits part of it well and part of it equivocally.[†]

Intrinsic ("peculiar") velocities are a conceivable difficulty in dealing with very small redshifts. In principle, the difficulty could be overcome if sufficient randomized data are available. However, there is no model-independent indication that the problem is a serious one, apart from the motion of the Sun and Galaxy. The catalog of the de Vaucouleurs (1964) includes only 14 blue-shifted objects, with an average blue shift < 100 km/sec, among more than 740 for which redshifts and magnitudes are given.

In any event, the existing galaxy data at low redshifts are in poor agreement with the Hubble law. A lengthy study by G. de Vaucouleurs (1972) led him to postulate a local spatial anisotropy. This has been disputed by Sandage *et al.* (1972). The chronometric theory is in excellent agreement with the data, its prediction for the $m-z$ relation being substantially the empirical law $m = 2.5 \log z + \text{const}$ found by de Vaucouleurs. This law is confirmed by maximum-likelihood estimation, whether for the totality of 742 redshifted galaxies with $m-z-\theta$ data listed on the de Vaucouleurs tape (updated to 1972) of their guide (1964), or for subsamples selected on morphology, field of the sky, or both. It is in addition in distinctly better agreement with the classic data of Humason, Mayall, and Sandage than is the Hubble Law, as first indicated by Hawkins (1962), in the case of field galaxies.

Closely related to the redshift-magnitude relation is the redshift distribution law. Assuming a uniform spatial distribution of luminous objects, i.e., that the number of objects of a given type in a given region of space is proportional to the volume of the region, the fraction of objects out to a

[†] Quasi-phenomenologically (see below), the data of Sandage on the $m-z$ relation (for a sample derived from 41 clusters) is in considerably better agreement with the Hubble law than the chronometric prediction; but the latter does effect a 45% reduction in dispersion. On the other hand, the compilation by Noonan of all published redshifts for clusters (146 in all) is in much better agreement with the chronometric than the Hubble prediction regarding the $N(< z)$ relation.

given redshift z is well determined in both theories, and well known in the expansion theory; for small z , this fraction $F(z)$ varies approximately as z^3 , independently of the precise parameters of the theory (or exactly as z^3 in the original Hubble theory based on Euclidean space), and increases rapidly with increasing z in the observational range. To treat the matter in the chronometric theory, let $V(\rho)$ denote the volume of space up to distance ρ from the origin O ; then dV varies as $\sin^2 \rho d\rho$. Integrating, it follows that

$$V(\rho) = \frac{1}{2}(\rho - \sin \rho \cos \rho) = [\tan^{-1} z^{1/2} - z^{1/2}(1-z)(1+z)^{-2}],$$

expressing ρ in terms of z . This implies that $F(z)$ varies as $z^{3/2}$ for small z , in the chronometric theory, as was to be expected from the approximate quadratic dependence of z on distance for small distances. This represents a considerable difference from the behavior indicated by the expansion theory. The existing samples which are or may be free from serious selection effects are limited in number and size, but they favor the $\frac{3}{2}$ power law over the third-power law, whether galaxies or quasars are used.

When selection by luminosity is an important factor, the V/V_m test treated by Schmidt (1968) may still be used, provided the sample is complete out to a definite limiting magnitude. If this limiting magnitude is \bar{m} , then the ratio of the volumes $V(z)/V(\bar{z})$, where \bar{z} is the maximum redshift for which the object would remain in the sample (if located at the distance indicated by the redshift), and $V(z)$ denotes the volume of the region in space in which the redshift is bounded by z , is uniformly distributed in the interval $[0, 1]$, on the hypothesis that the luminous objects in question are uniformly distributed in space. In the Hubble theory, e.g., in its simplest form, $\bar{m} - m = 5 \log \bar{z} - 5 \log z$, whence V/V_m (setting $V(z) = V$ and $V(\bar{z}) = V_m$, to conform with the notation of Schmidt) takes the value $10^{-0.6(\bar{m}-m)}$.

In the chronometric theory, for objects of spectral index ~ 1

$$\bar{m} - m = 2.5 \log[\bar{z}/(\bar{z} + 1)] - 2.5 \log[z/(z + 1)];$$

a simple computation leads to the result

$$\bar{z} = \gamma/(1 - \gamma), \quad \gamma = [z/(z + 1)]10^{0.4(\bar{m}-m)};$$

if $\gamma > 1$, then the luminosity is so great that the object would be included in the sample anywhere in the space under consideration. Setting

$$\rho = 2 \arctan z^{1/2}, \quad \bar{\rho} = 2 \arctan \bar{z}^{1/2},$$

$$\frac{V}{V_m} = \left(\rho - \frac{\sin 2\rho}{2} \right) / \left(\bar{\rho} - \frac{\sin 2\bar{\rho}}{2} \right).$$

The given expression for V/V_m differs by little from the ratio $(z/\bar{z})^{3/2}$ in the indicated redshift range, being typically of the order of 1% greater. As $z \rightarrow 0$,

this expression converges to $10^{-0.6(m-m)}$, i.e., to the expansion-theoretic value, but for moderate values of z , the difference between the respective values of V/V_m may be significant. Even for small values of z , the test is potentially discriminatory on the basis of the model dependence of the magnitudes, via the corresponding dependence of the appropriate aperture.

The distribution laws differ markedly for large z , in as much as $V_{\text{chrono}}(z)$ attains a finite limiting value which is approached for much lower z than in the case of realistic closed Friedmann models. For example, $N(2.25 < z < 3)/N(z < 2.25)$ has the value 1.37 in the (nonevolutionary) Hubble theory, > 0.33 for the Friedmann models with $q_0 \leqq 1$, and the value 0.09 in the chronometric theory (in which the region $2.25 < z < 3$ corresponds to the zone in space where the polar angle ρ lies in the narrow range $112.6^\circ < \rho < 120^\circ$). The latter value is greater than, but in the light of the observational situation agrees within an acceptable level of random fluctuations, with the value observed for quasars; however (indeed, virtually as a consequence), the former do not, even allowing for various effects which may modify the value (absorption, K -effect, etc.).

To summarize, the redshift-magnitude relation, and the related redshift distribution, provide several quite disparate theoretical predictions of a direct and straightforward nature. Their confrontation with observation may therefore reasonably be expected to furnish counterindications for at least one of the theories, although not necessarily positive indications for the other.

3. Further cosmological tests

We attempt no exhaustive analysis, but treat only two additional tests which may fairly soon become statistically applicable as data improve.

a. The redshift-angular diameter relation

It must be emphasized that the theory treats the *metric* angular, rather than isophotal angular diameter. For the relation of the latter diameter to the redshift is quite complex and dependent on a variety of uncertain functions. On the other hand, the metric diameter is in general not directly observed, so that the relation derived is not readily checked against observation.

In the chronometric theory, an object of metric diameter d has at distance ρ the angular diameter $\theta = d/\sin \rho + O(d^2)$, employing the same natural units as earlier. For galaxies, d^2 is negligible, and employing the redshift-diameter relation, it follows that

$$\theta = d(1 + z)/2z^{1/2}.$$

The chronometric θ - z relation appears quite different from the Hubble relation $\theta \propto z^{-1}$, and from the relation treated by Sandage (1972a) $\theta \propto (1+z)^2/z$. Unfortunately, in the z range in which there are measurements that can reasonably be construed as metric diameters, the various theoretical diameters differ by far less than the intrinsic dispersion in the angular diameters. The main difficulty in the use of the θ - z relation is indeed that of determining the angular diameter of a more-or-less constant metric diameter. The isophotal and metric diameters in general may behave differently as functions of redshift.

The very large sample represented by the de Vaucouleurs tape gives $\theta \propto z^{-1/2}$ to a much better approximation than $\theta \propto z^{-1}$. As in the case of the m - z relation, the dispersion from the expansion prediction is always of the same order of magnitude as the dispersion in the apparent quantities, while the dispersion from the chronometric prediction is materially less, being generally of the same order of magnitude as that from the least-squares fit. Again, this is true for the entire sample with appropriate data, or for subsamples selected on morphology, field of sky, redshift interval, etc. Also, here, as in the case of the m - z relation, proper analytical allowance for the observational cutoff in apparent magnitude, i.e., for the conceivable material z -dependence of the sample arising from the possible existence of significant numbers of intrinsically bright but apparently faint galaxies which have been excluded from the sample, merely slightly improves the fit of the chronometric relation.

The much smaller sample of brightest cluster galaxies treated by Sandage (1972a) is represented by him as following an approximate Hubble law, $\theta \propto z^{-1}$. However, quite apart from the apparent selection effects previously noted in connection with this sample, the results in the θ - z analysis are quite sensitive to the inclusion or exclusion of the objects at extreme and isolated redshift ranges. For example, when the local region $cz < 4000$ is excluded, and also those beyond the gap of > 2000 in the sample values of cz near $cz = 18,000$, in the sample of galaxies whose isophotal diameters were estimated from 48-inch Schmidt plates, there is little difference between the fits of the $\theta \propto z^{-1}$ and $\theta \propto z^{-1/2}$ curves. This subsample of thirty-five galaxies, defined by restriction to the range $4000 < cz < 18,000$, constitutes the major and most coherent portion of the cited sample. The dispersions in the deviations of $\log \theta$ from the $-\log z + \text{const}$ and $-0.5 \log z + \text{const}$ lines are, respectively, 0.115 and 0.119. The sample of nineteen galaxies measured from 200-inch plates is quite irregular in its redshift distribution and devoid of published statistically viable selection criteria; its statistical weight compared to the vastly larger BGC sample and the various subsamples indicated appears consequently to be quite small.

The systematic observations by Baum (1972) of galaxy diameters are nevertheless statistically too limited, as well perhaps as too complex in

theoretical interpretation, to differentiate between the relevant θ - z relations. The compilations of double radio source angular diameters by Legg (1970) provide diameters which are probably substantially metric, but include quite heterogeneous data, and are too limited in sample size for definite statistical conclusions to be drawn. If one computes the discriminatory variance of the linear diameters in Legg's data, say in kiloparsecs (kpc), it is found that it is substantially smaller in the chronometric theory than in a typical expanding-universe theory. However, this is a result of the smaller overall distance scale of the chronometric model, based on the value $H \sim 80$ at 10 Mpc; the logarithms of the linear diameters in the two theories have variances of the same order of magnitude. The compilation of radio angular diameter data by Miley (1971) is likewise too heterogeneous and/or limited in sample size to be statistically discriminatory. The variation of apparent angular diameter with frequency, and its dependence on spectral index, are further obstructions to the use of radio angular diameters without much more data and analysis. But the θ - z observations are effective in indicating a nontrivial dependence of θ on z for larger z , and the corollary correlation of z with distance.

b. The log N -log S relation

At the present time, uncertainties as to luminosity and spectral functions, as well as observational ambiguities involving faint sources, limit the precision of this test. However, there appears to be a substantial qualitative difference in this respect also between the chronometric theory and nonevolutionary expansion theories. In the latter theories, it seems quite difficult to obtain values of the index $\beta = -\partial \log N / \partial \log S$ which are greater than the Euclidean value 1.5, with what appear as a priori reasonable choices for spectral and luminosity functions; cf. e.g., Longair and Rees (1972). In the chronometric theory, such larger values are readily attained. Moreover, with simple reasonable models for the luminosity function and choice of spectral index, a $N(S)/N_0(S)$ curve is obtained which shows the key observed qualitative features of the observational N - S relation (cf. Longair and Rees (1972); here $N_0(S)$ denotes the corresponding function in an Euclidean universe, i.e., $N_0(S) \propto S^{-3/2}$).

Consider, to begin, with a uniformly distributed class of objects of fixed luminosity L , and having spectral index α . Let z denote the redshift of a source and ρ the corresponding distance in natural units: $\rho = 2 \tan^{-1} z^{1/2}$. In the chronometric theory, the observed luminosity is proportional to $(1+z)^{2-\alpha} z^{-1}$ as earlier derived; the expected number $N_L(S)$ of sources apparently brighter than S , within the luminosity class under consideration, is then proportional to the volume of space within which the indicated function of z (or equivalently, function of ρ) is greater than S .

It follows that

$$N(S) \propto \int_{L_{\text{obs}}(\rho) \geq S} \sin^2 \rho \, d\rho,$$

where $L_{\text{obs}}(\rho) = L(1+z)^{2-\alpha} z^{-1}$, expressed as a function of ρ . The behavior of $N(S)$ and the corresponding population-brightness index $\beta = -\partial \log N / \partial \log S$ depends significantly on α , and especially on whether $\alpha \geq 1$ or $\alpha \leq 1$. If $\alpha \geq 1$, $L_{\text{obs}}(\rho)$ is a monotone decreasing function of ρ , and, for $\alpha = 1$, it follows that

$$N(S) \propto (\rho - \sin \rho \cos \rho), \quad \rho = \cos^{-1}(1 - 2(L/S));$$

$$\beta = \frac{2 \sin \rho (1 - \cos \rho)}{\rho - \sin \rho \cos \rho}.$$

If $\alpha < 1$, $L_{\text{obs}}(\rho)$ decreases down to a certain minimum at $z = 1/(1-\alpha)$, and then increases again as ρ (or z) continues to increase. It follows that

$$N(S) \propto \int_0^{\rho_1} \sin^2 \rho \, d\rho + \int_{\rho_2}^{\pi} \sin^2 \rho \, d\rho,$$

where ρ_1 and ρ_2 are determined by the equation

$$LS^{-1} = 2^{\alpha-2} (1 - \cos \rho)(1 + \cos \rho)^{1-\alpha},$$

and the inequalities

$$0 < \rho_1 \leq \rho_2 < \pi.$$

Here L is a parameter proportional to the intrinsic luminosity of the source. It results from a simple computation that

$$\begin{aligned} \beta &= 2 \left(\frac{\sin^3 \rho_1}{\alpha + (2-\alpha) \cos \rho_1} - \frac{\sin^3 \rho_2}{\alpha + (2-\alpha) \cos \rho_2} \right) \\ &\times \left(\rho_1 - \sin \rho_1 \cos \rho_1 + \pi - \rho_2 + \sin \rho_2 \cos \rho_2 \right)^{-1}. \end{aligned}$$

It follows that β becomes infinite as the source strength decreases to that for which $\rho_1 = \rho_2$, i.e., for which the source is observable anywhere in the universe. For smaller S , $\beta \equiv 0$, since N can become no larger. The situation is well represented by the simple case $\alpha = 0$, which gives

$$\beta = \sin^3 \rho (\cos \rho)^{-1} (\rho - \sin \rho \cos \rho)^{-1}; \quad \rho = \sin^{-1}(L/S)^{1/2}.$$

The situation for $0 < \alpha < 1$ is qualitatively obtainable by interpolation between the values $\alpha = 0$ and $\alpha = 1$. Typically, as S decreases from high values, β begins eventually to increase perceptibly and rises eventually to ∞ , but for

TABLE 1

The population-brightness index $\beta = -\partial \log N / \partial \log S$ for sources of fixed intrinsic luminosity and spectral index α in the chronometric theory

$\log S$	$\alpha = 0$	$\alpha = 0.7$	$\alpha = 1$	β
2.0	1.503	1.501	1.499	
1.8	1.505	1.501	1.498	
1.6	1.508	1.502	1.496	
1.4	1.512	1.503	1.494	
1.2	1.520	1.505	1.490	
1.0	1.533	1.508	1.485	
0.8	1.554	1.515	1.475	
0.6	1.594	1.528	1.459	
0.4	1.675	1.563	1.432	
0.2	1.895	1.698	1.379	
0.0	∞	∞	1.275	
< 0	0	0	0	

fainter values of S it is identically zero. Table 1 shows the values of β for the cases $\alpha = 0$, 0.7, and 1, and can be used to estimate β roughly for other values of α by interpolation.

The discontinuous behavior near $S = L$ for $0 \leq \alpha < 1$ is smoothed out by a smooth luminosity function, but the same qualitative behavior is otherwise manifested. If $P(L)$ is the relative number of sources of intrinsic luminosity less than L , the resultant $N(S)$ takes the form $\int G_L(S) dP(L)$; if the spectral index is permitted to vary, there will in addition be a corresponding integral over its range. In presenting quantitative results, it is convenient to follow the practice of dealing with the ratio $N(S)/N_0(S)$, where $N_0(S)$ denotes the corresponding Euclidean quantity, and so is proportional to $S^{-3/2}$; the proportionality factor may conveniently be chosen so that $N/N_0 \sim 1$ for large S . The resulting expression is

$$N/N_0 = \frac{3}{2} \left(\int G_L(S) dP(L) \right) / \left(\int L^{3/2} dP(L) S^{3/2} \right).$$

The luminosity function for radio sources is not well determined, but is thought (expansion theoretically) to be rather broad. In Figure 4 the N/N_0 curve for a single luminosity class having spectral index 0 has been plotted, together with the smoothed-out curve resulting from a hypothetical lumino-

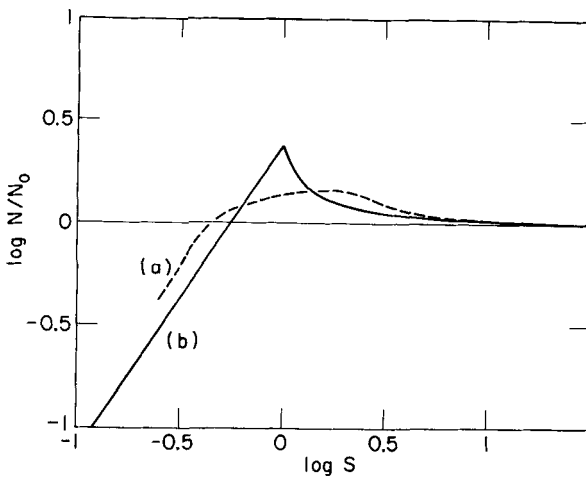


Figure 4 The chronometric N-S relation.

Curve (a), ~ 1 decade range in luminosity; curve (b), single luminosity class. Assumptions: (1) spatially uniform distribution of sources; (2) spectral index = 0. The rise above the horizontal axis corresponds to values of $-\partial \log N/\partial \log S$ in excess of the Euclidean value 1.5, and takes place for all values of the spectral index < 1 .

sity function corresponding to a range of 0.9 in $\log L$, $\log L$ being uniformly distributed in this range. A change in the L -scale merely translates the curve horizontally. The curve is qualitatively similar to observational curves (cf., e.g., Longair and Rees, 1972), showing the key features of a rise in population-luminosity index above $\frac{3}{2}$ as the source strength declines from very strong to strong, followed by a decline, eventually falling well below the Euclidean value for faint sources. Averaging over the spectral index, typically ~ 0.3 for flat sources or 0.7 for steep ones, but fairly broadly dispersed, will reduce the qualitative effects indicated, while the use of a less broad luminosity function would increase them. For $\alpha = 1$, the curve differs by little over the physically relevant range from the constant value unity; for very low flux levels, β falls to ~ 1.275 , before vanishing identically.

Besides the surely relevant and poorly known luminosity function and distribution of spectral indices, further factors may be relevant. Definitive statistically testing on the basis of the N-S relation will not be highly discriminatory until such matters are settled, and difficulties and discrepancies in the reported observations of faint sources are resolved. However, there is no apparent reason to anticipate that the various effects involved are of magnitudes sufficient to alter the disagreement of the observed N-S relation with a nonevolutionary Friedmann cosmology, or its agreement within statistical fluctuation with the present theory (cf. below).

4. The aperture correction for galaxies

It has long been recognized that the aperture correction to galaxy magnitudes is a matter of difficulty and delicacy, and yet at the same time of considerable importance to the redshift-magnitude relation. In particular, Humason *et al.* (1956) in their classic paper emphasized the highly material z -dependence of the aperture correction, and the necessity of compensating for it if valid results were to be obtained. In recent work Sandage (1972a) has again treated the aperture correction, and discussed within the framework of general relativistic models the practical problem of estimating the luminosity of portions of galaxies of fixed metric, rather than isophotal, diameter.

Unfortunately, no model-independent means of obtaining galaxy magnitudes for central portions of a fixed metric diameter is established. Within the limits of Friedmann models, a complex recursive procedure is indicated by Sandage, but demonstrations of the convergence of the method and the unicity of its results are lacking. Within the much broader limits encompassing general relativistic models, the present chronometric model, and others of comparable nature, it seems hopeless to seek a unique result.

This suggests that the magnitude-redshift relation for galaxies should primarily be employed as a means of testing hypotheses. In particular a $\partial m / \partial \log z = 5$ apparent slope for large-aperture measurements of "standard candles" is not entirely a simple observational fact, but in significant part a theoretical inference which is in agreement with observations, when the observations are made and reduced in accordance with the theory in question. In principle, it is possible that a different value for $\partial m / \partial \log z$ may be equally valid, from the standpoint of essentially the same observations, but a different theory. Indeed, this possibility is well exemplified by consideration of a conceivable attempt to avoid aperture corrections by observing only very narrow central portions of galaxies. Quite apart from the rapid decrease in surface brightness just beyond the center which might well obviate such an approach, it is demonstrable on theoretical grounds that such measurements would be incapable of discriminating at low redshifts (say less than 0.1) between the redshift laws $z \propto d^\alpha$ for a wide range of exponents α .

It will suffice to contrast the Hubble law $z \propto d$ (say $z = c_1 d$) and the Lundmark law $z \propto d^2$ (say $z = c_2 d^2$; Lundmark (1925) fitted a quadratic polynomial, but his name may serve appropriately). These are here to be regarded as hypotheses, to be tested by observations on the same galaxies, forming "standard candles," of substantially constant absolute luminosity and surface brightness characteristics. The apertures must be adjusted in accordance with the respective hypotheses, to obtain the luminosity of central portions of each galaxy of constant metric diameter characteristics.

Consequently the apertures must be adjusted in accordance with the respective hypotheses, to obtain the luminosity of the central portion of each galaxy of a fixed metric diameter. If a portion of metric radius r is to be observed, the respective apertures then vary as a/z and $a/z^{1/2}$, respectively. The resulting situation can then be summarized as the

Theorem If either one of the Hubble or Lundmark laws is valid, then both sets of observations—at the respective appropriate apertures—will be in agreement with both corresponding laws.

Proof Let $L(\theta)$ denote the luminosity of a given galaxy as observed with aperture θ ; let $I(r)$ denote the surface brightness of the galaxy as a function of the distance r from the center. Then $L(\theta) \propto a^{-2} \int_0^{\theta a} I(r)r dr$, but for small apertures, $\int_0^{\theta a} I(r)r dr \sim I(0)(\theta a)^2/2$. It results that $L(\theta) \propto \theta^2$, implying that the corresponding magnitude $m(\theta) = -5 \log \theta + k$, k being a constant. Agreement between observations and the Hubble law means that if $\theta_1(z)$ denotes the appropriate aperture on the basis of the Hubble theory, then $m(\theta_1(z)) = 5 \log z + k'$, k' also being a constant. Agreement between observations and the Lundmark law similarly means that $m(\theta_2(z)) = 2.5 \log z + k''$, where $\theta_2(z)$ is the appropriate aperture on the basis of the Lundmark law. Since $\theta_1(z) \propto z^{-1}$ on the basis of the Hubble law, and $\theta_2(z) \propto z^{-1/2}$ for the Lundmark law, $m(\theta_1(z)) - m(\theta_2(z)) = 2.5 \log z$, which is precisely the difference in magnitudes which would be observed.

Thus there is not even a theoretical possibility of using observations at small apertures to discriminate between the Hubble and Lundmark redshift-magnitude laws for galaxies. On the other hand, at large apertures, contamination from stars, the brightness of the night sky, etc. become serious limitations. There remains a possibility that observations at intermediate apertures may sufficiently avoid both problems; but the only published data that appear to be statistically applicable to the question do not substantiate the possibility.

The bright cluster galaxy observations of Peterson (1970a), taken at apertures $\theta_1(z)$, can be corrected by a standard curve to the apertures $\theta_2(z)$; these corrections are relatively crude in that there is quite considerable variation between the surface-brightness curves $I(r)$ for such galaxies. Nevertheless, no statistically significant difference between the fits to these data of the Hubble and Lundmark laws is apparent. It should be of interest to make direct measurements of the magnitude of the Peterson galaxies at the apertures indicated by the chronometric theory, and to make measurements of additional galaxies, chosen in a statistically controlled manner, at both apertures $\theta_1(z)$ and $\theta_2(z)$. It should be borne in mind, however, that these apertures depend also on the Hubble parameter (itself z -dependent in the

chronometric theory); therefore, measurements at several corresponding apertures should be taken.

The apparent limitations on the redshift-magnitude relation for galaxies in discriminating between the two laws means neither that galaxy observations as a whole are without discriminatory potential, nor that the redshift-magnitude relation is inherently ineffective. Indeed, the Schmidt V/V_m test is applicable to samples of galaxies which are complete to fixed apparent magnitudes, and has significant results for the Peterson sample: it is spatially extremely nonuniform according to this test, within the expanding-universe framework, but does not deviate significantly from spatial uniformity according to the chronometric theory. This suggests that apparent local superclustering emphasized by G. de Vaucouleurs (1970), following relevant observations of Holmberg, may not necessarily be physically real, but quite possibly largely a consequence of the theoretical framework within which the observations are analyzed. Observations in other fields which are complete out to fixed apparent magnitudes, or selected from complete lists in a statistically random fashion, could be used both for a definitive check on the redshift-magnitude relation, as indicated, and to test overall spatial uniformity. In any event, the redshift-magnitude relation for quasars is useful for discriminating between the expansion and chronometric theories; not only are aperture corrections not required, but their qualitative implications at larger redshifts are entirely different.

Consider now the practical problem of estimating the observed magnitude of a given galaxy at aperture θ' , given the observed magnitude at aperture θ . Most applicable methods take the surface brightness at distance r from the center of the galaxy, normal to the line of sight, to have the form $I(r/a)$, where a is a parameter dependent on the galaxy in question; admittedly the notion of "center," and especially of distance in other than E0 galaxies must be suitably interpreted. The function I has been variously graphically presented, or taken specific analytical form. For computational purposes, the latter is more convenient; the simplest form is the Reynolds-Hubble law: $I(r) \propto (1 + r)^{-2}$, except for large r ; we shall follow Abell's form for large r , i.e., $(1 + r)^{-3}$, joining it continuously to the earlier form at $r = 21.4$ as indicated by Abell and Mihalas (1966). It would make no essential difference in the following (i.e., for cosmological testing) if we used instead the form given by de Vaucouleurs, or even the Hubble form for large r as well. If the distance of the galaxy is d , then the aperture correction Δm is given by the equation

$$\Delta m = 2.5 \log[J(\theta'd/a)/J(\theta d/a)],$$

where $J(r) = \int_0^r sI(s) ds$. For the Abell standard form,

$$J(x) = \ln(1 + x) + (1 + x)^{-1} - 1 \quad \text{when } x \leq 21.4,$$

$$J(x) = 22.4 \left(\frac{1}{2(1+x)^2} - \frac{1}{1+x} \right) + 3.131 \quad \text{when } x > 21.4.$$

Thus the correction is determined when d and a are known, in addition to the aperture angles.

The determination of d must be made within the theoretical framework being tested, and will vary with the assumed value of the Hubble parameter. Taking, e.g., H as 100 at 15 Mpc, the chronometric and expansionary theories will give distances for the Peterson galaxies, having redshifts in the range 0.01–0.06, which differ by a factor which varies from about 0.3 to 0.7, the chronometric distance being the smaller. In Peterson's work the apertures are determined to yield in the expansionary framework fixed metric diameters of 20 kpc. Within the chronometric framework the actual metric diameters corresponding to the apertures employed are θd_c , where d_c denotes the chronometric-theoretical distance, which takes the form d_c (in kiloparsecs) = $\theta(\text{arc tan } z^{1/2})^\circ \times 0.017979$ if θ is measured in seconds, and H is as indicated (and so agrees with the value used by Peterson). Thus on the chronometric hypothesis, the observed magnitudes must be diminished by $2.5 \log[J(10/a)/J(d_c/2a)]$, to obtain the true magnitude of the central 20-kpc-diameter portion.

One thereby obtains a well-determined aperture correction, once the parameter a is specified. The determination of a again depends, however, on the theoretical model, for this determines distances, on which the conversion from angular to linear diameters depends. The chronometric a_c , for example, could in principle be determined as follows. Let m_1 and m_2 be the observed magnitudes of a galaxy at redshift z , with apertures θ_1 and θ_2 , where, say, $\theta_1 < \theta_2$. Then

$$m_1 - m_2 = -2.5 \log[J(\theta_1 d/a)/J(\theta_2 d/a)],$$

where in natural units $d = 2 \tan^{-1} z^{1/2}$, the θ_j being here in radians and a in natural units. The value $a = a_c$ determined from this equation evidently depends on the assumed value of the Hubble parameter, and will differ from the value obtained by using the expansion-theoretic distance. It is therefore convenient that the aperture correction is not highly sensitive to the precise value of a , apart from a zero point correction which is irrelevant in cosmological tests. The values of a obtained in the indicated fashion actually show considerable dispersion, even within the limited class of apparent bright cluster galaxies. In the absence of systematic published work on the subject, we shall simply take $a = 1$ kpc; this may interpolate between a modal value (perhaps 0.7) and a value perhaps more likely to minimize the root mean square deviation from the true correction (perhaps 2.0), as inferred from

analysis along the foregoing lines of data given by Fish (1964) and Sandage (1972b). The results of the analysis of the Peterson galaxies would not change materially if any value of a in the range 0.5–2 were employed instead. However, due to variation in a , and to the approximation for any individual galaxy involved in using a fixed surface brightness curve, an additional dispersion is introduced into the magnitudes which should eventually appear as a slightly increased dispersion in the absolute magnitudes of the galaxies, as determined from the best-fitting theoretical redshift-magnitude curve.

Since $J(10/a)$ is independent of the particular galaxy, it would suffice for cosmological testing to replace the Peterson magnitudes m by the corrected magnitudes $m' = m + 2.5 \log J(d_c/2)$. It should now be evident how the procedure may be applied to an arbitrary sample of galaxies of a specified type. These specifications must, however, be compatible with the considerations of the following section.

5. Statistical effect of the selection of the brightest objects

If one deletes from a heterogeneous list of luminous objects, quasars or galaxies, all objects fainter than a certain theoretical absolute magnitude—chronometric, expansionary, or otherwise—it has in general the effect of reducing the variance in absolute magnitude of those that are left, for all physically reasonable luminosity functions. This is the case irrespective of the validity of the theory in question, for in effect one is simply truncating a distribution beyond a certain point. The consequent reduction in variance is a statistical verity, and in no wise indicates that bright objects of the category in question form an intrinsically more homogeneous class, observation of which confirms the theory, unless the reduction is significantly greater than would arise on a statistical basis. The latter reduction is considerable, as the following analysis of a normal distribution shows. A similar analysis would apply to a mixture of normal distributions of different means; it seems unlikely that the overall figures will change greatly, for plausible types of mixtures, and we here limit the treatment to the simple cited case.

Given a zero-mean, unit-variance normal variate x , suppose the population above a value a is deleted, corresponding to the “faintest” $100p\%$ of the population. Thus the equation

$$(2\pi)^{-1/2} \int_{-\infty}^a \exp(-x^2/2) dx = 1 - p$$

gives a in relation to p . We then consider the new probability law P_a :

$$dP_a = \begin{cases} (2\pi)^{-1/2}(1-p)^{-1} \exp(-x^2/2) dx & \text{when } x < a, \\ 0 & \text{when } x > a. \end{cases}$$

The mean m_a of this new distribution is readily computed as $(2\pi)^{-1/2} \times (1-p)^{-1} \exp(-a^2/2)$, as is the variance in terms of the incomplete gamma function.

Table 2 gives the corresponding numerical results. Roughly speaking, deleting two-thirds of the faintest objects decreases the variance by about two-thirds. The table should be applied at each fixed redshift, as the fraction p deleted will generally vary with the redshift. The increase in dispersion for $p > 0.7$ can be understood as the effect of removing almost all of the distribution except the comparatively flat and hence widely dispersed tail.

TABLE 2
Statistical effects of selection of brightest objects

Fraction of objects deleted	Reduction in mean	Variance of remaining objects	σ_a
0.1	0.1960	0.6499	0.8061
0.2	0.3450	0.5463	0.7391
0.3	0.4967	0.4723	0.6873
0.4	0.6439	0.4194	0.6476
0.5	0.7979	0.3633	0.6208
0.6	0.9656	0.3162	0.5623
0.7	1.1590	0.3121	0.5587
0.8	1.4000	0.4185	0.6469
0.9	1.7545	0.7307	0.8548

The statistical theory has been compared with the results of selection on the absolute (theoretical) magnitudes for the Peterson sample. Deleting the faintest half of the galaxies on these bases leads to reductions in the variance of the absolute magnitudes, and in average absolute magnitudes, in quite good agreement with the statistical theory. This is equally the case whether the chronometric or the Hubble theory is employed.

6. The Peterson galaxies

Among the best data from the standpoint of statistical control are those of Peterson (1970a). These provide a complete sample of 44 bright cluster galaxies complete in a specified field to a limiting apparent magnitude of 15. The major portion of the present section is concerned with the analysis of these data along the general lines earlier indicated.

We shall later treat galaxy observations in specified categories reported by Arakelyan, de Vaucouleurs, and Sargent, among others, and discuss briefly the recently published data of Sandage. The work of de Vaucouleurs concerns nearby galaxies, and appears comprehensive and objective within

reasonable statistical limits. Sargent's work contains a study of 24 Seyfert-like Markarian galaxies, characterized and observed in an apparently objective and uniform fashion. Together with the Peterson galaxies, these provide three quite different groups of galaxies. The Sandage observations overlap significantly with those of Peterson; unlike the latter, the sample that they form is not delineated in a statistically explicit fashion; for this and other reasons it does not appear possible to use them for a statistically rigorous test of the chronometric hypothesis.

Before giving the details of the analysis of the Peterson data, the central conclusions will be summarized briefly.

(a) The dispersion of the Peterson magnitudes from the best-fitting Hubble line is 0.33 mag; that from the best-fitting constant-intrinsic-luminosity chronometric curve is 0.36. The slightly greater dispersion of the chronometric theory is not statistically significant, and may well be due to the utilization of data gathered basically on the expansion hypothesis, aperture corrections being made on the basis of a fixed curve, whereas the surface brightness profiles of the galaxies do in fact vary considerably (see below regarding this question).

(b) Because of the completeness of the sample, the Schmidt luminosity-volume test is applicable. Assuming a spatially uniform population of galaxies, the ratios V/V_m defined by Schmidt should be uniformly distributed in the interval from 0 to 1. It is found that in actuality, they are highly skewed, and their deviation from spatial uniformity, as measured by the Kolmogorov-Smirnov statistic, is so large as to correspond to a probability of 5×10^{-5} of obtaining such a skew sample, assuming that the population is in fact spatially uniform.

(c) It is well known that it is extremely difficult to obtain a rigorously complete sample out to a given magnitude, and it is therefore conceivable that the Peterson sample is not entirely complete out to a limiting magnitude of 15, but is such to a lower magnitude, such as 14. However, a test of spatial uniformity of the subsample of 23 galaxies brighter than this magnitude still shows considerable skewness; the probability level, due largely to the relative smallness of the sample, rises to 0.025, and so is still significant by conventional standards, although not strongly so.

(d) Because the galaxy apparent magnitudes are model-dependent, in particular the measuring aperture was determined by Peterson in accordance with the expansion hypothesis, completeness out to a prescribed limiting magnitude is likewise model-dependent. Consequently, the Peterson sample is not necessarily complete out to a fixed limiting magnitude under the chronometric hypothesis; the aperture corrections may significantly affect the relative apparent brightness of galaxies near the limiting magni-

tude. These effects are, however, unlikely to exceed 0.5 mag, and it seems quite safe to suppose that a sample which is complete out to a given limiting magnitude m under the expansion hypothesis is also complete out to a brighter magnitude $m - 1$ under the chronometric hypothesis, with the same metric diameter and a fixed zero-point adjustment of the magnitude scale, so that similar numbers of galaxies are involved in samples complete out to given limits. A limiting magnitude of 13.2 on the chronometric scale was therefore adopted, as comparable to the limiting magnitude of 14 in the expansion hypothesis; this, in fact, selected the identical subsample of 23 galaxies.

The application of the Schmidt V/V_m test within the chronometric framework to this subsample accepts the hypothesis of spatial uniformity, at a highly satisfactory probability level.

(e) The results indicated in (b)–(d) suggest that apparent inhomogeneities in the radial component of the spatial distributions of galaxies may be due to the mode of analysis, and specifically to the employment of the expansion hypothesis, rather than to actual spatial nonuniformity.

The main quantitative results are given in Table 3, whose columns are as follows: (1) is the Abell cluster number. (2) is the measured visual magnitude m at an aperture appropriate to a fixed metric diameter of 20 kpc, on the basis of the Friedman model with $q_0 = \frac{1}{2}$, as reported by Peterson. (3) is the actual semidiameter (radius) of the observed region on the basis of the chronometric hypothesis, with the assumption that

$$H = 100 \text{ kmsec}^{-1} \text{ Mpc}^{-1}$$

at 15 Mpc. (4) is the visual magnitude $m + \Delta m$, corrected on the chronometric hypothesis to a fixed metric diameter of 20 kpc, with the use of the Reynolds–Hubble–Abell surface brightness law earlier indicated. (5) is the mean net aperture correction $\Delta m - \bar{\Delta}m$. (6) is the V/V_m implied by the Hubble model ($m = 5 \log z + \text{const}$, Euclidean space). (7) is the ratio of the number of galaxies in the sample whose V/V_m does not exceed the value in column (7), to the total sample number (spatial uniformity means precisely that (6) – (7) tends to zero as the sample size increases indefinitely). (8) is the actual difference (6) – (7), whose maximum absolute value is the Kolmogorov–Smirnov statistic D . (9), (10), and (11) are the same as (6), (7), and (8), for the subsample of 23 galaxies with the expansion-theoretic apparent magnitude (column (2)) brighter than 14. (12), (13), and (14) are the same within the chronometric hypothesis, for the subsample whose chronometric-theoretic magnitude (column (4)) is brighter than 13.2 (approximately corresponding to the cutoff at magnitude 14 for the expansion-theoretic magnitude, and leading to the identical subsample).

TABLE 3
Analysis of spatial uniformity for Peterson galaxies

1	2	3	4	5	6	7	8	9	10	11	12	13	14
76	13.83	3.84	13.10	0.06	0.20	0.48	-0.28	0.79	0.91	-0.12	0.87	0.89	-0.02
119	14.28	3.57	13.52	0.12	0.37	0.68	-0.31						
147	14.74	3.58	13.98	0.12	0.70	0.95	-0.25						
151	14.29	3.32	13.46	0.19	0.38	0.70	-0.32						
194	12.34	5.45	11.93	-0.23	0.03	0.07	-0.04	0.10	0.13	-0.03	0.16	0.13	0.03
262	12.54	5.59	12.15	-0.25	0.04	0.18	-0.14	0.13	0.17	-0.04	0.22	0.17	0.05
347	12.61	5.45	12.20	-0.23	0.04	0.18	-0.14	0.15	0.26	-0.11	0.24	0.26	-0.02
376	14.72	3.43	13.92	0.16	0.68	0.91	-0.23						
400	13.21	5.01	12.73	-0.16	0.09	0.34	-0.25	0.34	0.57	-0.23	0.51	0.57	-0.06
407	14.70	3.47	13.91	0.15	0.66	0.89	-0.23						
426	12.13	5.38	11.71	-0.22	0.02	0.05	-0.03	0.08	0.09	-0.01	0.12	0.09	0.03
505	14.43	3.27	13.59	0.20	0.46	0.82	-0.36						
539	13.74	4.41	13.16	-0.06	0.23	0.52	-0.29	0.70	0.87	-0.17	0.95	0.96	-0.01
548	14.13	3.77	13.42	0.07	0.30	0.59	-0.29						
569	12.71	5.27	12.27	-0.20	0.04	0.18	-0.14	0.17	0.35	-0.18	0.27	0.30	-0.03
576	14.37	3.72	13.65	0.06	0.42	0.77	-0.35						
634	13.61	4.50	13.05	-0.08	0.15	0.41	-0.26	0.58	0.78	-0.20	0.81	0.78	0.03
671	14.23	3.40	13.42	0.17	0.35	0.66	-0.31						
754	14.34	3.29	13.50	0.20	0.40	0.75	-0.35						
779	13.22	5.13	12.76	-0.18	0.09	0.34	-0.25	0.34	0.61	-0.27	0.53	0.61	-0.08
993	14.48	3.30	13.65	0.19	0.49	0.84	-0.35						
1060	11.60	6.70	11.34	-0.38	0.01	0.02	-0.01	0.04	0.04	0	0.07	0.04	0.03
1139	14.20	3.84	13.50	0.06	0.33	0.61	-0.28						
1185	13.58	3.97	12.91	0.03	0.14	0.39	-0.25	0.56	0.74	-0.18	0.67	0.70	-0.03
1213	14.24	4.34	13.65	0.05	0.35	0.66	-0.31						
1228	14.10	4.00	13.44	0.02	0.29	0.57	-0.28						
1257	14.52	4.02	13.86	0.02	0.52	0.86	-0.34						
1314	13.65	4.04	13.00	0.01	0.16	0.43	-0.27	0.62	0.83	-0.21	0.76	0.74	0.02
1318	12.75	5.28	12.31	-0.20	0.05	0.20	-0.15	0.18	0.39	-0.21	0.28	0.35	-0.07
1367	12.56	5.09	12.10	-0.18	0.04	0.18	-0.14	0.14	0.22	-0.18	0.87	0.89	0
1377	14.73	3.35	13.90	0.18	0.69	0.93	-0.24						
1656	12.69	4.84	12.19	-0.14	0.04	0.18	-0.14	0.16	0.30	-0.14	0.24	0.26	-0.02
1736	14.33	3.62	13.58	0.11	0.40	0.75	-0.35						
2052	13.83	3.96	13.16	0.03	0.20	0.48	-0.28	0.79	0.96	-0.17	0.95	0.96	-0.01
2147	13.86	3.96	13.19	0.03	0.21	0.50	-0.29	0.82	1.00	-0.18	0.99	1.00	-0.01
2151	14.04	3.97	13.37	0.03	0.27	0.55	-0.28						
2152	14.40	3.58	13.64	0.12	0.44	0.80	-0.26						
2162	13.48	4.15	12.85	-0.01	0.12	0.36	-0.24	0.49	0.70	-0.21	0.62	0.65	-0.03
2197	13.20	4.12	12.56	0	0.09	0.34	-0.25	0.33	0.52	-0.19	0.40	0.48	-0.08
2199	13.02	4.14	12.39	-0.01	0.07	0.25	-0.18	0.26	0.48	-0.22	0.31	0.43	-0.12
2319	14.78	3.25	13.93	0.21	0.74	1.00	-0.26						
2634	13.22	4.18	12.60	-0.02	0.09	0.34	-0.25	0.34	0.65	-0.31	0.43	0.52	-0.09
2657	14.77	3.64	14.03	0.10	0.73	0.98	-0.25						
2666	12.95	4.45	12.36	-0.05	0.06	0.23	-0.17	0.23	0.43	-0.20	0.30	0.39	-0.09

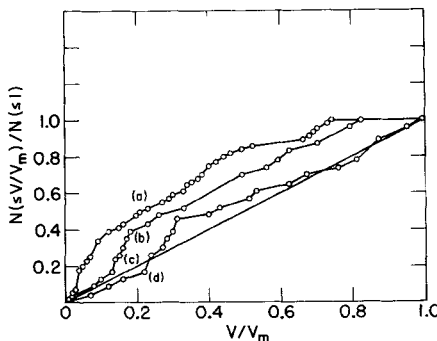


Figure 5 The V/V_m test for the Peterson sample.

\circ , individual galaxies, values computed on the following bases: (a) Hubble theory, limiting magnitude 15 (all 44 galaxies); (b) Hubble theory, limiting magnitude 14 (23 galaxies) (d) chronometric theory, limiting magnitude 14.2 (same 23 galaxies as in (b)). (c) Theoretical line for radial spatial uniformity. Thus apparent radial spatial uniformity is materially a function of the theory employed.

The only part of the aperture correction that is relevant to cosmological testing is the deviation from the mean correction given in column (5); this is small, having a root mean square of 0.15 mag. The respective Kolmogorov-Smirnov statistics D for the three cases (i.e., the maxima of the absolute values of the entries in columns (8), (11), and (14), respectively) are 0.36, 0.31, and 0.12. Assuming a spatially uniform population, the respective probabilities P of obtaining values of D this large are 2×10^{-5} , 0.024, and >0.5 , employing here the asymptotic law $P \sim 2 \exp(-2nD^2)$, where n is the sample size. This formula is asymptotic as $n \rightarrow \infty$; however, it is considered to give a good approximation for relatively small values of n ; the results are consistent with the confidence intervals given in Pearson and Hartley (1972).

Some of the results are summarized in Figure 5, in which the fraction observed having V/V_m less than a given value λ is compared with λ , in each of the three statistical situations under consideration here. The abscissa is then V/V_m , or the volume out to the redshift of the object is the theory in question, divided by the maximum volume within which the object would remain in the sample, according to the theory. The ordinate is the cumulative frequency, expressed as a fraction of the total number of objects in the sample, of objects whose V/V_m is not exceeded by the abscissa. The straight line segment between (0, 0) and (1, 1) is the theoretical line expected for an infinitely large sample of objects uniformly distributed in space; above this line, in order, come the observed line for the subsample of 23 galaxies limiting magnitude 13.2 according to the chronometric theory; the subsample of limiting magnitude 14 according to the Hubble theory (actually the same as just indicated), and the entire sample (44 galaxies) according to the Hubble theory.

7. Markarian galaxies and N-galaxies

A relatively objectively defined sample of galaxies of the former type has been observed by Sargent (1972). These galaxies resemble Seyfert galaxies, and aperture effects for them should be relatively marginal. It is therefore of interest to compare the (m , z) pairs observed by Sargent with the theoretical $m-z$ relation for a single type of luminous object, for which the present galaxies appear to be a relatively good candidate. In any event, it seems appropriate to begin with the hypothesis that they form a single luminosity class as the simplest tenable one. It is found that the chronometric curve, adjusted to the average absolute magnitude of the galaxies as given by the chronometric theory, fits within a dispersion of 0.77 mag the Sargent observations. The corresponding dispersion as given by the Hubble theory is 1.12; the sample dispersion is 0.87. The qualitative point here is not so much that the chronometric dispersion is less than the expansion-theoretic dispersion; the sample is too small for statistical significance, although in conjunction with other samples presented here it is statistically relevant. Rather it is the surprising excess of the expansion-theoretic over the sample dispersion; an excess of the magnitude here found seems quite unlikely, on the expansion-theoretic hypothesis, but to make a formal statistical analysis would seem supererogatory, in view of the weight of other evidence and the always possible defense of unknown selection effects. Not only does the chronometric theory supply a reasonable model, and one distinctly better than the expansionary one in this instance, but it also alters in a reassuring way the absolute luminosity of these objects vis-à-vis quasars, as well as vis-à-vis the classical Seyferts. In many important respects, other than their absolute luminosities as given by the expansionary theory, these objects appear very closely related, and possibly substantially identical. However, on the expansion theory, quasars are several magnitudes brighter than the present Markarian galaxies, and these in turn are according to Sargent (1971) brighter than the classical Seyfert galaxies. These apparent differences in luminosity are seen to result from the theoretical analysis, and to be not necessarily real, by an analysis from the chronometric standpoint, according to which there is little difference between the intrinsic luminosities of these three groups of objects. See also Rees and Sargent (1972).

Figure 6 exemplifies some of these points. The DeVeny quasar lines are based on the sample of 158 quasars described later; the magnitude-redshift theoretical curves for these have been corrected (in accordance with an oral communication from W. L. W. Sargent) to represent photographic magnitudes comparable to those reported in Sargent (1972) by taking $m_p \sim m_v + 0.4$ for the present galaxies.

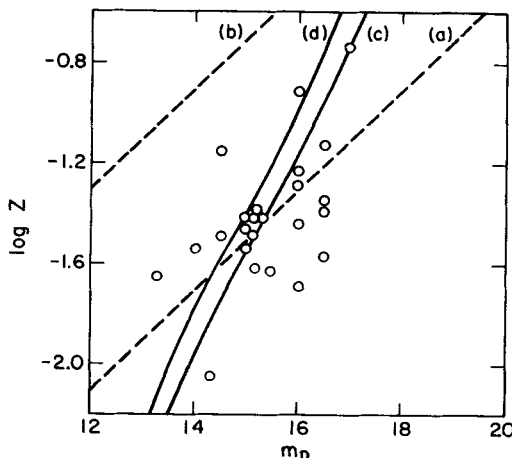


Figure 6 The redshift-magnitude relation for Seyfert-like Markarian galaxies studied by Sargent (1972).

(a) Best-fitting Hubble line to present galaxies ($\sigma = 1.12$); (b) best-fitting Hubble line to quasars studied by DeVeny *et al.* (1971); (c) best-fitting chronometric curve to present galaxies ($\sigma = 0.77$); (d) best-fitting chronometric curve to DeVeny quasars. In particular, quasars and Seyfert-like galaxies have little difference in intrinsic luminosity on the chronometric hypothesis, although the difference is quite large on the expansion hypothesis.

An analogous situation is presented by the N-galaxies. Their close relationship to quasars has been remarked by many authors, and Lynden-Bell (1971) has proposed that they constitute "miniquasars," similar to but less luminous than quasars. On the expansion hypothesis, N-galaxies average ~ 3 magnitudes fainter than the average quasar (as represented by the DeVeny list), but in other important respects they resemble quasars. The fact is that on the chronometric hypothesis, the N-galaxies have average intrinsic luminosity within 0.5 mag of the average quasar. Moreover, the chronometric $m-z$ curve fits the N-galaxy data with a distinctly smaller dispersion than does the Hubble line.

Admittedly, the number of N-galaxies having reliable magnitudes and redshifts is too small for the difference in dispersion to be statistically significant, but in conjunction with the other considerations of this section, the data for N-galaxies provide a measure of support for the chronometric hypothesis. Figure 7 shows the redshifts and magnitudes for the N-galaxies considered by Sandage (1967). The corrected magnitudes given by Sandage have been used, and the optically highly variable galaxy 3C 391, as reported by Sandage (1967), has been excluded. The standard deviations of the residuals of the observed magnitudes from the best-fitting theoretical lines are 0.49 for the chronometric theory and 0.68 for the expansion theory.

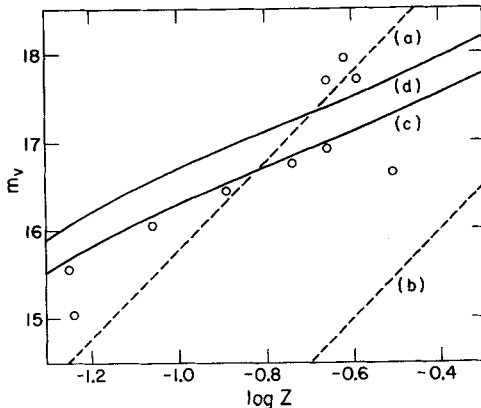


Figure 7 The redshift-magnitude relation for N-galaxies listed by Sandage (1967).

(a) Best-fitting Hubble line to present galaxies ($\sigma = 0.68$); (b) best-fitting Hubble line to quasars studied by DeVeney *et al.* (1971); (c) best-fitting chronometric curve to present galaxies ($\sigma = 0.51$); (d) best-fitting chronometric curve to DeVeney quasars. Again, these galaxies differ little from quasars in intrinsic luminosity on the chronometric hypothesis, but differ substantially on the expansion hypothesis.

The interpretation of these results within the chronometric theory, as regards the relation between quasars on the one hand and Seyfert-like or N-galaxies on the other is necessarily rather speculative, and of a different nature from the considerations involved in systematic hypothesis testing. Nevertheless it may not be amiss and indeed is probably peripherally relevant to note the indication that such galaxies are not only similar to but are perhaps identical with a certain category of quasar of average intrinsic luminosity. That is, if at larger redshifts, many of these galaxies might well appear to be quasars. Observations on spectral functions required for material confirmation may not be available for some time, but it may be noted parenthetically that the analysis of quasar observations (cf. below) provides some circumstantial evidence: (a) chronometrically there is a statistically insignificant but nevertheless noticeable deficiency of quasars in the redshift range 0.0–0.3, which could be removed by hypothesizing the identity of N- and certain Seyfert-like galaxies with certain classes of quasars; (b) the model-independent distribution of luminosities of quasars (cf. below) does not deviate in a statistically significant way from a normal distribution, but there are nevertheless some clearly marked groupings suggesting that it is more precisely a superposition of normal distributions, of effectively non-overlapping ranges. The brightest fifth of the quasars in the DeVeney list ("brightest" in a model-independent sense detailed below) have an optical luminosity ~ 1.2 mag brighter than the average quasar in the list; and there is a noticeable gap in luminosity between these bright quasars and the

average ones. The latter quasars thereby appear to constitute "miniquasars" relative to the bright ones, in a sense analogous to that employed by Lynden-Bell (1971), whose theoretical proposal, expanded and modified in the fashion just suggested, appears to be in agreement with present observations. The recent observations of Sandage (1973) on N-galaxies lend further support to the conjecture that N-galaxies at higher redshifts may appear as quasars.

That these results are not reflections of small sample size or of coincidental selections is confirmed by the study of a substantial sample of Markarian galaxies listed by Arakelyan *et al.* (1972). These are largely at the higher redshifts thought to be beyond the local supercluster postulated by some in order to reconcile the apparent square-law dependence of redshift on distance for low-redshift galaxies with the expanding-universe theory. No special selection effects relatively favorable to a square law are known for these data. However, the square law decreases the dispersion in apparent magnitude, while the linear law increases it. Specifically, the dispersions in apparent magnitude (a) and in absolute magnitude based respectively on the (b) chronometric prediction (differing trivially from the square law in this redshift range) and (c) Hubble law, are as follows. For the 60 galaxies with $cz > 3000 \text{ km sec}^{-1}$ (average value, 8000), (a) 0.89, (b) 0.84, (c) 1.04. For the full sample of 69 galaxies, (a) 1.09, (b) 1.01, (c) 1.51. The results are qualitatively unaltered if the galaxies are arranged in order of increasing redshift, and divided into bins containing equal numbers of galaxies, the brightest, second brightest, etc., in each bin being selected; or if the observations at extreme redshifts are deleted from the sample.

8. The redshift-magnitude relation for nearby galaxies

The major study by G. de Vaucouleurs (1972) of the redshift-magnitude relation for about 100 nearby groups of galaxies confirms the apparent quadratic dependence of redshift on distance, which was noted by Hawkins (1962) on the basis of the observations of Humason *et al.* (1956) (regarding historical origins, cf. also Lundmark, 1920, 1925). This is consistent with the chronometric theory, but deviates from the law of Hubble (1929).

It has been proposed by de Vaucouleurs that the expansion theory is basically correct, but that a local spatial anisotropy distorts the redshift-magnitude relation. The hierarchical model proposed by de Vaucouleurs is related in direction to that originally proposed by Charlier, as well as more recent ideas of Holmberg; it appears to be in satisfactory agreement with low-redshift observations for the $m-z$ relation of galaxies. It is, however, scientifically less economical that the chronometric theory, in that the latter involves no sacrifice of spatial homogeneity or additional parameters.

As discussed by G. de Vaucouleurs (1972), there is a persistent anomaly in the determination of Hubble's parameter by different observations, and specifically between the lower values obtained from observations of Virgo cluster objects and the higher values obtained from observations including the present redshift-magnitude data. A further advantage of the chronometric over the expansion-theoretic model is that it reconciles the different values on the basis of the different distances to the objects under observation. Thus the velocity/distance relation of these groups is apparently non-linear for $\Delta < 30$ Mpc. The velocity/distance ratio increases from $H \cong 50$ to 150 km sec $^{-1}$ Mpc $^{-1}$ when Δ increases from $\Delta \cong 5$ to $\Delta \cong 25$ Mpc, according to de Vaucouleurs (1972). On the chronometric hypothesis, the value $H = 50$ at a distance $\Delta = 5$ is equivalent to the value $H = 86$ at $\Delta = 15$; similarly the value $H = 150$ is equivalent to the value $H = 116$ at $\Delta = 15$; they are thus within 16% of the value $H = 100$ at $\Delta = 15$ Mpc which has been adopted in the present work. This is a level of accuracy comparable with optimistic informed estimates of the attainable accuracy (cf. Sandage, 1970). It is relevant to note also that one of the most scrupulous estimates of the Hubble parameter, that due to Holmberg (1964), of 80 km sec $^{-1}$ Mpc $^{-1}$, while not specifically based on a particular value for the distance Δ , may reasonably be considered to correspond to $\Delta \sim 10$; it is then equivalent to the value $H = 98$ at $\Delta = 15$. This differs insignificantly from the value $H = 100$ at $\Delta = 15$ employed here, as does the eclectically based estimate $H = 95$ by van den Bergh (1970). From the chronometric standpoint, there is thus no significant anomaly in the differing values of the Hubble parameter as determined by most leading investigators. The only exception, the recent determination $H \sim 50$ by Sandage, is based on quite different observations and new distance scales, and seems explicable on this basis. The work of Abell (1972) emphasized primarily the uncertainty in the Hubble parameter; a possible low value for H is cited basically as an illustration of the dependence of its determination on the assumption made regarding the comparative luminosity function of the Virgo cluster; and the difficulty of resolution of the fundamental question of an operational and model-independent selection procedure for "cluster" tends seriously to moot statistically cosmological cluster samples.

The foregoing indications regarding the phenomenology of low-redshift galaxies suggest a comprehensive statistical analysis of the de Vaucouleurs tape, representing an updating to 1972 of the material in G. de Vaucouleurs and A. de Vaucouleurs (1964). Included here are many more galaxies than those on which the Hubble law was originally based. Such an analysis was conducted jointly with J. F. Nicoll, employing all of the data of objectively delineated subsamples, entirely without corrections or other uncertain emendations, and standard contemporary principles of statistical estimation

and hypothesis testing. The results are extremely favorable to the square redshift-distance law, both at the model-building and hypothesis-testing levels. They are quite unfavorable to the Hubble law at the model-building level, but at the hypothesis testing level the law may be marginally acceptable, with some emendations.

Making the purely phenomenological assumption that $z \propto r^p$, where z is the redshift and r the distance, apart from peculiar motions, for some constant exponent p , and sufficiently small distances r , simply embodies the observed facts that redshifts generally increase with distance and vanish near the Galaxy. Statistically, it is assumed that bright galaxies form a true statistical population, at least for redshifts ≤ 0.03 , i.e., there is no evolution in this range. Where relevant it is assumed further that the spatial distribution of the galaxies is radially homogeneous; no assumption as to isotropy is required. It then follows that the probability density for r varies as $r^2 dr$, whence that for z varies as $z^{3q-1} dz$, where $q = p^{-1}$.

The exponent p may be estimated from observed relations between the magnitudes, redshifts, and angular diameters of galaxies, in accordance with the maximum-likelihood procedure. For any value of p , the apparent luminosity will vary with the absolute luminosity in accordance with the inverse square law, the redshift factor $(1+z)^{-1}$, and possible theory-dependent factors which may be presumed negligible for $z \leq 0.03$, as they surely are for all theories considered realistic. The apparent angular diameter θ will similarly vary with the absolute diameter Δ , and inversely with r . It follows that $m = 5q \log z + M$ and $\log \theta = -q \log z + A$, where $A = \log \Delta$, apart from terms of order z or less, which are here negligible. Absolute magnitudes M and logarithmic diameters A may be defined by these equations.

The joint probability distribution of z , M , and A takes the form $P(z)P(M, A)$, in view of the stochastic independence of M and A from z , where $P(z) = Cz^{3q-1}$ with $C = 3q[z_2^{3q} - z_1^{3q}]^{-1}$ if the redshift interval under consideration is $z_1 < z < z_2$, and $P(M, A)$ takes the form in terms of observed quantities: $P(m - 5q \log z - \bar{M}, \log \theta + q \log z - \bar{A})$, where \bar{M} and \bar{A} are the population means. The unknown function $P(M, A)$ will be assumed otherwise to depend only on the standard deviations σ_M and σ_A of M and A , and their correlation ρ , by the normal law. This is standard phenomenological procedure; serves to ensure the coincidence of maximum-likelihood and least-square estimation for the parameter involved in $P(M, A)$; and may be confirmed by statistical testing of the resulting sample distributions of absolute quantities.

The various bi- and univariate distributions then follow by integration, and depend on parameters that are functions of the foregoing. The maximum-likelihood procedure consists in choosing the parameters to maximize the corresponding probability density for the observed sample. With

an imposed cutoff in apparent magnitude of m_L , the new probability density $P(z, M, A)$ is derived by multiplication of $P(z)P(M, A)$ by $(\iiint_{m \leq m_L} P(z)P(M, A) dz dM dA)^{-1}$ for $m \leq m_L$, and by 0 for $m > m_L$. The corresponding maximum-likelihood estimates cannot be given in analytically explicit form, but are determinable by successive approximation procedures.

In addition to the familiar $m-z$, $\theta-z$, and $N(z)$ relations, it is interesting to consider the $N(V/V_m)$ relation. The original Schmidt V/V_m test (see Schmidt, 1968) involved no a priori limitations on the redshifts involved, but it is essential for observational reasons (incompleteness in redshift determinations for larger z), as well as to enhance its discriminatory capacity, to adapt it to the case in which it is a priori required that $z_1 < z < z_2$, where z_1 and z_2 are given. The V ($= V(z)$) then excludes the region up to the redshift z_1 , so $V(z) \propto z^{3q} - z_1^{3q}$, while the V_m is $V(z_m)$, where z_m is given by the equation $m_L - m = (5q) \log(z_m/z)$ provided z_m is determined from this equation is $\leq z_2$; otherwise $z_m = z_2$ and $V_m = V(z_2) - V(z_1)$. Thus

$$V/V_m = (z^{3q} - z_1^{3q})(z_m^{3q} - z_1^{3q})^{-1},$$

where z_m is the indicated p -dependent function of m , z , m_L , and z_2 . The principle of the Schmidt test, i.e., the uniform distribution in $[0, 1]$ of V/V_m , on the assumption of radial spatial homogeneity, applies equally well to this generalized situation; and, unlike the original case ($z_1 = 0, z_2 = \infty$), the test is in practice effectively discriminatory between different redshift-distance relations, even when applied to low-redshift objects.

The deviation of an observed from the theoretical uniform distribution can be measured by the Kolmogorov-Smirnov statistic D , which is the maximum absolute difference between the cumulative observed and theoretical distributions. Alternatively, an approximately normal statistic X similar to that employed by Schmidt (1968) is given by the mean of the V/V_m , centered to zero mean and normalized to unit variance, i.e.,

$$X = (12/N)^{1/2} \sum (V/V_m - \frac{1}{2});$$

however, X may vanish although the distributions are different. In either case, the value of p that minimizes the deviation (and so maximizes the corresponding probability) provides an analogue to the maximum-likelihood estimate, and the corresponding confidence intervals for p effectively substitute for dispersions in the estimates.

The de Vaucouleurs catalog includes galaxies having redshifts up to $\sim cz = 10,000$ and magnitudes up to ~ 15 , and is estimated to be overall $\sim 50\%$ complete out to a magnitude of 13. Completeness is probably much greater in limited redshift regions, and its approximate validity out to $cz \sim 2000$ is suggested by the observed $N(< z)$ relation shown in Figure 8.

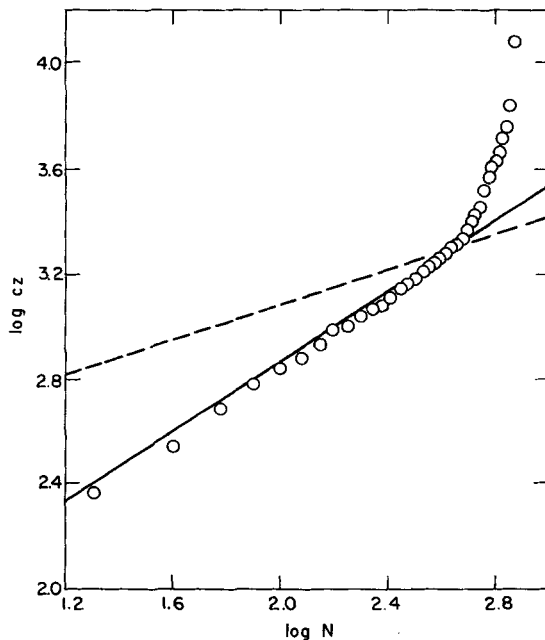


Figure 8 The $\log N$ - $\log z$ relation for all galaxies included in the de Vaucouleurs tape, having $m-z-\theta$ data (742 galaxies).

○, observational points; — and ---, the lines $\log N (\leq cz) - \log N (\leq 2000) = (3/p) \log(cz/2000)$, for the values $p = 2$ and $p = 1$, respectively. These represent the theoretical intrinsic number of galaxies in the indicated redshift regions, on the assumption of a uniform spatial distribution of galaxies. Progressive incompleteness in redshift determinations is anticipated for $z \gg 0$, and is indicated by the strong deviation in this range of the observational relation from the very nearly linear one found for $cz \lesssim 2000$.

For greater conservatism, the test has also been carried out with a limiting magnitude of 12.5. It seems likely that the sample is nearly complete to this limit; indeed results with brighter limits are similar but less definitive because of smaller sample size. For statistical validity, actual completeness is not required, but only randomness within the complete population, in a radial direction, out to the distance corresponding to $cz = 2000$. There is no special reason to doubt that this holds.

a. Estimates of p

In addition to the $m-z$ and $m-\theta$ relations, the $m-z-\theta$ relation for all 742 galaxies having these data in the de Vaucouleurs catalog were employed for maximum-likelihood estimation. The results regarding ρ are shown in Table 4.

TABLE 4
Maximum-likelihood estimates of the redshift-distance exponent

Sample	Full catalog (742 galaxies)		Subsample with $500 \leq cz \leq 2000, B(0) \leq 13$ (350 galaxies)	
	Relation	Exponent	Exponent	Dispersion in exponent
$m-z$		2.05	2.39	0.28
$\theta-z$		1.96	1.92	0.26
$m-\theta-z$		2.04	2.39	0.29
$N-z$			2.57	0.31
$m-N-z$			2.48	0.21
$\theta-N-z$			2.32	0.22
$m-\theta-N-z$			2.48	0.21

In order to assay the sensitivity of the results to conceivable selection effects, estimates were also made for a number of subsamples, selected on redshift range, apparent magnitude, morphological type, and field of observation. No evidence for significant sensitivity was found (cf. the discussion below). A subsample which is representative and reasonable on a priori grounds as well as on the basis of internal indications, is that defined by the limits $500 \leq cz \leq 2000$ and $B(0) \leq 13$. The higher cutoff in cz eliminates a region in which there is a clear phenomenological break in the $N-z$ relation, as shown in Figure 8, and anticipated as a result of incompleteness in redshift determinations for higher redshifts. The results regarding p for this subsample of 350 galaxies, including those based on relations involving N , which would be inappropriate for the full catalog, are shown on the right in Table 4.

The median value of p is 2.39 (the mean is 2.36); the difference from the value $p = 2$ is not statistically significant, in view of the median dispersion of 0.26 (mean of 0.25). However, the excess over 2, as compared with the results from the full sample, is in the direction of a magnitude truncation effect, and indeed the explicit incorporation of an a priori magnitude cutoff into the maximum-likelihood procedure leads to estimates closer to $p = 2$. The relatively lengthy computations for the modified procedure have been carried out for several cutoffs and two redshift intervals on the basis of the observed $m-z$ relation, and are given in Table 5.

In view of the indication from the original maximum-likelihood estimates (in particular, the z -independence of the distribution of residuals from the corresponding theoretical $m-z$ law; cf. Figure 1) that $m = 13$ should be

TABLE 5
Estimates incorporating an a priori magnitude cutoff

Limiting magnitude	Redshift range:	$500 \leq cz \leq 2000$			$500 \leq cz \leq 1800$		
		Sample size	p	σ_p	Sample size	p	σ_p
13.00		350	1.86	0.18	303	1.86	0.20
12.90		339	1.86	0.19	293	1.92	0.22
12.85		330	1.95	0.22	288	1.96	0.24
12.80		325	1.94	0.23	286	1.90	0.25

beyond the faintness necessary in the range $cz \leq 2000$ to include all but a small fraction of the relevant population, the marginal effect of allowance for the magnitude cutoff on the estimates was to be expected.

b. Estimates of galaxy parameters

The maximum-likelihood estimates of the basic parameters of the joint absolute magnitude-diameter distribution are shown in Table 6. For comparison purposes, the same parameters as estimated from the data on the basis of the prior hypotheses that $p = 1$ or 2 are also shown.

For each sample, the estimated parameters are rather insensitive to the relation employed, particularly in the case of the dispersions, which do not

TABLE 6
Maximum-likelihood estimates of galaxy parameters

Relation	Sample: Full catalog (742 galaxies)					Subsample (350 galaxies)				
	\bar{M}	σ_M	\bar{A}	σ_A	ρ	\bar{M}	σ_M	\bar{A}	σ_A	ρ
$m-z$	17.92	0.93	—	—	—	16.79	0.72	—	—	—
$\theta-z$	—	—	0.14	0.23	—	—	—	0.16	0.21	—
$m-\theta-z$	17.94	0.93	0.18	0.23	0.76	16.78	0.72	0.41	0.21	0.70
$m-N-z$	—	—	—	—	—	16.60	0.72	—	—	—
$\theta-N-z$	—	—	—	—	—	—	—	0.38	0.21	—
$m-\theta-N-z$	—	—	—	—	—	16.60	0.72	0.44	0.21	0.70
$p = 2^a$	18.05	0.93	0.16	0.23	0.76	17.77	0.72	0.21	0.21	0.70
$p = 1^a$	23.72	1.36	-0.97	0.30	0.87	23.76	0.85	-0.99	0.22	0.74

^a Here a value of p is assumed a priori, and the maximum-likelihood procedure is applied to the other parameters (least-square estimation in these cases).

differ within the accuracy quoted between their values for $p = 2$ and the maximum-likelihood estimates of p . As anticipated from the cutoff on apparent magnitude in the subsample, it has generally smaller dispersions and brighter mean magnitudes than the full catalog. For $p = 1$, the dispersions are distinctly larger than for $p = 2$, and are in fact generally larger than corresponding ones in the raw data. Specifically, the latter are, for the full sample, $\sigma_m = 1.33$ and $\sigma_{\log \theta} = 0.30$; for the subsample, $\sigma_m = 0.79$ and $\sigma_{\log \theta} = 0.22$. This negative predictive power for the $p = 1$ assumption is equally the case for the N - z relation for the subsample, where $D = 0.27$ for $p = 1$ and $D = 0.04$ for the deviation of the observed relation from a law of uniform distribution in redshift.

The allowance for the observational cutoff in magnitude has naturally the effect of increasing the estimated dispersion in absolute magnitude as well as the estimated mean magnitude. The results of this more refined analysis are $\sigma \sim 0.92$ and $M \sim 18.1$, for all of the samples in Table 6. It is interesting that these values do not differ significantly from those estimated for the full sample without allowance for the observational magnitude truncation.

c. The Schmidt V/V_m test

As earlier indicated, this test is independent of magnitude truncation, whether in all of space or in a fixed redshift interval, as is here appropriate. The influence of peculiar velocities may be largely suppressed by elimination of sufficiently low redshifts. In view of the earlier-cited dispersion of $< 100 \text{ km sec}^{-1}$ among blueshifted galaxies in the catalog, the elimination of galaxies with redshifts $\leq 500 \text{ km sec}^{-1}$ appears likely to achieve this end. At the same time it should serve to avoid ultralocal irregularities.

At the other extreme, the dependency on redshift of incompleteness in redshift determinations requires the elimination of correspondingly high redshifts. The close approximation to linearity of the phenomenological $\log N(< z)$ - $\log z$ relation up to but not beyond the limit $cz = 2000 \text{ km sec}^{-1}$ (cf. Figure 8), provides objective indications for the appropriateness of this redshift as an upper limit. Consequently the redshift limits $500 \leq cz \leq 2000$ have been adopted in the tests detailed here. Computations for slightly different ranges bounded by $cz = 300$ at the lower range and $cz = 1800$ at the upper, have shown insensitivity to the precise limits employed.

As earlier indicated, it is problematical whether the catalog galaxies brighter than 13^m in the redshift range ≤ 2000 form a random subsample of all such galaxies. However, this seems likely to be effectively the case with a limiting magnitude of 12.5. The results for both limiting magnitudes are given in Table 7.

TABLE 7

Maximum-probability estimates of the redshift-distance exponent from the $N - V/V_m$ relation

Redshift interval	Limiting magnitude	D estimate	X estimate
500-2000	13.0 (350 galaxies)	2.24	2.25
	12.5 (286 galaxies)	2.17	2.05
500-1800	13.0 (303 galaxies)	2.20	2.21
	12.5 (254 galaxies)	2.01	1.92
300-2000	13.0 (379 galaxies)	2.08	2.09
	12.5 (312 galaxies)	1.82	1.84
300-1800	13.0 (332 galaxies)	2.05	2.05
	12.5 (280 galaxies)	1.75	1.75
0-2000	13.0 (409 galaxies)	1.93	2.00
	12.5 (340 galaxies)	1.77	1.81

Confidence intervals for these estimates may be determined, and the V/V_m procedure clarified, by reference to Table 8, which gives for each limiting magnitude and a range of values of p the corresponding values of D , the probability $P(D)$ of obtaining a deviation as large as D , and X . In particular, with the more conservative limiting magnitude of 12.5, the hypothesis that $p = 1$ leads to probabilities of deviations as large as those

TABLE 8

Deviations from spatial uniformity as indicated by the $N - V/V_m$ relation for galaxies with $500 \leq cz \leq 2000$

p	Limiting magnitude 13			Limiting magnitude 12.5		
	D	$P(D)$	X	D	$P(D)$	X
10.0	0.165	0.00000001	6.15	0.134	0.00007	4.27
5.0	0.114	0.0002	4.09	0.099	0.008	2.95
3.0	0.064	0.110	1.83	0.057	0.304	1.52
2.5	0.042	0.570	0.72	0.041	0.726	0.84
2.3	0.029	0.928	0.16	0.032	0.924	0.50
2.2	0.029	0.931	-0.15	0.026	0.989	0.31
2.1	0.030	0.904	-0.47	0.025	0.995	0.11
2.0	0.038	0.684	-0.83	0.030	0.960	-0.11
1.8	0.049	0.363	-1.58	0.041	0.734	-0.58
1.6	0.075	0.036	-2.43	0.058	0.296	-1.12
1.4	0.091	0.006	-3.43	0.071	0.115	-1.70
1.2	0.119	0.0001	-4.60	0.078	0.061	-2.37
1.0	0.149	0.0000004	-5.92	0.104	0.004	-3.11

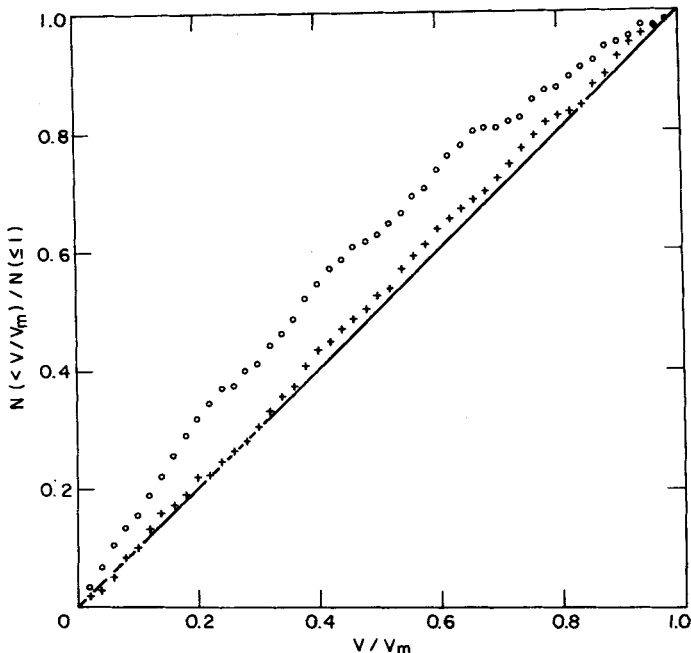


Figure 9 The $N(<V/V_m)$ relation for the subsample of the galaxies included in the de Vaucouleurs tape in the redshift range $500 \leq cz \leq 2000$, and not fainter than $13''$, on the basis of the $p = 1$ and 2 hypotheses (\circ and \times , respectively).

The deviation from spatial uniformity (—) for a hypothetical linear redshift-distance law is highly significant for a sample of the present size (350 galaxies); in the case of a hypothetical square law, the agreement is quite satisfactory.

observed in D and X of 0.004 and 0.001, respectively; for $p = 2$, the corresponding probabilities are 0.96 and 0.83. Figure 9 shows the sample $N(V/V_m)$ relation for $p = 1$ (open circles) and $p = 2$ (crosses) together with the line representing theoretical spatial uniformity in the radial direction.

d. Discussion

On a straightforward phenomenological basis, the results strongly support a value of $p \sim 2$, and reject the value $p = 1$. As in virtually any situation in which controlled random sampling is inherently difficult, some refinements in procedure might be contemplated. The major ones, and the only ones that appear to have nontrivial potential for alteration of the main conclusion are: (a) selection on morphological type; (b) limitation of the region of the sky in order to reduce the possible effects of different telescope locations and parameters.

Comprehensive quantitative examination of the possible effect (a) shows that it is not real. The relative strength of the indications for the value $p = 2$ as against the value $p = 1$ is quite unaffected by selection on morphological type. For the most refined estimates, i.e., those that allow explicitly for an a priori magnitude cutoff, a substantial sample is necessary to ensure proper convergence of the successive approximations procedure; consequently, the subsample of galaxies that are either elliptical or spiral was studied in this connection. The results, summarized in Table 9, which is comparable to Table 5 treating all types of galaxies, yield an average estimate of $p = 1.88 \pm 0.21$, based as earlier on the subsample in the restricted redshift range $500 \leq cz \leq 2000$.

TABLE 9

Maximum-likelihood estimates incorporating an a priori magnitude cutoff, for the subsample of all galaxies with data which are either elliptical or spiral, and have $500 \leq cz \leq 2000$

Limiting magnitude	Sample size	Estimate of p	Dispersion in p
13.00	271	1.89	0.20
12.95	268	1.87	0.20
12.90	264	1.85	0.20
12.85	259	1.89	0.22
12.80	255	1.89	0.24

Results for morphologically selected subsamples of the full sample having $m-z-\theta$ data, are generally quite similar. The results are summarized in Table 10, which is comparable to Table 4, some of whose results are repeated for ready comparison. For the classic $m-z$ relation, which in the present analysis appears the most stable, the estimate of p , averaged with equal weight over the subsamples of ellipticals, spirals, and lenticulars, is 2.03 ± 0.26 . No less compelling is the scrutiny of the resulting dispersions. Those from the $p = 1$ law are larger than those in the apparent quantity observed, whether magnitudes or logarithmic diameters, for most of the samples, and appear never to be significantly less than those in the raw data. On the other hand, the dispersions from the $p = 2$ law are quite materially less than those in the apparent quantities, and do not differ appreciably if at all from the dispersions from the optimal value of p .

Similarly, potential effect (b) is not quantitatively visible on separate analysis of the northern and southern hemispheres, galactic or celestial. The results are summarized in Table 11, which is statistically comparable to Tables 4 and 10, all galaxies with $m-z-\theta$ data in the indicated portion of the

TABLE 10
Effect of selection on morphological type

Type	Estimates of p			Dispersions in magnitude				Dispersions in $\log A$			
	$m-z$	$\theta-z$	$m-\theta-z$	σ_m	σ_{M_1}	σ_{M_2}	$\sigma_{M_{m-z}}$	σ_a	σ_{A_1}	σ_{A_2}	$\sigma_{A_{m-z}}$
All (742)	2.04 ± 0.07	1.97 ± 0.08	2.04 ± 0.07	1.33	1.36	0.93	0.93	0.304	0.300	0.231	0.231
Elliptical (163)	2.15 ± 0.18	3.69 ± 0.45	3.27 ± 0.41	1.24	1.33	0.90	0.90	0.184	0.309	0.176	0.155
Spirals (396)	2.01 ± 0.11	1.84 ± 0.10	1.98 ± 0.10	1.29	1.29	0.93	0.93	0.285	0.265	0.209	0.208
Lenticulars (158)	1.94 ± 0.13	2.51 ± 0.23	2.13 ± 0.16	1.21	1.17	0.79	0.79	0.218	0.271	0.170	0.166
Ellipticals + spirals (559)	1.95 ± 0.08	1.80 ± 0.08	1.94 ± 0.08	1.34	1.31	0.94	0.94	0.312	0.286	0.232	0.231

sky being included in the sample. Averaging over the four possibilities yields $p = 2.06 \pm 0.12$. Again, scrutiny of the resulting dispersions in magnitude and logarithmic diameter unequivocally reinforces the phenomenological indications that $p \sim 2$. As earlier, dispersions of deviations from the $p = 1$ law are generally larger than those in the apparent quantities, and are in

TABLE 11
Effect of selection by region of sky

Portion of sky	Estimates of p			Dispersions in magnitude				Dispersions in $\log A$			
	$m-z$	$\theta-z$	$m-\theta-z$	σ_m	σ_{M_1}	σ_{M_2}	$\sigma_{M_{m-z}}$	σ_a	σ_{A_1}	σ_{A_2}	$\sigma_{A_{m-z}}$
Whole sky (742)	2.04 ± 0.07	1.97 ± 0.08	2.04 ± 0.07	1.33	1.36	0.93	0.93	0.304	0.300	0.231	0.231
North celestial (525)	2.08 ± 0.09	2.13 ± 0.11	2.09 ± 0.09	1.30	1.35	0.90	0.90	0.290	0.306	0.226	0.226
North galactic (480)	2.19 ± 0.11	2.15 ± 0.14	2.19 ± 0.11	1.19	1.29	0.89	0.89	0.278	0.292	0.227	0.227
South celestial (217)	2.04 ± 0.14	1.67 ± 0.12	2.03 ± 0.14	1.34	1.36	0.94	0.94	0.333	0.285	0.243	0.240
South galactic (262)	1.90 ± 0.10	1.80 ± 0.10	1.89 ± 0.10	1.53	1.44	0.99	0.99	0.342	0.308	0.238	0.237

hardly any cases materially less than the latter. On the other hand, those from the $p = 2$ law are again quite materially less than those in the apparent quantities, and as earlier, in all cases less than those from the $p = 1$ law. Indeed, the raw comparison of dispersions of the residuals from the respective laws tends actually to overestimate the quality of the fit of the linear law, since for any theory of the form $m = f(z) + M$, $\sigma_m^2 = \sigma_f^2 + \sigma_M^2$, i.e., $\sigma_M^2 = \sigma_m^2 - \sigma_f^2$, the anticipated reduction in variance of the apparent magnitudes is thus σ_f^2 , which is four times greater for the $p = 1$ law than for the $p = 2$ law.

Selection on both morphology and field of observation leads to further reduction in sample size, beyond which statistical investigation would appear likely to be moot. The results of this consequently virtually definitive refinement in sample selection, shown in Table 12, strikingly confirm the earlier conclusions. The average value of p for the three morphological types—elliptical, spiral, and lenticular—in the four indicated hemispheres of the sky, and as derived from the $m-z$ relation, is 2.07 ± 0.24 . In all cases the estimate is well within two standard deviations of the value $p = 2$. In the majority of cases, the dispersion in magnitude from the $p = 1$ line exceeds that in apparent magnitude and in no cases is it materially less, while in all cases the dispersion from the $p = 2$ line is considerably less than that in the apparent magnitudes, and within one percent of the minimal dispersion obtainable by a least-squares fit. The situation is generally quite similar for the $\theta-z$ and $m-\theta-z$ relations, except that the standard errors of estimate are greater and the results are consequently not quite as striking, although in precisely the same direction.

Due to the relatively small sample sizes, it would be inappropriate to make statistical analyses based on the postulate of radial spatial homogeneity, as is the V/V_m test described earlier, until a theoretical statistical procedure is available to deal with large local clusters such as Virgo and Fornax. These inevitably bias the spatial distribution of sufficiently small samples, and it would be improper, or at least statistically moot, simply to delete a priori local clusters designated in other than a functorial statistical fashion, i.e., by an objective procedure devoid of preconceived hypotheses as to the form of putative clusters.

On the other hand, the phenomenological viewpoint is primarily that of model-building, which is logically quite distinct from that of hypothesis testing. The lack of indication for the law $p = 1$ in the $m-z-\theta$ relation for low-redshift galaxies does not in itself imply that this law is statistically definitely unacceptable, for the degree of apparent magnitude truncation is considerable on the hypothesis that $p = 1$. However, the de Vaucouleurs data give a variety of further indications for the $p = 2$ law and counterindications for the $p = 1$ law.

TABLE 12

Effect of joint selection on morphological type and region of sky^a

North celestial	North galactic	South celestial	South galactic
Ellipticals			
$2.17 \pm 0.20/3.59 \pm 0.48/3.23 \pm 0.47$ 1.38/1.51/0.95/0.95 0.204/0.354/0.191/0.164 (103)	$2.32 \pm 0.31/3.92 \pm 0.81/3.17 \pm 0.58$ 1.18/1.34/0.94/0.93 0.194/0.306/0.192/0.174 (94)	$2.84 \pm 0.76/5.07 \pm 2.34/3.84 \pm 1.38$ 0.78/0.94/0.71/0.70 0.141/0.205/0.148/0.136 (60)	$2.07 \pm 0.22/3.85 \pm 0.56/4.47 \pm 0.99$ 1.24/1.29/0.83/0.83 0.156/0.307/0.151/0.120 (69)
Spirals			
$2.20 \pm 0.15/2.06 \pm 0.15/2.21 \pm 0.15$ 1.18/1.30/0.89/0.88 0.269/0.275/0.210/0.210 (290)	$2.19 \pm 0.16/2.11 \pm 0.17/2.18 \pm 0.16$ 1.15/1.24/0.88/0.88 0.253/0.263/0.201/0.201 (271)	$1.73 \pm 0.14/1.53 \pm 0.11/1.63 \pm 0.12$ 1.46/1.24/0.94/0.93 0.316/0.232/0.198/0.189 (106)	$1.79 \pm 0.13/1.57 \pm 0.11/1.73 \pm 0.13$ 1.54/1.36/1.00/0.99 0.343/0.263/0.221/0.214 (125)
Lenticulars			
$2.11 \pm 0.17/2.92 \pm 0.33/2.41 \pm 0.22$ 1.11/1.18/0.72/0.72 0.192/0.277/0.158/0.148 (116)	$2.06 \pm 0.19/2.42 \pm 0.28/2.17 \pm 0.21$ 1.06/1.09/0.72/0.72 0.202/0.242/0.156/0.153 (98)	$1.65 \pm 0.21/1.82 \pm 0.29/1.67 \pm 0.22$ 1.37/1.11/0.89/0.88 0.276/0.253/0.199/0.198 (42)	$1.73 \pm 0.19/2.42 \pm 0.39/1.95 \pm 0.26$ 1.35/1.16/0.89/0.88 0.236/0.279/0.187/0.184 (60)
Ellipticals and spirals			
$2.06 \pm 0.10/2.00 \pm 0.12/2.06 \pm 0.10$ 1.32/1.36/0.93/0.93 0.301/0.302/0.230/0.230 (393)	$2.14 \pm 0.13/2.02 \pm 0.14/2.14 \pm 0.13$ 1.20/1.28/0.91/0.91 0.282/0.284/0.227/0.227 (365)	$1.74 \pm 0.12/1.40 \pm 0.10/1.71 \pm 0.12$ 1.32/1.14/0.88/0.88 0.334/0.245/0.237/0.225 (166)	$1.76 \pm 0.10/1.61 \pm 0.10/1.74 \pm 0.10$ 1.56/1.34/0.97/0.96 0.357/0.286/0.241/0.235 (194)

^a Within each classification: top line: maximum likelihood estimates together with corresponding dispersions, for the $m-z$, $\theta-z$, and $m-\theta-z$ relations in order, for the indicated subsample of the basic sample of 742 galaxies with requisite data; middle line: dispersions in apparent magnitude, and in absolute magnitude for $p = 1$, $p = 2$, and $p = \text{maximum-likelihood estimate}$, respectively; bottom line: the same for the logarithmic diameters. The number in parentheses is the sample size.

First, as is expected for a correct law, there is no significant trend with z in the absolute magnitudes based on the $p = 2$ law, while there is a pronounced trend for those based on the $p = 1$ law (cf. Figure 1). Second, the $m-z$ relations of the galaxies in fixed redshift ranges, whether selected on brightness in bins containing fixed number of galaxies, or formed into a sample in their totality, are in very good agreement with the $p = 2$ law, but on the whole are no closer to the $p = 1$ law than they are to constancy. Representative results of this nature are given in Table 13, for all galaxies in

TABLE 13

Dispersions and mean magnitudes of bright low-redshift galaxies over assorted redshift ranges

Number of galaxies	Range in cz	σ_m	σ_{M_1}	σ_{M_2}	Mean m	Mean M_1	Mean M_2
NA	500–1100	0.99	1.00	0.97	11.57	24.44	18.01
251	500–1500	0.95	0.98	0.91	11.76	24.18	17.98
384	500–2000	0.90	0.98	0.85	11.91	23.89	17.91
159	600–1200	0.92	0.93	0.90	11.67	24.27	17.97
257	600–1600	0.93	0.96	0.90	11.82	24.06	17.95
368	600–2000	0.88	0.94	0.84	11.95	23.86	17.91

fixed redshift ranges, and Table 14, for relatively bright galaxies in bins. It is interesting to note that the spread in mean magnitude over different redshift ranges, for the same type of object, is much less for the $p = 2$ law than for the $p = 1$ law, the latter spread being on the whole no less than that in the apparent magnitudes. Thus in Table 13, the spread is 0.10 for the $p = 2$ absolute magnitudes, 0.38 for the apparent magnitudes, and 0.58 for the $p = 1$ absolute magnitudes. Similarly, for the fourth brightest galaxies in bins containing 10 galaxies each, these spreads are respectively 0.11, 0.61, and 0.50, over the redshift ranges considered in Table 14. Again, for the tenth brightest galaxies in bins containing 20 galaxies each, the ranges are 0.03, 0.33, and 0.34. The narrow spread of the $p = 2$ absolute magnitudes, and the generally undiminished spread of the $p = 1$ absolute magnitudes relative to that in the apparent magnitudes, is what would be expected on the $p = 2$ hypothesis, but is surprising on the $p = 1$ hypothesis. In particular, it is difficult to see how observational apparent magnitude truncation, admittedly a priori a conceivably significant factor, could result in such close agreement with the $p = 2$ law for such a variety of redshift ranges, bin sizes, and choices of relative galaxy brightness within each bin, if in fact p were equal to 1.

In any event, on the $p = 1$ hypothesis, any catalog complete out to a

TABLE 14
Dispersions and mean magnitudes of ranked galaxies in bins^a

Sample criterion	Number of galaxies	Range in cz	σ_m	σ_{M_1}	σ_{M_2}	Mean approximate magnitude	Mean M_1	Mean M_2
First brightest, in groups of 10	50	500–3000	0.70	0.62	0.46	10.81	22.45	16.64
Second brightest, in groups of 10	50	500–3000	0.68	0.54	0.39	11.28	22.91	17.10
Third brightest, in groups of 10	50	500–3000	0.63	0.55	0.37	11.57	23.21	17.40
Fourth brightest, in groups of 10	38	500–2000	0.50	0.49	0.30	11.61	23.61	17.61
Fourth brightest, in groups of 10	50	500–3000	0.55	0.56	0.29	11.78	23.42	17.61
Fourth brightest, in groups of 10	61	500–5000	0.74	0.61	0.29	12.04	23.26	17.66
Fourth brightest, in groups of 10	67	500– ∞	0.93	0.63	0.34	12.22	23.19	17.72
Fifth brightest, in groups of 10	50	500–3000	0.49	0.62	0.30	11.98	23.61	17.80
Tenth brightest, in groups of 20	20	500–2000	0.39	0.55	0.25	11.92	23.88	17.91
Tenth brightest in groups of 20	25	500–3000	0.43	0.61	0.24	12.05	23.70	17.88
Tenth brightest, in groups of 20	30	500–5000	0.61	0.67	0.24	12.25	23.54	17.90
Brightest of 11 at middle redshift of group of 11 ^b	33	500–2000	0.63	0.54	0.44	10.62	22.60	16.61

^a The term “rth brightest object in groups of s” refers to the procedure of arranging the source data in order of redshift, followed by subdivision into disjoint groups of size s (proceeding in the same order), followed finally by selection of the rth brightest object from each group.

^b Again arranging objects in order of increasing redshift, those groups of 11 successive objects whose middle object is as bright as any in the group were picked out, and the sample formed from their middle objects.

limiting apparent magnitude \bar{m}_{app} yields a fair sample in the range $z_1 < z < z_2$ if all objects intrinsically fainter than $\bar{M}_{p=1} = \bar{m}_{app} - 5 \log z_2$ are deleted. The absolute magnitudes $M_{p=1}$ for the resulting subsample should then exhibit a significant trend with z only if there is a corresponding luminosity evolution. The trend may be appropriately tested by comparing the mean of the subsample in the range $z_1 < z < z_3$ with that of the subsample in the range $z_3 < z < z_2$ by a t -test, z_3 being chosen so that the two subsamples have approximately the same size. (This test is “robust” for

fairly large samples, meaning that no assumption of normality of the luminosity function is involved.) In fact, with the data of the de Vaucouleurs (1964), and the values $cz_1 = 500$ and $cz_2 = 2000$, and \bar{m} in the range $12.5 \leq \bar{m} \leq 13$, the normal test statistic t is ~ 2.8 , corresponding to a probability ~ 0.0025 , indicative of a rapidity of evolution for nearby galaxies quite beyond normal expansion-theoretic conceptions. On the chronometric hypothesis, the corresponding t -value is 0.99, as is quite consistent with z -independence of the mean luminosity of bright galaxies. Additionally, if there is serious selection on luminosity for $cz \lesssim 2000$ in the de Vaucouleurs catalog, the population of deviations from mean magnitude of the subsample of galaxies in the vicinity of a fixed redshift should be noticeably redshift-dependent. A Smirnov two-sample test of these local model-independent luminosity functions in the vicinity of the redshifts $cz = 500$, 1000, 1500, 2000, and 2500, based on the groups of 20 galaxies nearest each redshift, reveals no significant differences between the distributions at the 5% level.

Continuing with the model-building discussion, a conceivable explanation for the phenomenological quadratic redshift-distance law within the expansion framework is the local superclustering proposed by G. de Vaucouleurs (1972). On the other hand, local superclustering would appear to involve significant radial spatial inhomogeneity. This is not at all confirmed by the Kolmogorov-Smirnov V/V_m test.

There is some evidence that the square redshift-distance law may persist at higher redshifts. The anomaly in the range $14 \leq m \leq 15$ reported by Rubin *et al.* (1973) is reduced from the significant level of five standard deviations to the insignificant one of two standard deviations if the linear law is replaced by a square one. The galaxies studied by Arakelyan *et al.* (1972) and described earlier are largely at higher redshifts and involve no known selection effects relatively favorable to a square law. However, the latter law decreases the dispersion in apparent magnitude, while the linear law increases it. The compilation of published redshifts of clusters of galaxies by Noonan (1973) exhibits a roughly linear $\log N$ - $\log z$ relation for the 56 clusters in the range $z < 0.04$, of slope 1.46, which deviates only marginally from the square-law slope of 1.5 but considerably from the linear law slope of 3. The strong linearity shown by the Sandage sample of brightest cluster galaxies is, for reasons of small sample size, material model-dependence of the appropriate apertures of measurement for very large galaxies and unpublished selection criteria, not entirely conclusive as regards galaxies as a whole. In any event, the mean slope of ~ 1 for the (rather irregular) $\log N$ - $\log z$ relation of the subsample in the range $z < 0.04$ is in better agreement with the square than with the linear law; and the former law does effect a significant ($\sim 50\%$) reduction in the dispersion of apparent mag-

nitudes, in contrast with the absence of any reduction typically shown by the latter law for samples of other objects. It is interesting also that the $N(<z)$ relation of the Sandage sample, although highly irregular, varies roughly linearly with z rather than as $z^{3/2}$ for small redshifts, and even in the redshift interval $z < 0.04$ deviates considerably from the $N(<z)$ relation of the Noonan list of all galaxy clusters with published redshifts. Further analysis of the Sandage samples is given in the next section.

In summary, the data given on the de Vaucouleurs tape indicate that the hypothesis that $p = 1$ may be acceptable, with substantial emendations in the nature of superclustering, extreme breadth of the luminosity function, and the like. However, it is not phenomenologically indicated by the observations on low-redshift galaxies, which suggest rather the hypothesis that $p = 2$. This hypothesis leads to a narrow luminosity function, of breadth < 1 mag, and appears to be acceptable on the basis of all observable relations within the sample thus far examined.

9. The redshift-magnitude relation for Sandage's brightest cluster galaxies

In assessing the implications of this relation, it is necessary to bear the following circumstances in mind:

(a) The brightest cluster galaxy evolved in the work of Hubble, Humason, Mayall, and Sandage, as a means of confirmation and elaboration of the Hubble theory. Its independent status as a "standard candle" has not been established, and there is opposing evidence (cf. Abell, 1972; Peterson, 1970b; Zwicky, 1970).

(b) A sample sometimes cited as one of the main observational bases for the Hubble relation, given as Table 2 by Sandage (1972b), while undoubtedly of outstanding accuracy, appears to be of uncertain statistical uniformity. No objective criterion for a galaxy to be included in the sample has been published, nor indeed is it expressly claimed in the cited source that it is an appropriate sample for testing the redshift-magnitude relation. A superficial examination of the redshifts' ranges and numbers of galaxies indicates so clearly that it is in no sense an approximation to a complete sample out to a fixed limiting apparent magnitude, that a test of this via, e.g., the Schmidt V/V_m test may appear supererogatory. Rather the sample seems suitable for determination of the value of the deceleration parameter, on the basis of the prior hypothesis that a Friedmann model is valid. A sample well suited to this purpose may however be totally inappropriate for a test of this prior hypothesis.

(c) The statistical theory of the apparent uniformity of luminosity of the brightest galaxies in rich clusters, first clearly enunciated by Scott (1957),

remains quite tenable (cf. Peterson, 1970b). If valid, the appropriateness of observations on bright cluster galaxies as a means of validating a theoretical hypothesis is further reduced.

(d) The small dispersion in absolute magnitude from the expansion-theoretic standpoint of the 41 galaxies studied by Sandage (1972b), of the order of 0.3, is in itself not at all a statistical verification of uniformity of their actual physical intrinsic luminosities, in view of the not necessarily random character of the sample involved, as well as neglect of evolutionary corrections. A concrete illustration of the ease with which such small dispersions may be attained by selection is afforded by the case of quasars, which in their totality are well known to fit expansion-theoretic redshift-magnitude curves with large dispersion, of the order of 1.7 mag in the case of the comprehensive list due to DeVeney *et al.* (1971). It is easy to select a subsample of 41 quasars which fit the curve with a dispersion of less than 0.3 mag, as is evident from a plot of the data (cf. below). Needless to write, no serious investigator would consider such a procedure valid; but the result of selection by a sufficiently refined physical criterion, or for a different statistical purpose such as the minimization of the variance of an estimate of a parameter (such as q_0) may be de facto virtually identical with this.

Finally, the Sandage (m, z) pairs cannot be corrected in any clear-cut fashion to obtain the magnitudes that should have been obtained if apertures appropriate to the chronometric theory had been used. In the case of the Peterson data, the precise apertures pertinent to the recorded magnitudes are given; such data are not available for the Sandage pairs. Indeed, the actual procedures employed in obtaining the final magnitudes from the observations are quite complex, and in particular: (a) the procedure employed is galaxy-dependent (in some cases a standard curve was used to correct to a presumed aperture, in others interpolation, etc.); (b) the standard aperture correction curve is presented in a fashion that implicitly assumes a certain relation between metric and isophotal diameters, which arises in the theory of Friedmann models, and is not valid in the chronometric theory; (c) the eye-fits used in processing data are difficult to treat in a statistically controlled fashion within the framework of an alternative theory.

The regrettable conclusion emerges that there is no entirely correct means to utilize the data presented in Table 2 of Sandage (1972b) in a statistically valid test of the chronometric hypothesis. More generally, it is doubtful whether data gathered for the efficient determination of q_0 on the hypothesis that a Friedmann model holds can legitimately and practically serve at the same time to test the latter, or an alternative, cosmological hypothesis. The actual dispersion from the chronometric theory for constant-luminosity objects of the Sandage (m, z) pairs necessarily differs by

very little from the standard deviation of the difference between the theoretical curves

$$(5 \log z) - [2.5 \log z - 2.5 \log(1 + z)]$$

over the range of redshifts represented by the sample. With a *formal* correction for aperture based on the assumption that the correction procedure employed for the Peterson galaxies is somehow de facto valid for the Sandage galaxies, the actual dispersion of the 79 aperture-corrected (m, z) pairs in the redshift range $0.01 < z < 0.21$ from the chronometric curve is 0.74 mag. (In order to obtain a maximally homogeneous subsample it seemed appropriate to exclude five galaxies which are widely separated in redshift from the others in Sandage's total list of 84 brightest cluster galaxies.) The considerably smaller dispersion of 0.30 mag given by Sandage for the dispersion in expansion-theoretic absolute magnitude is explicable in terms of a variety of effects: an underestimate of the aperture correction, the Scott effect, inherent variability in the intrinsic luminosity of brightest cluster galaxies as indicated by Abell (1972), etc. The gross deviation from radial spatial uniformity in the sample is suggestive of a strong selection effect, which is borne out by the following analysis, and which alone is of magnitude quite sufficient to explain a chronometric dispersion of the value reported.

The cited data themselves indicate quite significant differences between the sample galaxies, exhibiting much variability and tending to support the statistical theory of the nature of the brightest cluster galaxy, as opposed to the theory that it is physically distinctive. For 22 of the galaxies, magnitudes are given at two or more apertures; from such data it is possible to estimate the Hubble radius of the galaxy according to the equation

$$m_1 - m_2 = -2.5 \log \left[\frac{\int_0^{r_1} rI(r/a) dr}{\int_0^{r_2} rI(r/a) dr} \right],$$

where m_1 and m_2 are the magnitudes, r_1 and r_2 are the radii at the galaxy corresponding to the given apertures θ_1 and θ_2 , and I is the function earlier defined. The determination of radii r_j from the apertures θ_j together with the redshift z depends on the Hubble parameter H and also on the model. Taking as in Sandage's work $H = 50$ and using the simple Friedmann model with $q_0 = 1$ (the values of a are quite insensitive to the value of q_0) gives a fully specified equation for a which is readily solvable by successive approximations, using the largest and smallest values of the aperture listed by Sandage (1972b). The values of a which are thereby obtained are quite variable, ranging from below 0.05 kpc to above 45 kpc. While these extremes may well result from errors in magnitude observations, a large part of the variation must arise from other sources. The standard deviation of $\log a$

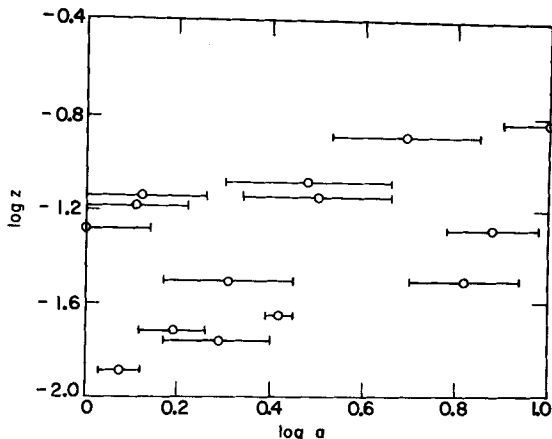


Figure 10 The Hubble core radius-redshift relation for the brightest cluster galaxies with suitable data studied by Sandage (1972b).

The error bars for individual galaxies are small relative to the differences in core radius between the galaxies, indicating nonuniformity in intrinsic size.

is 0.57; if four relatively extreme values of a are deleted, a quite connected group of values is obtained of dispersion 0.28 in $\log a$. The actual (z , $\log a$) pairs are shown in Figure 10. A change in the Hubble parameter would affect all values of a equally, and hence not alter the dispersion in $\log a$. The change in the model from the chronometric to the Hubble one has the effect of multiplying the value of a determined on the basis of the chronometric theory by the ratio of the distances according to the respective models. For the redshift range involved here, this ratio does not differ effectively from $\text{const} \times z^{1/2}$. This factor does not, however, produce a significant reduction in the dispersion in a .

Such dispersion should arise in major part from that in magnitude measurements, although this can be expected to be quite small in view of the accuracy of these measurements as described by Sandage (1972b). However, when the two apertures of measurements θ_{\min} and θ_{\max} are relatively close, the dispersion in magnitude measurement is particularly likely to be reflected in an apparent dispersion in $\log a$. As a final means of estimating a conservative lower bound for $\sigma_{\log a}$, a subsample has been formed consisting of only those galaxies for which $\theta_{\max}/\theta_{\min} > 1.75$, and for which there is unambiguous data. For the resulting sample of seven galaxies, the dispersion in $\log a'$, where a' denotes the Hubble radius as determined on the basis of Hubble-law distances, is 0.18, which in view of the accuracy of the magnitudes can reasonably be attributed primarily to substantial variation in the size of the galaxies.

Such dispersion in $\log a$ therefore indicates considerable variability in an aspect which is strongly correlated with intrinsic luminosity. The relation between angular diameter and absolute luminosity has been treated in a comprehensive and precise study by Holmberg (1969), who finds (p. 326) that $M = -6.00 \log A + \text{const}$, within a dispersion of 0.40 mag. It follows that $\sigma_M \sim 6\sigma_{\log A}$, for any group of, e.g., elliptical galaxies (the constant is slightly type-dependent). Making the plausible assumption that the Hubble radius is sufficiently closely related to the diameter that a similar relation holds with A replaced by a , it follows that the order of magnitude estimate $\sigma_M \sim 6\sigma_{\log a}$ is likely to be valid. For the purpose of estimating the expected sample variance in absolute magnitude, the largest of the quoted standard deviations in $\log a$ may be the most relevant, but again, using the smallest figure, 0.18, for conservatism, it follows that a dispersion of the order of ~ 1.14 mag in absolute magnitude is to be expected for the galaxies in the group in question. This dispersion is of the same order as the actual dispersion of the data from the chronometric curve. There is no published basis for estimating the dispersion in $\log a$ for the entire group of 84 galaxies, but there is no apparent reason to doubt that the group for which data are given are representative at least of the correct order of magnitude. The smallness of the dispersion in expansion-theoretic absolute magnitude reported by Sandage suggests either an implicit selection effect, for which there are other indications, or an extraordinary physical uniqueness for brightest cluster galaxies which exempts them from even rough obedience to Holmberg's law. In the absence of any independent evidence for this exceptional behavior, the order of magnitude of the dispersion from the chronometric curve of the Sandage (m, z) pairs is no greater and indeed less than was to be expected from the dispersion in the Hubble radii a of that subsample for which Sandage has given data sufficient for its estimation.

Since the foregoing was written, Gunn and Oke (1975) have questioned procedures apparently involved in the earlier treatment of bright cluster galaxy samples. These include the attempted deletion of cD (supergiant) galaxies from the sample, despite the difficulty of recognizing them at large redshifts, and the subtraction of the background cluster luminosity, despite the difficulty of isolating that part of the luminosity due to the subject galaxy itself. It is evident that systematic deletion of particularly bright galaxies at larger redshifts would tend to bias the observational redshift-magnitude relation in the direction of increasing slope for the $m - \log z$ relation. It could also affect the distribution of intrinsic diameters of the sample. The ambiguity in the subtraction of the cluster background luminosity would not have this effect, but could simulate it in its impact on the dispersion in $\log a$. It is evident that these considerations only enhance the general conclusions reached regarding the statistical admissi-

bility of the Sandage sample, even if the second one may contribute significantly to the surprisingly large apparent dispersion in the absolute diameters of the sample galaxies. Finally, the difficult problem of a statistically sound definition of "cluster," earlier alluded to, is a further point to consider in assessing the significance of the bright cluster galaxy samples.

More recently, Sandage and Tammann (1975) have treated the $m-z$ relation for ScI galaxies, again primarily for the estimation of q_0 and of intrinsic luminosities. Their reported result that $\partial m/\partial \log z \sim 5$ for these galaxies is obtained by combining two distinct samples, one consisting of classic ScI galaxies, and another of faint galaxies at generally much higher redshifts, whose identification as ScI galaxies is of quite another character and uncertain. The large difference between the average redshifts of the two samples results in an extreme sensitivity of the slope in the $m-z$ relation to a possible substantial difference in average intrinsic luminosity between the two samples.

Indeed, the $m-z$ relation of each of the separate samples is much better fitted by a line of slope 2.5 than one of slope 5. The respective dispersions in (a) apparent magnitude, (b) expansion-theoretic absolute magnitude ($q_0 = 1$), (c) chronometric absolute magnitude, are as follows. For the classic ScI galaxies (all unexceptionable data in Table 6 of Sandage and Tammann (1975), with $cz > 500$, a group of 22 galaxies), (a) 0.80, (b) 0.78, (c) 0.57. For the Sandage-Tammann sample of 60 galaxies among those in the list of 69 galaxies given as their Table 1: (a) 0.66, (b) 0.62, (c) 0.49. For the combined sample of 82 galaxies, the results are: (a) 1.55, (b) 0.67, (c) 0.90. These results imply that for the combined sample, the distribution of expansion-theoretic absolute magnitudes will show a pronounced cyclical trend. Since in addition to a major uncertainty as to the propriety of the classification of the faint galaxies as supergiants, the distribution of redshifts for the overall sample appears strongly nonrandom, the two samples of Sandage and Tammann are hardly consistent with the expansion hypothesis. Indeed, each sample itself deviates by $\gtrsim 4$ standard deviations from expectation, if the sample is assumed fair and the Hubble law is valid, as measured by the normalized reduced variance statistic introduced in Segal (1975). Each sample, however, is separately quite consistent with the chronometric hypothesis within $\lesssim 1$ standard deviation.

To summarize, the data for large or objectively designated galaxy samples are not at all phenomenologically indicative of a nonevolutionary expansion of the universe, but rather of the $m - z - \theta - N$ relations predicted by the chronometric redshift hypothesis. The data for samples that are small or may otherwise be less cogent statistically is generally similar, except for that on brightest cluster galaxies, which appears exceptional and equivocal. Greater definitiveness in the testing of the two hypotheses could probably

best be achieved by additional observations or samples—randomized if necessary in specified fields—that are complete in redshift and out to specified limiting magnitudes. There is no model-independent reason to anticipate that such samples will be relatively more favorable to the expansion hypothesis, and indeed the sample of Colla *et al.* (1975) of this nature, published too recently to be detailed here, appears to be in satisfactory agreement with the chronometric $m - z$ and $N(<z)$ predictions, but poor agreement with the expansion-theoretic ones. In particular, the X -statistics earlier referred to (these are approximately normally distributed with zero mean and unit variance for a fair sample and correct theory), based on the raw data for the fifty-four radio ellipticals in the sample, are, respectively, -2.1 and 4.7 ; for the subsample of forty-four with $z < 0.05$, especially unlikely to be strongly affected by the observational magnitude cutoff, the values are -1.9 and 3.5 . These represent formal probability ratios in favor of the chronometric theory of $>10^5$ and 10^2 , respectively.

10. Preliminary discussion of quasars

It has sometimes been asserted that quasar data have been disappointingly inapplicable to cosmological testing, by virtue of the large dispersion in their characteristics indicated by the data. The actual data, however, do not bear out this negative point of view regarding quasars, to the extent that model-independent analysis is possible. Moreover, from the standpoint of the chronometric hypothesis, their dispersion is quite moderate.

A priori one might expect that quasars would form an intrinsically more homogeneous class than galaxies. The cases in which there is some question as to whether a given object is a quasar are relatively few; the well-known variability in brightness is limited to a small fraction of the quasars, and introduces a dispersion in the magnitude too small to be of any significance in cosmological testing. Further, while relatively few quasars have been found as the result of statistically controlled observation, there are several important samples of this type, and the very heterogeneity of selection and of the telescopes involved in observation of the totality of known quasars should tend to prevent any strong bias from affecting the observations as a whole. Certainly, any selection effect on quasars has been fairly constant in the past six to seven years, for the $m-z-N(z)$ relation based on the ~ 70 quasars for which reliable data were available circa 1966 does not appear to differ appreciably from that based on the ≤ 200 quasars known today.

Actually, quasar data are in quite good agreement with the chronometric hypothesis, on the simplest possible model-independent hypotheses:

(1) spatial and temporal homogeneity (the latter meaning "no evolution," in particular);

(2) the quasars form a single luminosity class apart from a moderate roughly Gaussian random fluctuation. On the other hand, they are consistent with the expansion hypothesis only with the adjunction of model-dependent assumptions: (a) strong temporal evolution and spatial inhomogeneity; (b) a broad luminosity function, involving the existence of relatively large numbers of faint quasars for which there is little direct observational evidence.

Both assumptions (a) and (b) require the use of the observations themselves to determine the many parameters needed to specify fully the assumptions. The predictive power of the expansion hypothesis is thereby quite limited in regard to quasars, and its verification in the indicated sense would be possible with relatively arbitrary data. The recent work of Schmidt (1972a) details from the standpoint of the expansion hypothesis the parameters of the quasar population (cf. also the references to earlier work given there). The testing of the expansion hypothesis which is undertaken here is designed to parallel as closely as possible the tests applied to the chronometric hypothesis, in order to afford a fair and objective comparison, and so differ in format and, in part, in detail and in the quasar samples employed. The qualitative conclusions obtained are in no respect in disagreement with those of Schmidt (1972a), but his work stresses the determination of the quasar parameters on the assumption of the expansion hypothesis, while the present work is concerned rather with the comparison between the expansion hypothesis and the chronometric hypothesis. See also Longair and Scheuer (1967) for an analysis of the quasar $m-z$ relation from a largely expansion-theoretic standpoint.

The major statistically controlled data regarding quasars are the lists by Schmidt (1968) of 3C quasars; that of Lynds and Wills (1972) of 4C quasars; of Braccesi *et al.* (1970) of radio-quiet quasars; and the summary material by Schmidt (1970) regarding radio-quiet quasars. Possibly subject to relevant selection effects, but so much larger in sample size as well as heterogeneous in selection as quite possibly to possess comparable statistical power, is the compilation by De Veny *et al.* (1971) of published data on quasars up to 1971. In addition there are recent lists of radio and radio-quiet quasars due to Sandage (1972c), of unspecified statistical applicability, and older lists such as that given by Burbridge (1967), the latter being of interest in relation to the question of the temporal stability of conclusions drawn from comprehensive heterogeneous lists.

These data have been treated in a systematic but simple statistical fashion. First, the redshift-magnitude relation has been compared with

those predicted by the respective theories, on the assumption that the objects under consideration form essentially a single luminosity class with moderate dispersion. This assumption is confirmed by quantitative analysis, apart from the possibility of "temporal evolution" in the expansion model. In the vicinity of a fixed redshift, the dispersion in quasar apparent visual magnitudes as given by DeVeny *et al.* averages 0.8 mag, for redshifts $z > 0.2$ (for $z < 0.2$ the dispersion is ~ 1.3 if 3C 273 is excluded, the increase possibly being due to a slight degree of selection on luminosity, and/or the difficulty of distinguishing quasars from similar luminous objects, such as Seyfert galaxies). The precise situation as regards the DeVeny list and other quasar samples will be treated later, but an overall view of the situation is provided by Figures 11-13.

Figure 11 gives the standard deviation as a function of redshift for the apparent magnitudes of the quasars in the DeVeny list, at an approximately fixed redshift. Excluding quasars whose magnitudes are qualified as U, E, or

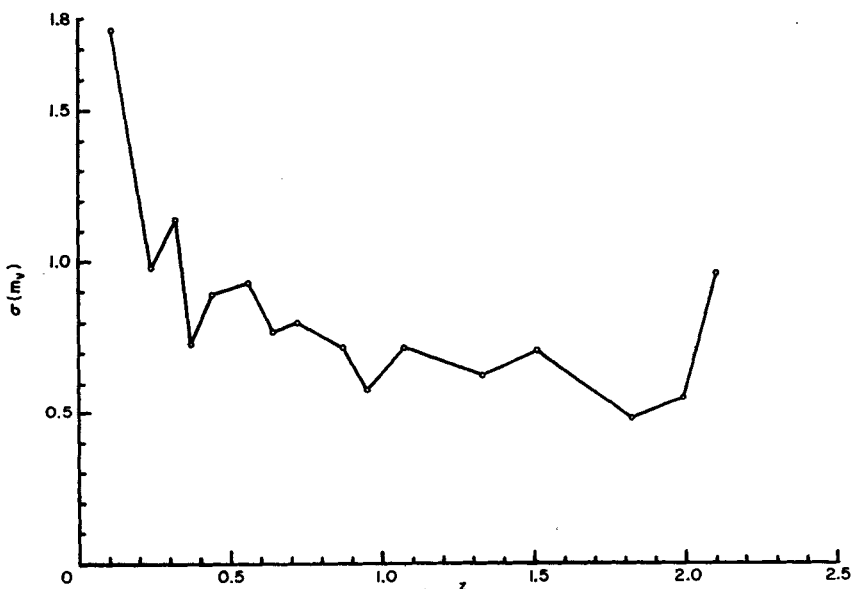


Figure 11 Dispersion $\sigma(m_v)$ in quasar apparent magnitudes as a function of redshift.

All quasars in the list by DeVeny *et al.* (1971) having unqualified data, 158 in all, were divided into 16 groups of 10 quasars (8 in the last) of approximately equal redshift. The dispersion in each group of 10 quasars is plotted against the median redshift of the group (median taken as average of fifth and sixth largest redshifts in the group). For $z > 0.2$, the dispersion is comparable with that for bright galaxies on the same basis, and is not indicative of a material observational cutoff in apparent magnitude.

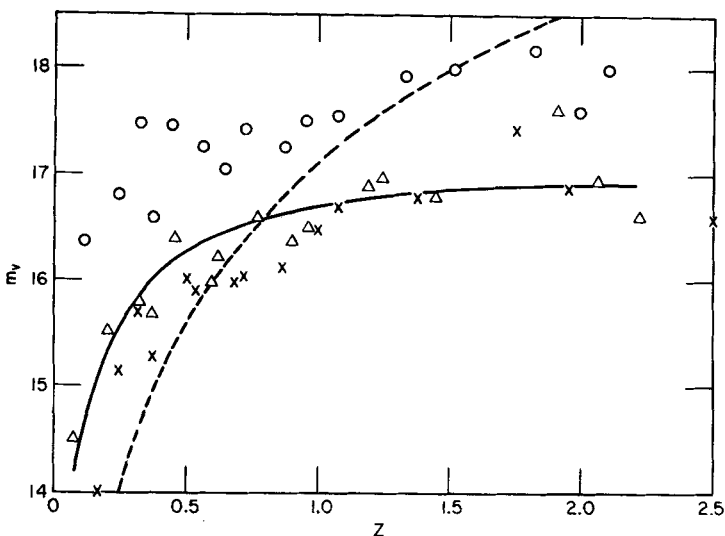


Figure 12 Redshift-magnitude relations for quasars from 16 groups of ~ 10 quasars ordered by redshift.

○, means of each group; △, second brightest quasar in each group; ×, first-brightest quasar in each group. The curves are theoretical constant intrinsic luminosity lines, with constant adjusted from the second-brightest quasar observations, on the following hypotheses: —, chronometric theory, $\sigma = 0.26$; ---, expansion theory ($q_0 = 1$), $\sigma = 1.32$. For the first-brightest and mean quasars in each group, the respective theoretical curves must be correspondingly lowered and raised, and again provide an excellent fit in the case of the chronometric theory and a poor one in the case of the Hubble line.

P in this list, there are 158 quasars having measured redshifts and apparent magnitudes. These were divided into groups of size 10 in order of increasing redshift, the last group comprising eight quasars. The quantity $\sigma(m_i)$ plotted against redshift in Figure 11 is $[n^{-1} \sum (m_i - \bar{m})^2]^{1/2}$, where n is the number of quasars in the group, m_i denotes the apparent magnitude, and \bar{m} the mean of the magnitudes in the group. The quasars in each group have slightly different redshifts, but on either the expansion or the chronometric hypothesis, these differences should contribute entirely marginal amounts to the dispersion of the group. Thus for example the widest redshift range is the last, which is $2.07 \leq z \leq 2.72$; the expansion-theoretical dispersion in apparent magnitude for the quasars in question, assuming they have the same intrinsic luminosity, is 0.19, and is still less on the chronometric hypothesis. The effect on the computed dispersion is likely to be much less; if the theoretical deviations are uncorrelated with the variations in intrinsic luminosity, the effect on the computed dispersion of 0.96 would be to reduce it to 0.94. Thus Figure 11 gives an effectively model-independent indication

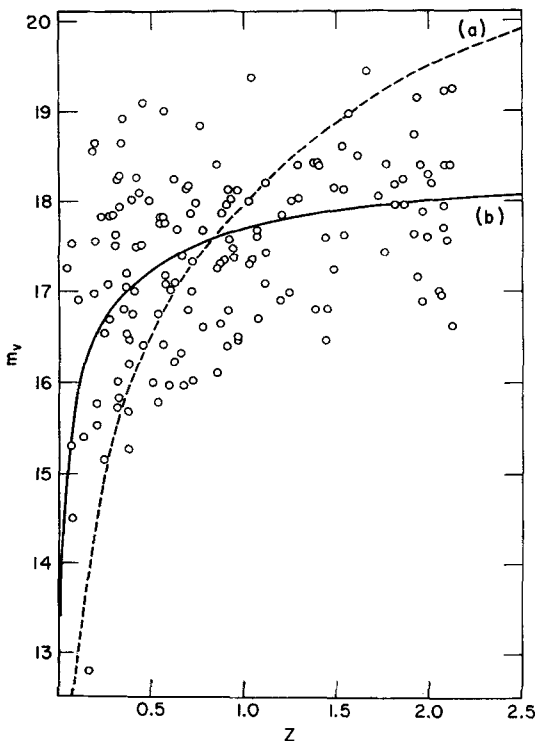


Figure 13 The redshift-magnitude relation for quasars.

○, All quasars with unqualified data in the list of DeVeny *et al.* (1971). Curves are the constant intrinsic luminosity curves for (a) the Friedmann model with $q_0 = 1$ and (b) the chronometric theory, with respective average luminosities fitted to the data. The chronometric curve closely approximates the mean position of the quasars at any given redshift; the Hubble curve is clearly systematically below the data for lower redshifts and above for higher redshifts.

of the observed dispersion in apparent magnitude for quasars at fixed redshift. (It would not be correct for a model in which magnitude varied rapidly with redshift, but any such model would be in gross contradiction with quasar observation, and need not be considered here.)

The lack of any pronounced downward trend in dispersion as a function of redshift, for redshifts > 0.2 , is an indication of the absence of serious selection effects, as regards selection on luminosity. This indication is reinforced by Figure 12, which shows the redshift-magnitude relations for (a) the brightest quasar in each group; (b) the second brightest quasar in each group; (c) the mean quasar in each group (i.e., the mean magnitude plotted at the median redshift, which differs insignificantly from the geometric or

arithmetic mean redshift here). If there were serious selection effects, the differences in magnitude between these respective observational curves would be likely to decrease with increasing redshift. In fact, these differences show no significant trend with redshift.

We shall treat in detail statistically controlled samples as well as the DeVeny list; but in view of the latter's model-independent apparent freedom from serious selection effects, it may reasonably be expected to afford a solid indication of the acceptability of the respective theoretical hypotheses, and/or their relative discrimination. In Figure 12, the best-fitting single-luminosity-class theoretical curves on either hypothesis, for the second-brightest quasar sample, are also plotted. It is evident that the expansion-hypothesis relation has a much greater dispersion from the observations than the chronometric relation; this is actually the case for the other two samples, as well. Figure 13 shows the totality of 158 quasars in the DeVeny list (having unquestioned magnitudes and redshifts), together with the theoretical chronometric and Hubble-theoretic curves of constant intrinsic luminosity, adjusted to the samples. The chronometric line appears virtually an optimal fit for a monotone increasing $m-z$ relation (cf. also below).

The quantitative situation regarding this approach to the redshift-magnitude analysis of the DeVeny quasars is summarized in the following tables. Table 15 lists: (1) the redshift rank of groups of quasars, each having

TABLE 15

Redshift-magnitude observational and theoretical data for quasars in groups ordered by redshift

1	2	3	4	5	6	7	8	9	10	11
1	0.11	16.38	1.76	Mk 205	0.070	14.50	-3.16	0.06	0.158	12.80
2	0.24	16.79	0.98	PKS 2135 - 14	0.200	15.53	-1.91	0.08	0.240	15.15
3	0.32	17.47	1.14	PKS 2251 + 11	0.323	15.82	-1.16	-0.05	0.311	15.72
4	0.37	16.60	0.73	Ton 202	0.366	15.68	-0.75	-0.29	0.371	15.28
5	0.44	17.46	0.89	PHL 658	0.450	16.40	-1.02	0.27	0.501	15.99
6	0.56	17.25	0.93	3C 345	0.594	15.96	0.02	-0.37	0.530	15.78
7	0.64	17.05	0.77	MSH 03 - 19	0.614	16.22	-0.17	-0.13	0.677	15.97
8	0.72	17.43	0.80	3C 175	0.768	16.60	-0.06	0.11	0.720	16.02
9	0.87	17.25	0.72	4C -03.79	0.901	16.38	0.50	-0.21	0.859	16.10
10	0.95	17.49	0.58	3C 94	0.962	16.49	0.54	-0.14	0.980	16.47
11	1.07	17.55	0.72	PKS 1127 - 14	1.187	16.90	0.58	0.16	1.070	16.70
12	1.33	17.92	0.63	BSO 1	1.241	16.98	0.60	0.22	1.375	16.79
13	1.51	17.99	0.91	3C 298	1.439	16.79	1.11	-0.04	1.434	16.46
14	1.82	18.18	0.48	PHL 1222	1.910	17.63	0.89	0.69	1.750	17.43
15	1.99	17.61	0.55	PHL 1305	2.064	16.96	1.72	-0.01	1.955	16.88
16	2.10	18.00	0.96	PHL 8462	2.224	16.63	2.22	-0.37	2.720	16.60

10 members except group 16, having eight; (2) the median redshift of the group; (3) the arithmetic mean of the magnitudes of the group; (4) the standard deviation of these magnitudes about their mean (this is the conventional, and hence biased statistic; the figures should be increased by 5% for an unbiased estimate); (5) a conventional name for the second brightest object in each group; (6) the redshift z of this object; (7) the magnitude m of the object; (8) the Hubble deviation, i.e., the difference $m - 5 \log z + c$, the constant c being chosen so that the average difference vanishes; (9) the chronometric deviation, i.e., the difference

$$m - 2.5 \log z + 2.5 \log(1+z) + c',$$

the constant c' being chosen so that the average of these differences vanishes; (10) the redshift of the brightest object in each group; (11) the magnitude of this object. No essential improvement in the dispersion of the expansion theory would be expected from the use of a Friedmann model in place of the simple Euclidean version; explicit computations were made with the Einstein-de-Sitter model, which actually produced an increase in dispersion. The main conclusion to emerge, that the dispersion of the expansion theory is of the order of 3 or more times greater than that of the chronometric theory, as regards the $m-z$ relation for the indicated model-independent objects, should be unaffected by the use of another Friedmann model with a value of q_0 in the range generally considered realistic.

The actual dispersions are summarized in Table 16. Under "sample" is

TABLE 16
Dispersions and means for redshift-magnitude relations of quasars in groups ordered by redshift

Data	Theory		
	Chronometric	Expansion ^b	Sample
Second brightest in group	$\sigma = 0.26$	$\sigma = 1.32$	$\sigma = 0.71$
Group means	$\sigma = 0.29$	$\sigma = 1.34$	$\bar{m} = 16.34$ $\sigma = 0.49$
First brightest in group	$\sigma = 0.29^a, 0.60$	$\sigma = 1.02^a, 0.99$	$\bar{m} = 17.40$ $\sigma = 0.60^a, 1.01$ $\bar{m} = 16.01$

^a Excluding 3C 273.

^b Expansion theory: Friedmann model, $q_0 = 1$.

given the dispersion in the apparent magnitudes of the objects selected from each group, and also the mean apparent magnitude. There is clearly no qualitative difference between the results of using the second, first, or mean quasar in each group.

11. The N - z relation for quasars

The foregoing analysis has been primarily in the nature of model formation. It does not precisely constitute testing of hypotheses as to the correct model. It indicates that the chronometric hypothesis is quite satisfactory as regards the m - z relation for quasars, but that the expansion hypothesis appears to require emendation to be consistent with this relation. However, it remains to check out both hypotheses on other, statistically more controlled quasar samples; to test both hypotheses against other observational relations; to examine the modifications of these tests when the original hypotheses are augmented by auxiliary ones. In particular, the auxiliary hypotheses of strong temporal evolution in the properties of quasars, and the related one that they form a quite broad rather than roughly single intrinsic luminosity class, have been proposed in connection with the expansion hypothesis, and should be considered.

We continue now with our description of the statistical procedure for tests based on quasars. The next relation considered is that between $N(z) = N(< z)$, the number of quasars at redshifts $< z$, and z . In order to arrive at a definite relation, our earlier assumption to the effect that the objects form a single luminosity class with moderate dispersion must be augmented by an assumption as to their spatial distribution; it will be assumed that this is approximately uniform, i.e., the number of quasars in a given volume of space is generally proportional to the volume. This assumption will again be confirmed by the quantitative analysis of the quasar observations on the chronometric hypothesis, but in any event it is the physically most reasonable and mathematically simplest a priori distribution from which to commence model building or preliminary testing (as in the work of Schmidt, 1968, based on the expansion hypothesis). As a means of obtaining a preliminary overall indication, we again turn to comprehensive, independently compiled data.

As is well known, there are few quasars known of redshift > 2.5 , and it is reasonable to anticipate that selection effects are present at somewhat lower redshift. Thus it would be surprising if the DeVeny quasar list approximated a random sample of quasars out to redshift 2.9, nearly the largest known redshift; but as z decreases, it becomes increasingly likely that those at lower redshifts approximate a random sample out to redshift z . We shall

apply the Kolmogorov-Smirnov test for the comparison of the observed with the theoretical redshift distributions to various redshift intervals of this type. In addition, the redshift intervals (0.5, 1.0) and (1, 2) will be considered, as a check on the possible influence of lower redshifts, where anomalies may arise from classification difficulties. The results are that the chronometric hypothesis is accepted, at notably high levels of probability in most cases, while the expansion hypothesis is rejected in virtually all cases, at conventional significance levels.

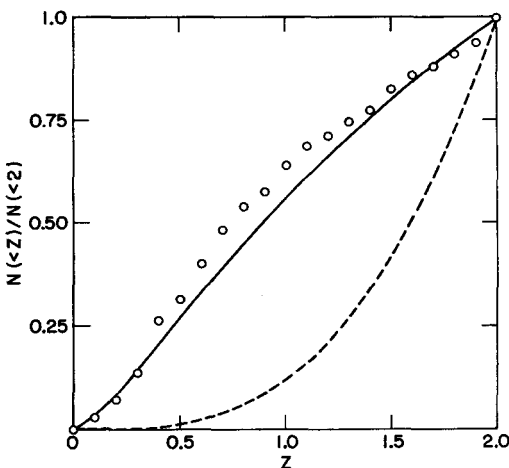


Figure 14 The $N-z$ relation for quasars in the redshift range $0 < z < 2$.

○, cumulative fraction of quasars in the list by DeVeny *et al.* (1971) having unquestioned data, in the cited redshift range (146 quasars in all); —, expected distribution on the chronometric hypothesis; ---, expected distribution on the Hubble theory for a random sample. Theoretical assumptions: spatial and temporal homogeneity. The quite satisfactory agreement of the chronometric prediction with the observations serves to confirm both the chronometric hypothesis and the assumption that the sample is fair. On the expansion hypothesis, this assumption is open to question due to the faintness expected for objects at larger redshift, but Figures 15 and 16 do not reveal any material improvement in the fit of the expansion prediction to the observations when consideration is limited to quasars in restricted redshift ranges.

Figures 14 and 15 show the observed and theoretical fractions of quasars of redshift bounded by a given value z . This form of presentation, as opposed to that of the differential fractions, has the advantage of being readily subject to statistical analysis. The Kolmogorov-Smirnov statistic, which is the maximum of the (absolute values of the) deviations of the observed and theoretical fractions, has a distribution which is independent of the true redshift distribution (this is strictly true only for continuous distributions, but in all events it yields an upper bound on the probabilities,

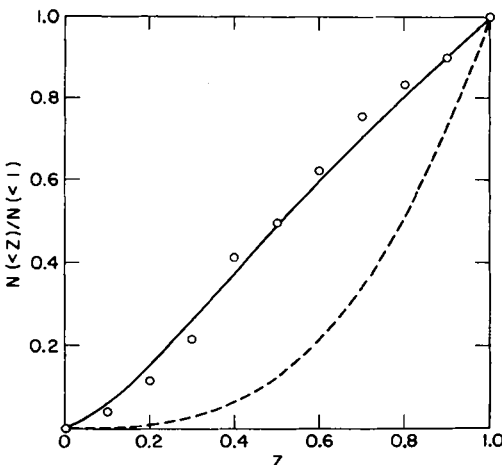


Figure 15 The N - z relation for quasars in the redshift range $0 < z < 1$.

○, cumulative fraction of quasars in the list by DeVeny *et al.* (1971) having unquestioned data (98 quasars in the cited range); —, expected distribution on the chronometric hypothesis; ---, expected distribution on the Hubble theory for a random sample. Theoretical assumptions: spatial and temporal homogeneity. See the comment on Figure 14.

and there is no reason to anticipate a discontinuous distribution in the present case). It is clear visually that the observed distribution is well fitted, in all redshift intervals $(0, a)$, for $a \leq 2$, by the theoretical chronometric distribution, while its deviation from the expansion-theoretical distribution is even greater than that between the two theoretical distributions. The situation is the same when the lower redshifts are excluded as in the intervals $(0.5, 1)$ and $(1, 2)$.

These results do not signalize rejection of the expansion hypothesis as such, but only its conjunction with the auxiliary hypothesis indicated. Spatial uniformity of the distribution may be in question, and in Schmidt (1968) and numerous analyses of quasar distributions technically along different lines from the present one, although related in general idea, the conclusion has been reached that it does not hold, if the expansion-theoretic hypothesis is correct. A fuller comparison with these earlier developments will be given later in connection with the chronometric results for the quasar samples treated by Schmidt *et al.*, but a preliminary indication of the extent to which the general hypothesis of z -dependence of the spatial distribution of quasars (mathematically equivalent to temporal evolution in the Friedmann model framework) may be accepted by the data may be obtained as follows.

Accepting provisionally this hypothesis, it would be anticipated that over relatively small redshift intervals the redshift distribution should conform to a nonevolutionary model. In fact, over very few intervals beginning

at $z = 0$ is this the case; apart from the decrease in sample size involved, which limits the statistical significance of the conclusions, and considering the decrease in z -range, the expansion hypothesis fits about as poorly over the intervals $(0, a)$ for small a as for large values of a . This result might be explained on the basis of local anomalies, in particular the difficulty of discriminating between quasars and Seyfert and N-galaxies, and other large redshift emissionline objects. Virtually all such known galaxies having quasarlike features are at redshifts ≤ 0.3 . The redshift intervals $(0.3, a)$ for values of a somewhat greater than 0.3 should therefore be substantially free from local anomalies and contaminations by nonquasars, and at the same time represent regions of space sufficiently close (on the expansion hypothesis) that selection effects on luminosity should be minimal. These intervals would therefore appear a priori as probably the most favorable ones for showing the approximate spatial uniformity of quasars over small redshift intervals, say ~ 0.2 , on the basis of the expansion hypothesis.

In fact, the exclusion of the initial redshift interval $(0, 0.3)$ does not significantly improve the fit of the expansion-theoretical distribution to the observations, over shorter redshift intervals, as shown by Table 17 for the intervals $(0.3, 0.3 + b)$ for $b = 0.2, 0.3, 0.4$. In all cases, the chronometric curve agrees with the observational line within quite probable random fluctuations, while in most cases the deviation of the expansion curve from the observational line is significant at conservative statistical levels.

TABLE 17
Kolmogoroff-Smirnov tests of the $N(z)$ relation for quasars

Redshift interval	Number in sample	Chronometric D^a	Chronometric probability ^b	Hubble D^*	Hubble probability
0-2.0	146	0.09	0.19	0.42	10^{-22}
0-1.0	98	0.05	~ 1.00	0.38	2×10^{-12}
0-0.5	48	0.10	0.76	0.32	2×10^{-4}
0.5-1.0	50	0.12	0.47	0.29	5×10^{-4}
1.0-2.0	48	0.11	0.36	0.22	0.02
0-0.3	21	0.12	~ 1.00	0.28	0.07
0.3-0.5	27	0.28	0.09	0.35	0.003
0.3-0.6	40	0.16	0.26	0.30	0.002
0.3-0.7	52	0.12	0.45	0.27	0.001

^a D , the Kolmogoroff-Smirnov statistic, is the maximum of absolute value of difference between observed and theoretical cumulative frequency functions.

^b Probability is that of a D as large as that observed. Data from DeVeny *et al.* (1971), and comprise all quasars listed of unquestioned redshift and magnitude.

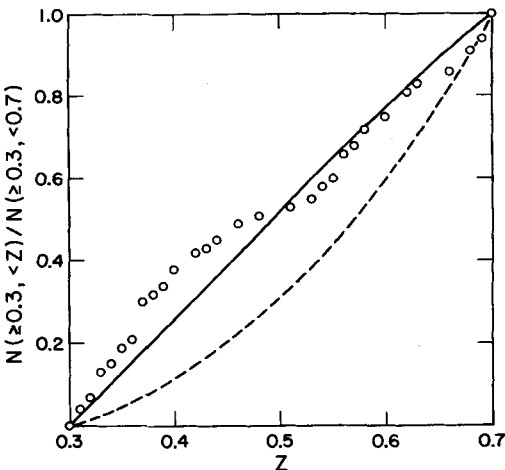


Figure 16 The N - z relation for quasars in the redshift range $0.3 < z < 0.7$.
The basis here is the same as in Figures 14 and 15. Compare the comment on Figure 14.

The entire interval $0.3 < z < 0.7$ is shown in Figure 16. The tentative indication seems virtually inescapable that on the expansion hypothesis, the temporal evolution must be so rapid that even over redshift intervals of the order of 0.2, the expansion cannot be regarded as approximately stationary. This indication naturally recalls the related indication provided by the apparent spatial distribution of the Peterson galaxies described earlier. At the same time, the chronometric hypothesis fits the data remarkably well; even on a correct hypothesis, there might well be some nontrivial interval for the variate in question within which the sample distribution differs significantly from the population distribution, but no such interval of order ≥ 0.1 is apparent for the present observations in relation to the chronometric hypothesis.

Table 17 summarizes the results of Kolmogorov-Smirnov tests in the indicated redshift intervals. In order of magnitude, the probabilities on the expansion hypothesis that the observed deviations could arise by chance seem much smaller than might have been anticipated prior to the present analysis. Those for the chronometric hypothesis are, however, correspondingly remarkably large; it would be improbable for them to be much larger, even granting the validity of the theory. The indication from this latter circumstance is that the DeVeny list is rather more representative out to redshifts ~ 2 than one had any right to expect. The speed and thoroughness of observational quasar work during the past decade has perhaps been underestimated.

12. The apparent magnitude distribution for quasars

There is one final distribution of quasar statistics which is generally taken account of and logical to treat in the present context, that of apparent magnitudes. Ideally, the joint z - $N(<z)$ - $N(<m)$ relation should be considered; however, the present state of the available statistics and also of the statistical art is such that it is unlikely to yield any definite useful information beyond that obtainable from analyses of single variates. We consider here therefore only the $N(<m)$ distribution, and shall neglect secondary effects such as deviation of the spectral index from unity (cf. the earlier treatment of the N - S relation for radio sources), and possible intergalactic absorption.

For a theory with an m - z relation of the form

$$m = f(z) + c,$$

and for a single luminosity class (i.e., fixed c), the apparent magnitude cumulative probability $P(<m)$ can be derived from the form of the function f , together with the distribution of z implied by the underlying geometry. If c itself is statistically distributed, then m becomes the sum of the variates $u = f(z)$ and $v = c$. Assuming that the luminosity function is independent of z , the distribution of m is then the convolution of the respective distribution functions for u and v .

There is no compelling reason to anticipate a normal distribution for the quasar intrinsic luminosities, but the chronometric luminosities are reasonably well approximated by this distribution; cf. Table 18, based on the 158 quasars in the DeVeny list. This is not the case for the expansion-theoretic luminosities, but the well-known law $N(m) \propto 10^{-0.6(m-m)}$ for the distribution of apparent magnitudes below a fixed limiting magnitude is independent of the luminosity function (cf. Longair and Rees, 1972). Since in fact the normal distribution is approximated for computational purposes by a linear combination of delta-functions, and the theoretical $N(m)$ relation is not very

TABLE 18
Distribution of chronometric intrinsic luminosities

Deviation m from mean magnitude	Observed frequency	Normal law frequency, $\sigma = 0.9$ mag
$1.5 < \Delta m$	0.06	0.05
$0.5 < \Delta m \leq 1.5$	0.21	0.24
$-0.5 \leq \Delta m \leq 0.5$	0.43	0.42
$-1.5 \leq \Delta m < -0.5$	0.28	0.24
$\Delta m < -1.5$	0.02	0.05

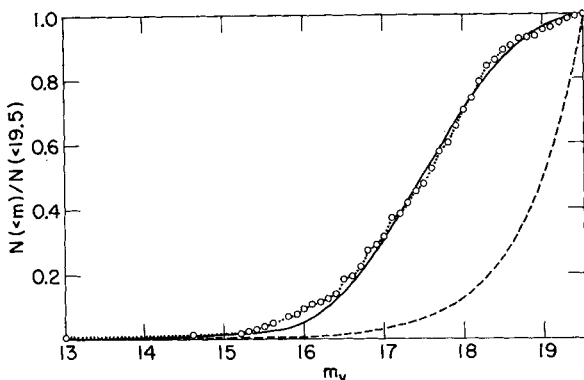


Figure 17 The $N(<m)$ relation for quasars up to a limiting magnitude of 19.5.

○, observational points; —, theoretical line for the chronometric theory, which depends on the observational luminosity function derived from the list of DeVeny *et al.*; ---, theoretical line for the Hubble theory and is independent of the luminosity function. In either case it is postulated that the sample is a random subsample of a complete sample. From an expansion-theoretic standpoint this may be questioned, but the restriction to the fairly conservative limiting magnitude of 18 in Figure 18 still does not bring the expansion prediction into agreement with observation.

sensitive to the precise form of the luminosity function, the use of the normal law in the chronometric case does not differ significantly from the use of the empirical distribution function.

Accordingly, the convolution of the chronometric-theoretical constant luminosity curve with a Gaussian of dispersion 0.9 mag, approximately that found for the DeVeny list, has been computed and is compared in Figures 17 and 18 with the Hubble-theoretical curve and the observational apparent magnitude distribution for the same list, out to prescribed limiting magnitudes. The limiting magnitude of 19.5 in Figure 17 includes virtually all quasars on the list. It is evident that the chronometric curve and the observations are in extremely good agreement. On the other hand, the fit of the expansion-theoretic curve from the observations is quite poor; there is a notable deficiency of faint quasars, from the expansion-theoretic standpoint. In defense of the expansion theory, it might be argued that the sample is not known to be random, and that selection on luminosity might well be an important factor. That this is not very significantly the case is indicated by Figure 18, in which the limiting magnitude is 18, only slightly fainter than the modal quasar magnitude for a variety of samples. On the other hand, while the data clearly supply confirmation of the chronometric hypothesis, in the absence of model-independent methods of estimating selection effects this apparent rejection of the (nonevolutionary) expansion hypothesis should be regarded as tentative. Definitive tests should be sought through the use of statistically controlled data, samples of which are later discussed.

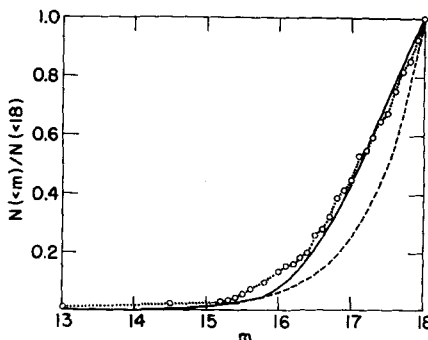


Figure 18 The $N(<m)$ relation for quasars up to a limiting magnitude of 18.
The basis here is the same as in Figure 17. Compare the comment regarding that figure.

13. The redshift-luminosity relation for quasars

In addition to comprehensive lists such as the DeVeny list used earlier, there are the following selective lists: (1) Schmidt (1968), 3C sources; (2) Lynds and Wills (1972), 4C sources; (3) Braccesi *et al.* (1970), optically selected quasars. The Schmidt and Lynds-Wills lists include radio luminosities, and the Braccesi list includes infrared luminosities. The results of testing the $m-z$ relation are indicated in Table 19. It is evident that the chronometric hypothesis is generally much more satisfactory in relation to the cited data. The chronometric dispersions are reassuringly uniform, ranging from $\lesssim 1$ mag for unselected quasars down as brighter quasars are selected. The Schmidt (1968) and Lynds and Wills (1972) lists being primarily radio-selected, it was to be expected that for a correct theory, the dispersions in the apparent radio luminosities should be relatively small, as they are relative to the dispersions in optical magnitudes. The Braccesi list being optically selected, it was similarly to be expected that it would show relatively small dispersions in apparent optical luminosities, as is the case. These appear to be the statistically best controlled data available, and are consistent in yielding dispersions of the order of 0.8 for samples which are complete, but include quasars of fairly low luminosities, in the model-independent sense of luminosity relative to other sample members of approximately equal redshift.

On the other hand, the expansion-theoretic dispersions are quite variable; in all cases higher than the chronometric and sample dispersions, for the most part quite substantially so. In model-independent terms, 3C 273 is exceptional in that it is more than 4 mag brighter than the average of the six quasars having the most similar redshifts (three greater, and three less

TABLE 19
The redshift-magnitude relation for quasar samples

Sample	Sample Size	Dispersions (magnitudes)		
		Chronometric	Hubble	Sample
DeVeny, all objects having unquestioned z and V	158	0.95	1.67	1.02
DeVeny, replacing magnitude by average magnitude of seven quasars of nearest redshift (three above, three below)	152	0.32	1.23	0.52
DeVeny, locally brightest ^a 20% ("local brightness" measured by excess of magnitude above average of those of the six quasars of nearest redshift)	32	0.31	1.08	0.65
DeVeny, locally brightest ^a 10%	16	0.28	1.08	0.54
Schmidt, complete 3C sample	32 ^a	0.80 ^a	1.12 ^a	0.88 ^a
	33	0.97	1.12	1.16
Lynds-Wills, complete 4C sample	30	0.89	1.32	0.99
Braccesi, all with unquestioned redshifts	27	0.79	2.28	0.58
Schmidt, complete 3C sample, radio magnitudes ^b	32 ^a	0.72 ^a	1.27 ^a	0.67 ^a
	33	0.73	1.27	0.75
Lynds-Wills, complete 4C sample, radio magnitudes ^b	30	0.80	1.54	0.72
Braccesi, infrared magnitudes	27	0.88	2.32	0.64

^a Excluding 3C 273.

^b Reported values as corrected were converted to the Pogson scale.

than that of 3C 273; cf. below); for no other quasar is this difference as much as 2 mag. Consequently, it may be excluded on a rational statistical basis, and it seems more illuminating to do so. The overall indication from Table 19 is that the chronometric theory generally provides a distinctly and uniformly better fit.

Equally statistically significant with the comparison between the dispersions of the respective theories is the comparison between their dispersions and that from the sample mean. In all cases except the complete samples, the

deviations from the chronometric theory have a lesser dispersion than those from the sample mean, as would be expected from a correct theory. In the event of a large dispersion in intrinsic luminosity, chance fluctuations could produce a slightly larger dispersion from a correct theory than from the sample mean, particularly when there is strong selection on apparent luminosity, as in the case of a complete sample, but it is extremely unlikely to produce a substantially larger dispersion. This applies to the much greater dispersion from the expansion theory than from the sample mean, in all cases except that of the Schmidt sample. This dispersion from the Hubble line is too large to be consistent at any acceptable probability level with a small dispersion in the intrinsic luminosities. On the other hand, if the latter dispersion is large, the relatively small dispersion of the magnitudes from the constant sample mean is then extremely improbable, in view of the considerable variation in $5 \log z$ over the redshift range in question.

The conclusion seems inescapable that these data are in conflict with the expansion hypothesis, unless it be assumed that the intrinsic luminosities do not form a z -independent population. The need for this assumption, which from the standpoint of the expansion-theoretic hypothesis is naturally regarded as luminosity evolution, seems not seriously disputed by proponents of the expansion hypothesis, and need not be belabored here. It seems necessary to stress, however, that the assumption virtually eliminates the predictive power of the expansion theory as regards the luminosities of large-redshift objects. No such assumption is required for the chronometric hypothesis, which has quite significant predictive power. For example, the expansion hypothesis carries no implication regarding the probable magnitude of quasars which may be observed at redshifts ~ 3.5 , which is essentially different in principle from that obtainable by simple extrapolation of the empirical $m-z$ relation. According to the chronometric hypothesis in totally uncorrected form (with $\alpha = 1$), $m = 2.5 \log z - 2.5 \log(1+z) + c$, then fitting the mean intrinsic luminosity index c to the DeVeny data, $c \sim 18.4$, yields the results $m \sim 18.1$. Interestingly, the quasar OH 471 reported by Carswell and Strittmatter (1973) of redshift 3.4 and the quasar OQ 172 reported by Wampler *et al.* (1973) of redshift 3.5 are approximately of this apparent magnitude, although their intrinsic luminosities are quite unprecedented from the expansion-theoretic standpoint, and would further exacerbate the problem of the quasar energy mechanism in this theory.

As a final aspect of the quasar $m-z$ relation, we shall essay a test of the hypothesis that the *bright* quasars follow the chronometric and/or the expansion-theoretic law, employing an entirely model-independent definition of "bright," which also avoids the necessity for grouping quasars as has done earlier. This at the same time affords a model-independent estimate of the quasar dispersion in intrinsic luminosity. We shall define

"bright" as bright relative to quasars at approximately equal redshift; more specifically, for any quasar we shall define the "excess brightness" Δm as the excess of the average magnitude of the six quasars obtained by selecting from the DeVeny list the three of nearest larger redshift and the three of nearest smaller redshift, over the magnitude of the quasar in question. We shall then consider the redshift-magnitude relation for the 10 and 20% of the sample for which this relative brightness is greatest. As earlier noted, the quasar 3C 273 is clearly exceptional in its relation to the distribution of excess brightnesses, having $\Delta m > 4$, while for all other quasars $\Delta m < 2$; accordingly, it will be excluded from these samples, which will be called for brevity the brightest tenth and fifth.

The results are included in Table 19 and shown in part in Figure 19. The brightest tenth of the DeVeny list has a chronometric dispersion of 0.28 mag, entirely without correction, less than that of the best samples of bright cluster galaxies. The dispersion of the same quasars from the Hubble

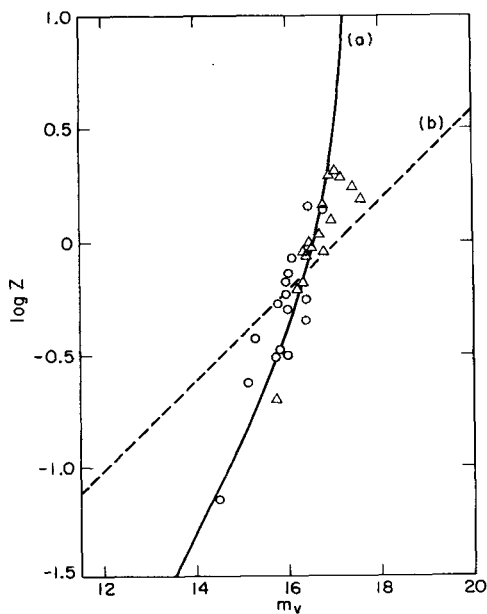


Figure 19 The redshift-magnitude relation for the locally brightest fifth of the quasars in the list of DeVeny et al.

O, quasars in the locally brightest tenth; Δ , quasars in the second-brightest tenth. Curves are best-fitting theoretical constant-intrinsic-luminosity curves for: (a) chronometric theory; (b) Hubble theory. As is representative for brighter quasars, selected in any fashion not making explicit use of a particular model, the dispersion from the Hubble line is more than three times that from the chronometric curve.

line is, however, 1.08 mag, i.e., even these bright quasars bear virtually no significant relation to the Hubble line. For the brightest fifth, consisting of 32 quasars, the dispersions are respectively 0.31 and 1.08 mag. (It should be noted that the sample dispersion is 0.65, less than that from the Hubble line.) These dispersions are fully comparable with those obtained for most samples of bright cluster galaxies after correction for color and galactic absorption. This suggests that the relatively bright quasars form a "standard candle" at least to the same extent as brightest cluster galaxies may do so; the standardization is further augmentable by selection on radio spectral indices, as proposed by Setti and Woltjer (1973) (cf. below).

It should perhaps be noted that work of Bahcall and Hills (1973), which appeared after this manuscript was largely complete, is directed toward establishing that the "brightest" quasars follow the Hubble law. The definition of "brightest" is in part model-dependent, and only seven quasars are included in the final sample found to have a dispersion of 0.3 from the Hubble line. This dispersion is no less than that from the chronometric prediction of the present model-independent samples of size 16 and 32.

Finally, we mention that various quasar samples of undesignated selection criteria show the same $m-z$ relation behavior as the ones just discussed. The largest such list, apart from the DeVeney list, is that of Sandage (1972c). The chronometric dispersion is markedly less than the Hubble line dispersion for the complete Sandage list, the subsample of 15 radio-quiet quasars, and also for radio luminosities. The analysis of the latter involves transformation of the model-dependent data listed by Sandage back to their presumed empirical form; this has been carried out by J. F. Nicoll. Nicoll's results also show that the evident trend in the Hubble absolute radio luminosity with z , remarked by Sandage and ascribed by him to selection, is entirely accounted for by the chronometric theory; see also Section 17.

14. The redshift-number relation for quasar subsamples

We next examine the quasar samples treated in the last section from the standpoint of the theoretical versus observed $N(<z)$ function. The observed and theoretical fractions, obtained by dividing respectively by the total number of quasars in the sample, or by the total volume of space out to the maximum redshift in the sample, are given in Figures 20–23. It is clear at a glance that the chronometric curve fits on the whole very well, but that the expansion-theoretic curve is in gross disagreement. This impression is fully confirmed by Kolmogorov-Smirnov tests, as indicated in Table 20. The indications given by the DeVeney heterogeneous list are fully supported by the more homogeneous samples.

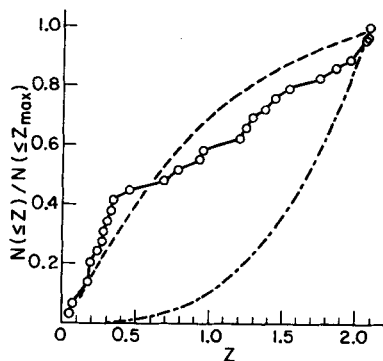


Figure 20 The N - z relation for the quasar sample of Braccesi et al. (1970).

Theoretical lines, assuming spatial and temporal homogeneity and approximate randomness of sample, are: —, chronometric theory; ---, Hubble theory. Of the samples of quasars treated here, this sample of relatively faint quasars probably involves the maximal selection on luminosity and spectrum. Nevertheless it is in satisfactory statistical agreement with the chronometric prediction on the basis of a Kolmogorov-Smirnov test.

As earlier, it might be argued that due to luminosity selection, these samples are not adequately random, and that this circumstance is the origin of the apparent gross deviation from the expansion theory. However, in this event the agreement between observation and theory should improve substantially if the sample is cut off at a lower redshift. Such a cutoff diminishes the sample size and thereby the significance level of any given deviation, but it can otherwise not produce satisfactory agreement between the observed

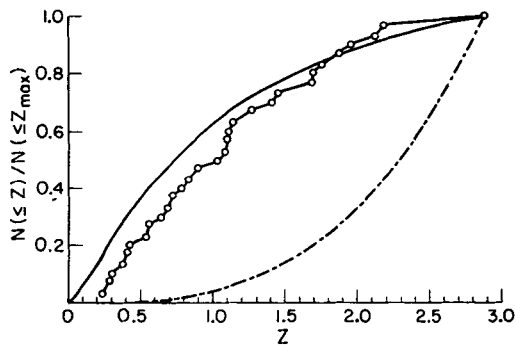


Figure 21 The same as Figure 20 for the complete sample of 4C quasars given by Lynds and Wills (1972).

○, individual quasar. The noticeable but not statistically significant apparent deficiency in the number of quasars at lower redshifts in this and the next sample may plausibly arise from the exclusion of quasarlike galaxies (notable Seyferts and N) which are found at these redshifts.

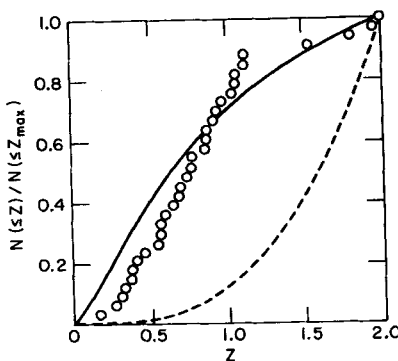


Figure 22 The same as Figure 21 for the complete sample of 3C quasars given by Schmidt (1968).

Compare the comment on Figure 21. Again the chronometric prediction for a random sample is in satisfactory statistical agreement with the observations.

$N(< z)$ and expansion-theoretic curves. For it is apparent that the slope of the observational curve is generally decreasing, in all cases, while the slope of the expansion-theoretic curve is materially increasing, at all redshifts. Adjustment by the scale factor involved in a cutoff at a lower redshift cannot change the sign of the second derivative of the $N(< z)$ curve, and so cannot eliminate this fundamental difference between the observations and the expansion theory.

In order to limit as much as possible extraneous sources of dispersion, to which deviations from the Hubble theory could conceivably be ascribed, two further tests were made. First, the samples were considered over a shorter redshift interval, $0.2 < z < 1$, in which one might anticipate some evolution, but much less than for the full redshift intervals of the samples. The deletion of the redshift range $z > 1$ should serve to diminish greatly any selection on luminosity which might be present in the samples. The deletion of the range $z < 0.2$ should serve to eliminate local anomalies. Nevertheless,

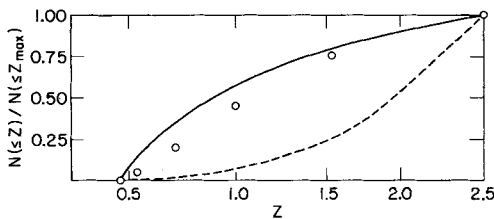


Figure 23 The same as Figure 21, for the Schmidt adopted distribution (1972a) of optical quasars of approximate magnitude 18.

Note: The plotted points represent summary data (observations on individual quasars not reported).

TABLE 20
Kolmogoroff-Smirnov test of the $N(z)$ relation for complete quasar samples

Sample	Number in sample	Chronometric D	Chronometric probability	Hubble D	Hubble probability
Schmidt 3C (1968)	33	0.19	0.16	0.58	$< 10^{-11}$
Schmidt optically selected ^a (1970)	19	0.24	0.21	0.49	$< 3 \times 10^{-4}$
Braccesi (1970)	27	0.22	0.14	0.58	$< 10^{-8}$
Lynds-Wills 4C (1972)	30	0.19	0.23	0.61	$< 10^{-9}$
Schmidt adopted redshift distribution of quasars of approximate magnitude 18 ^a (1972a)	number <i>N</i> not given	0.14	> 0.05 if <i>N</i> < 90	0.50	$< 10^{-4}$ if <i>N</i> > 20

^a Individual quasars were not listed, but only subtotals in specified redshift intervals. The D statistic used is the maximum over those z values for which data were given; and is therefore probably a slight underestimate of the true value.

as shown by Figure 24, the Hubble curve remains in gross disagreement with the observations, while the chronometric line fits very well, considering the limited sample sizes. The quantitative probabilities based on Kolmogorov-Smirnov tests are given in Table 21, in which, in addition, the DeVeney sample considered earlier and a sample of unspecified selection but substantial size given by Sandage (1972c) are included.

Second, the DeVeney sample was taken over the restricted redshift interval $0.25 \leq z < 2.25$ as a means of removing local effects and minimizing possible confusions between quasars, N-galaxies, and Seyfert galaxies at the lower end, and of avoiding the apparently anomalous cutoff at the other end, which may reflect changes in the spectral functions of quasars at higher frequencies, or other relevant but largely unexplored effects. The results shown in Figure 25 are again in excellent agreement with the chronometric theory and in gross disagreement with the Hubble theory. Results for the Sandage sample over the complete redshift range of the sample are shown in Figure 26, and show agreement similar to that of the results in Figure 25. All available evidence, including the list of Burbridge and Burbridge (1969), indicates that all reasonably comprehensive or complete samples are likely to show the same behavior as the samples earlier treated (cf. Figure 33).

A still more conclusive acceptance of the chronometric and rejection of the expansion hypotheses (both on a nonevolutionary basis and the assumption of approximately uniform spatial distributions for quasars) can be obtained from the Schmidt V/V_m test, treated next.

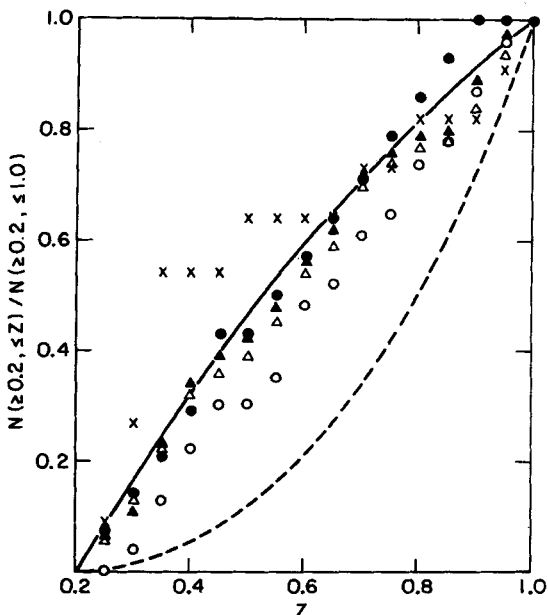


Figure 24 The N - z relation in the redshift range $0.2 < z < 1$ for quasar samples.

(a) \circ , Schmidt 3C sample; (b) \bullet , Lynds-Wills 4C sample; (c) \blacktriangle , DeVeny list; (d) \triangle , Sandage (1972b); (e) \times , Braccesi list. Otherwise on the same basis as Figures 20 and 21. The elimination of redshifts > 1 and the avoidance of possible local irregularities and classification difficulties by eliminating the region $z < 0.2$ do not materially improve the agreement of the expansion prediction with the observations. However, the chronometric prediction is in satisfactory agreement with the observations for all of the samples.

TABLE 21
The N - z relation for quasars in the range $0.2 < z < 1$ for diverse samples

Probability of observed maximum deviation as given by Kolmogoroff-Smirnov test			
Sample	Sample size	Chronometric theory	Hubble theory
DeVeny	119	~ 0.5	$< 10^{-15}$
Sandage	77	~ 0.5	$< 5 \times 10^{-9}$
Braccesi	11	> 0.2	< 0.01
Lynds-Wills	14	> 0.4	~ 0.03
Schmidt	22	> 0.2	~ 0.08

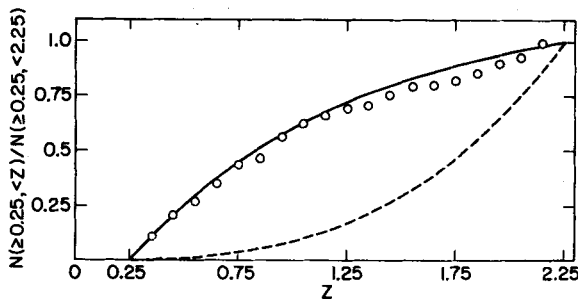


Figure 25 The N - z relation for quasars in the redshift range $0.25 < z < 2.25$.

Data: all quasars in DeVeny list with unquestioned redshifts and magnitudes. The cutoff above $z = 2.25$ used here corresponds to an observational one, and if removed would accentuate the discrepancy between the Hubble curve and the observations. A hypothetical extraordinarily broad luminosity function for quasars might serve to render the Hubble curve acceptable in relation to the observations, but would not explain the excellent agreement with the chronometric prediction. The deletion of quasars with $z < 0.25$ serves to remove from the comparison possible extraneous influences which cannot be resolved at this time. Compare the comment on Figure 24.

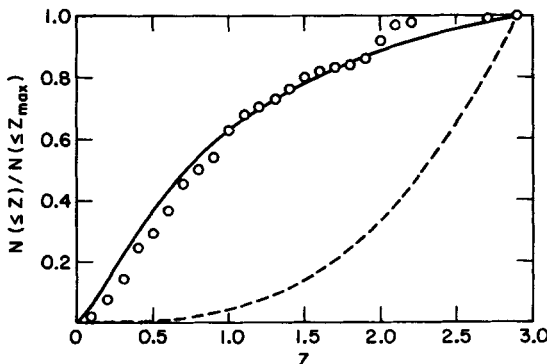


Figure 26 The N - z relation for the quasar list of Sandage (1972b).

The basis here is the same as earlier, except that the z values are limited to multiples of 0.1. Although no explicit selection criterion is given for the sample, it would appear on the chronometric hypothesis to be random in its redshift distribution.

15. The Schmidt V/V_m test for quasars in the chronometric theory

When samples of a specified type of luminous object are available which are complete down to specified limits of apparent luminosity, this provides a relatively universal and simple test for spatial uniformity. The availability of the Schmidt 3C quasar sample, the Lynds-Wills 4C quasar sample, and the Peterson galaxy sample—these are among the statistically most objective

and substantial data on hand—indicates the importance of adapting the test to the chronometric theory. It is not difficult to do so, and the tests provide a significant measure of assurance as to the validity of the chronometric theory. It should be recalled that on a nonevolutionary expanding-universe theory, all three samples show quite strong and statistically quite significant deviations from spatial uniformity.

In principle, the procedure of Schmidt,[†] further expounded by Lynds and Wills, applies to any geometry. The basic statistical principle of the V/V_m test is as follows. Let a space S be given, together with a volume element in S such that the total volume is finite; this total volume may then be normalized to the value 1. This volume element may be entirely arbitrary apart from the requirement that individual points have zero volume. Let $\{S(t)\}$ be a one-parameter family of subsets of S , which are continuously increasing with t , and such that every point of S is contained in some $S(t)$, while no point is contained in all $S(t)$. For an object uniformly distributed in S , let \bar{t} denote the least (or greatest lower bound) of the values of t for which the object is contained in $S(t)$. The volume of $S(\bar{t})$ is then a random variable V which takes on all values between 0 and 1. Furthermore, uniformity of the distribution of the object in S means precisely that the probability that the object will be in $S(t)$ is the volume of $S(t)$. This means that V is uniformly distributed in the interval $[0, 1]$. The choice of the one-parameter family $S(t)$ is in practice dictated by the theory under consideration; it is not mathematically unique, but there is generally a simplest reasonable choice.

The theoretical procedure for dealing specifically with the Schmidt V/V_m test will now be described, in the more general situation in which one considers only a fixed redshift region, $z < z_{\max}$, with z_{\max} not necessarily equal to ∞ , but large. The fundamental assumptions involved in the analysis are then somewhat more conservative, for it is postulated only that the objects in question are uniformly distributed in the region $z < z_{\max}$, and not necessarily in all of space; and that the observational sample(s) on which the analysis is based are complete (or constitute a random selection from a complete sample) only within the same region. Observationally, there is doubt as to the degree of accessibility of large redshift regions; as noted, e.g., by Burbridge (1971), the spectral function of quasars for large frequencies may fall off increasingly rapidly, making their observation more difficult (cf. in fact the last point in the observation of 4C 05.34 reported by Oke, 1970); spectroscopic selection may well be a factor in establishing redshifts and thus establishing that suspected quasars are indeed such (cf., e.g., Basu, 1973); intergalactic absorption, if present, would further limit the statistical validity of the inclusion of large redshift regions in the analysis.

[†] This appears to originate in part in work of P. Kafka (1967).

Consider, then, the region S of space in the chronometric theory in which $z < \tilde{z}$, where \tilde{z} is a fixed arbitrary value, taken for relevance and simplicity to be > 1 . For the most part, the regions $S(t)$ can be defined in the same way as in the expansion theory, as those out to a given redshift. There is, however, one case in which this is not possible. For an object in a complete sample at a redshift $z_1 > 1$, which is only slightly brighter than a limiting luminosity, and has a sufficiently flat spectrum, the region in which the object would be included in the sample is not the region of space out to a certain redshift, but consists rather of two disconnected pieces, of the form $z < z_1$ and $z_2 < z < \tilde{z}$. In this case, it would be incorrect to use the region below a given redshift. There is a natural choice of the one-parameter family of regions which is correct according to statistical theory, namely those of the form $z < t$ and $t' < z < \tilde{z}$, where $t < t'$ and the redshifts t and t' represent equal apparent luminosities for the spectral index in question. (Compare the earlier treatment of the chronotheoretic N - S relation.)

In the cases of the Lynds-Wills 4C and Schmidt 3C samples, most objects are sufficiently bright relative to the limiting magnitudes to be included in the sample wherever located in the redshift region $z < z_{\max}$ on the basis of the chronometric theory. Of the remaining objects none actually involve the pair of disconnected regions just described, in the redshift region $z < 3$. In, e.g., the Schmidt sample only one object (3C 323.1, of spectral index 0.66) is radio-limited and its spectrum is too steep to lead to the disconnected regions just described, in the relevant redshift regions. Chronometrically, only two objects in the Schmidt sample, 3C 191 and 3C 9, are optically limited; in the Lynds-Wills sample, one object (4C 18.34) is radio-limited and one (4C 12.39) is optically limited. In all these cases, the spectra are too steep to lead to disconnected regions.

The results are shown in Figures 27 and 28. The horizontal axis is the V/V_m for the individual quasar; this is naturally theory-dependent, so there are two sets of points for the same observational datum. The value $z_{\max} = 3$ has been used, expressing the possibility that completeness in the region $z > 3$ is best not assumed. This has substantially no effect on the expansion value of V/V_m , which have consequently been taken unchanged from the cited authors.

As was to be expected from the near independence of the apparent luminosity of quasars from their redshift on the chronometric theory, the corresponding V/V_m test gives results which differ by relatively little from the $N(z)$ comparison. In most cases the V_m for a quasar will be unity. The uniformity of the distribution of the V/V_m for quasars is then largely tantamount to the $N(< z)$ for quasars being proportional to the $V(z)$, and the Kolmogorov-Smirnov test for the uniformity of the V/V_m distribution is correspondingly related to the Kolmogorov-Smirnov test detailed earlier for the observed versus theoretical $N(< z)$ relation.

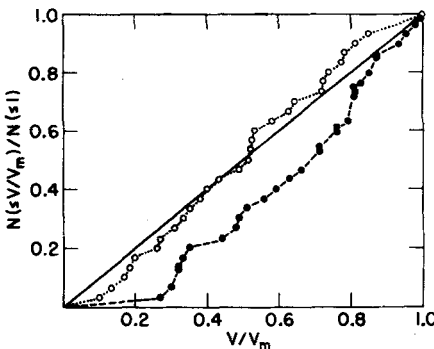


Figure 27 The Schmidt V/V_m test for the 30 quasars in the complete sample of Lynds and Wills.

○, chronometric analysis; ●, values given by Lynds and Wills for the Friedmann model with $q_0 = 1$; —, theoretical spatial uniformity. The chronometric values accept the hypothesis of spatial uniformity without any indication of luminosity and/or number evolution, unlike the expansion values.

For the expansion hypothesis this is not the case since the theoretical luminosity varies strongly with redshift in all redshift ranges. There is indeed a difference between the V/V_m test and the $N(<z)$ and also $N(m)$ test (the latter being discussed by Longair and Scheuer, 1970b, and by Lynds and Petrosian, 1972). However, as shown by Schmidt (1968) and also Lynds and Wills (1972) on the basis of this test, the expansion hypothesis is in poor

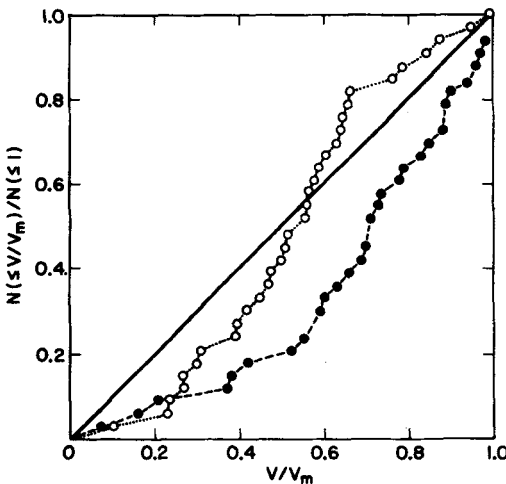


Figure 28 The Schmidt V/V_m test for the 33 quasars in the complete 3C sample of Schmidt. The basis here is the same as in Figure 27. The comment regarding that figure applies.

agreement with their data. Only with additional assumptions of luminosity and density evolution, as indicated by Schmidt (1972a,b,c), does the agreement become satisfactory, but this agreement is then virtually a matter of definition.

16. The angular diameter redshift relation for double radio sources

Given two theories regarding a variable y of the form:

$$y = f_j(x) + c \quad (j = 1, 2),$$

where c is postulated to be an x -independent random variable of dispersion σ , it is evident that one can discriminate between the theories observationally with a moderate amount of data only if this dispersion σ is not too large compared to the average dispersion between the theories, i.e., the root mean square $f_1(x) - f_2(x)$ over the relevant range of x . In the case of the θ - z relation, this signifies that one can discriminate effectively between the relations

$$\theta_{\text{app}} \propto (1+z)/z^{1/2} \quad (\text{chronometric}),$$

$$\theta_{\text{app}} \propto (1+z)^2/z \quad (\text{standard cosmology}),$$

or variants thereof, only if the intrinsic dispersion in $\log \theta$ is not large relative to the average difference between the respective theoretical laws.

The intrinsic, model-independent dispersion in $\log \theta$ can be estimated from data which includes sufficiently many objects that many pairs at approximately equal redshift occur. Taking the largest and most thoroughly documented data, those compiled by Miley (1971), one finds 22 pairs of quasars which are double radio sources at approximately equal redshifts (the largest logarithm in the ratio of the pairs being 0.047, most being much less). If θ and θ' denote the angular diameters for such pairs, the quantity $[(2n)^{-1} \sum (\log \theta - \log \theta')^2]^{0.5}$, where n is the number of pairs, is a statistically consistent estimate of the dispersion in $\log \theta$, assuming that the distribution of θ_{int} is z -independent. This estimate is found to be 0.44. On the other hand, the root mean square of $\log(1+z)/z^{1/2} - \log(1+z)^2/z$ over the redshifts included in the sample is 0.03; and this would not be significantly altered by using a slightly different expansion-theoretic form, e.g., the Einstein-de Sitter angular diameter, or the Euclidean one. Thus the dispersion in the data is of the order of more than 10 times the theoretical difference to be probed, and no statistically significant comparison can be obtained. The Legg samples are smaller in size, and otherwise similar; hence they are likewise unable to discriminate between different theoretical θ - z relations of the type considered here.

The actual dispersions computed with the use of the Miley data are 0.36 and 0.37 respectively for the deviations of the observed $\log \theta$ from the expansion-theoretic and chronometric predictions, respectively. It was impossible for the two dispersions to differ by more than 0.03, so the closeness of these values was to be anticipated. It is somewhat unusual that the dispersions are less than the intrinsic dispersion, but the diminution in variance below the intrinsic level is not nearly at a significant level. The Miley data include 50 quasars which are double radio sources whose angular diameters are not indicated as questionable, and the dispersion of $\log \theta$ for these data is 0.79; thus the reduction of dispersion in $\log \theta$ itself via either theory is substantial.

For galaxies, the Legg data give dispersions of 0.56 and 0.52 respectively for the deviations of $\log \theta$ from the Hubble and chronometric theories respectively. Qualitatively the results are similar to those for the Miley data, and serve to confirm the conclusions just reached.

17. Observation versus theory for radio sources

There seems to be agreement among major surveys on two qualitative features of the $N-S$ relation: (a) the elevation of the index $\beta = -\partial \log N / \partial \log S$ above the Hubble "Euclidean" value 1.5 (and a fortiori larger than attainable Friedmann values); (b) the decrease of N with increasing S , with $\beta \gtrsim 1$. In view of the uncertainty in the intrinsic luminosity function for radio sources, and the lack of published tabular data required for statistical analysis, it would be quite difficult to effect a Kolmogorov-Smirnov test of the data vis-à-vis the chronometric and expansion hypotheses, nor would any such test be conclusive at this time. It appears that little more can be said than that features (a) and (b) are difficult to reconcile with a nonevolutionary Friedmann cosmology, but are predicted by the chronometric theory, as earlier indicated.

The value of β may become infinite for a single luminosity class in the chronometric theory, but decreases rapidly as the breadth of the luminosity function increases. The values given in Figure 4 for a one-decade breadth in luminosity function agree reasonably well with the observations of Kellermann *et al.* (1971) and those of Pooley and Ryle (1968), when the latter are corrected for spectral index (cf. Kellermann *et al.*, 1971); the N/N_0 curve for the totality of radio sources should approximate the average of that in Figure 4 and the constant value 1, assuming an average spectral index ~ 0.6 . Roughly this order of magnitude for the breadth, on the basis of the chronometric theory, is indicated by an analysis of the data presented by Schmidt

(1972b), Table 1, giving a list of 41 3CR sources complete in a given field up to a given limit and including redshifts for all but six sources. On the expansion theory, the intrinsic luminosity F_{rad} is given by the relation

$$\log F_{\text{rad}} = \log f_{\text{rad}} + 2 \log z + \text{const};$$

a computation of the dispersion of the $\log F_{\text{rad}}$ computed from this relation for the 29 galaxies having precise redshifts in the sample gives $\sigma = 1.02$; for all the objects having precise redshifts, consisting in addition of six quasars, the dispersion is much higher. On the chronometric theory, the dispersion is $\sigma = 0.55$ for the 29 galaxies of the 35 objects having precise redshifts, and somewhat greater if all 35 objects are included.

The relation between the dispersions on the two theories is consistent with that found earlier, and cannot be regarded as a coincidence. It indicates that bright radio sources are more nearly standard objects than had been thought, and suggests that observations down to fainter limits and of additional redshifts may yield quite discriminatory cosmological information. However, on the chronometric hypothesis there is presently no significant evidence whatever that radio sources have been evolving either in luminosity or space density. In addition to the cited data of Schmidt on radio luminosities, the following recent lists of redshifts versus radio luminosities are extant: 4C quasars (Lynds and Wills, 1972); 3C quasars (Schmidt, 1968); radio galaxies and quasars (Sandage, 1972c). The Lynds-Wills and Schmidt lists have explicitly designated completeness features; the Sandage lists are larger but the criteria for inclusion are not given explicitly. It is interesting that in all cases (which are not entirely independent, the quasar lists being overlapping), the chronometric dispersion in the luminosity-redshift relation is less than or approximately of the same size as the dispersion in apparent luminosity, while the dispersion from the expansion-theoretic line ($q_0 = 1$) is 50 to 100% greater. The specific values are given in the following table. Radio magnitudes are uncorrected and have been converted to the Pogson scale to facilitate comparison with the visual magnitudes. The apparent radio luminosities were not given in Sandage (1972c), but were reconstituted by J. F. Nicoll (unpublished course paper, MIT), in accordance with the equation $m_R = 5 \log z - 2.5 \log L_R$, where L_R denotes the absolute expansion luminosity tabulated by Sandage; see Table 22.

Thus the phenomenological superiority of the chronometric luminosity-redshift relation extends to radio luminosities. Concomitantly, the breadth of the radio luminosity function is highly model-dependent. From the chronometric standpoint, the breadth is quite moderate; indeed, substantially the full radio luminosity function for the quasars and galaxies may well be observationally accessible in the next few years.

TABLE 22

Data source	Number and nature of objects	Apparent radio magnitude	Dispersions in	
			Chronometric absolute radio magnitude	Expansion absolute radio magnitude
Lynds and Wills (1972)	30 quasars (4C list)	0.79	0.84	1.51
Schmidt (1968)	33 quasars (3C list)	0.75	0.73	1.27
Sandage (1972c)	68 radio galaxies	1.24	1.36	2.38
Sandage (1972c)	132 quasars	1.23	1.26	1.79

18. The Setti-Woltjer quasar classes

Setti and Woltjer (1973) have proposed that the $m-z$ relation for sufficiently pure classes of quasars may be in rough agreement with the Hubble line. They have identified three classes, selected on their radio spectra, and found that the first class (those with steep spectra) show a definite trend with redshift, described as "a clear Hubble relation." The lack of such behavior for the relations of the other two classes is ascribed to a broad luminosity function.

It is interesting that the chronometric theory provides a considerably better fit for the $m-z$ relation of all three quasar classes than does the Hubble line. In addition, the observational $N(< z)$ relations may be compared with those theoretically predicted on the assumption of spatial homogeneity of the quasar distribution. The chronometric prediction provides a very good fit, but the Friedmann model predictions for values of q_0 generally thought realistic are in gross disparity with the observations.

In particular, the important corollary to the Setti-Woltjer study that quasars are at essentially cosmological distances, and their redshifts are increasing functions of distance, is unaffected; but if the much better-fitting chronometric theory is correct, the distances are probably an order of magnitude less than those given by realistic Friedmann models, and $(\partial \log z / \partial \log r) = 2r/\sin r$, measuring r in units of R , i.e. z increases very rapidly with distance in much of the quasar redshift range.

a. The $m-z$ relations

The dispersions in apparent magnitudes, and of the residuals of these magnitudes from the respective theoretical predictions are given in Table 23. All data satisfying the Setti-Woltjer criteria, and having unquestioned values of z , have been included in each sample. σ stands for the standard deviation of the indicated quantity; M represents an absolute magnitude, the subscripts c and e referring to the chronometric and expansion theories respectively, the latter being represented by the Friedmann model with $q_0 = 1$.

TABLE 23
The $m-z$ relation for the Setti-Woltjer quasar classes

Sample	Size	$\sigma(m)$	$\sigma(M_c)$	Expected $\sigma(M_c)$	$\sigma(M_e)$	Expected $\sigma(M_e)$
Q_s (\sim steep spectrum)	38	1.03	0.81	0.96	0.91	0.72 <i>i</i>
Q_f (\sim flat spectrum)	22	1.15	0.89	1.08	1.00	0.69 <i>i</i>
Q_o (radio quiet)	53	0.96	1.05	0.50	2.35	2.23 <i>i</i>
$Q_o, z \leq 0.5$	25	0.98	0.89	0.73	1.36	1.16 <i>i</i>

In any theory of the form $m = f(z) + M$, where $f(z)$ is an analytically prescribed function of z , while M is an intrinsic magnitude, it is to be expected on an elementary statistical basis that $\sigma(m)^2 = \sigma(f)^2 + \sigma(M)^2$, or $\sigma(M) \sim [\sigma(m)^2 - \sigma(f)^2]^{1/2}$. The latter quantity has been computed and entered in the table as "expected dispersion." Pure imaginary values signify that the dispersion in apparent magnitudes is less than would be expected on the hypothesis that the $m-z$ relation has the form indicated; the absolute value of the expected dispersion is then an indication of the extent to which the hypothesis deviates from expectation, on the basis of the sample in question.

The subsample of the optical quasars for which $z \leq 0.5$ has been included because it is large enough to be meaningful, and in order to minimize possible selection on luminosity, which is in all likelihood greatest for this particular type of quasar. It serves also to test, and actually to confirm, the a priori reasonable idea that the excess of $\sigma(M_c)$ over $\sigma(m)$ for the total optical sample is a consequence of the effective cutoff in apparent magnitudes for the optical quasars.

For each sample, the $\sigma(M_c)$ is substantially less than the $\sigma(M_e)$; for all samples except one, the $\sigma(M_c)$ is less than the $\sigma(m)$, and is in reasonably good agreement with the expected $\sigma(M_c)$. The $\sigma(M_e)$ is less than the $\sigma(m)$ for

the first two samples, but much greater than it for the optical sample; and in all cases the expected $\sigma(M_e)$ is quite different from the actual $\sigma(M_e)$.

The Q_S and Q_F samples are the purer subgroups identified by Setti and Woltjer. For Q_S this means $\alpha \geq 0.7$ and a suitable double radio structure. The Q_F have $\alpha < 0.6$ and are of relatively small angular diameter in a sense specified by Setti and Woltjer (designated P in their preprint).

b. The $N(< z)$ relations

On the assumption of spatial homogeneity, the $N(< z)$ for each type should vary approximately with the volume out to redshift z . The extent to which this is the case is shown by Figure 29. The chronometric prediction is in visibly good agreement with the observations; the Friedmann model with $q_0 = 1$, and the Hubble model, are respectively in poor and very poor agreement with observation. In all cases the redshift range has been limited to $0 < z < 2$, for uniformity and to minimize probable selection effects at higher redshifts; the sample sizes are thereby slightly reduced.

A quantitative measure of the deviations of the $N(< z)$ counts from theory is afforded by the Kolmogorov-Smirnov statistic D . This is the maxi-

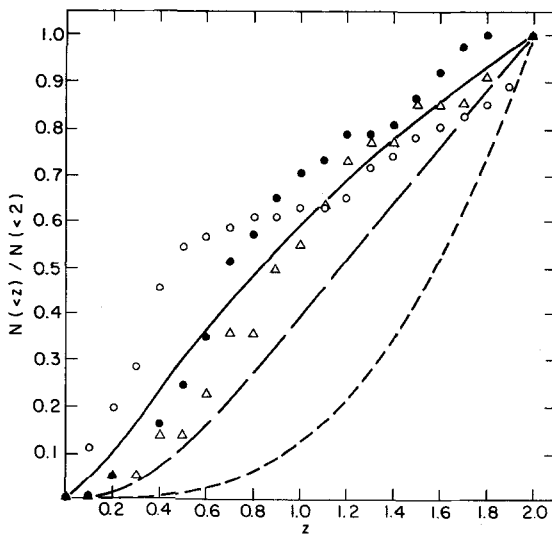


Figure 29 The redshift distributions of the Setti-Woltjer quasar classes in comparison with theoretical predictions.

—, chronometric theory; --, Friedmann model with $q_0 = 1$; -·-, Hubble theory. ●, Q_S ; △, Q_F ; ○, Q_O . Despite the observational selection which may be present, the chronometric prediction is statistically acceptable on the basis of Kolmogorov-Smirnov tests for all classes.

TABLE 24

Radial spatial homogeneity of the Setti-Woltjer quasars as measured by Smirnov deviations and probabilities

Sample	Size	D_e	$P(D_e)$	D_e	$P(D_e)$
$Q_S, z < 2$	37	0.11	$\gtrsim 0.5$	0.31	1.4×10^{-3}
$Q_F, z < 2$	20	0.12	$\gtrsim 0.5$	0.22	0.29
$Q_0, z < 2$	46	0.25	7.6×10^{-3}	0.43	6.0×10^{-8}
$Q_0, z < 0.5$	25	0.07	$\gtrsim 0.5$	0.34	6.2×10^{-3}

mum absolute difference between the fractions observed and predicted up to redshift z . It is given together with the corresponding probabilities in Table 24, the D_e referring to the Friedmann model with $q_0 = 1$.

Schmidt V/V_m tests, based on an assumption of effective randomness of the samples in the totalities of quasars of each type with $z < 2$ and reasonable prescribed limiting luminosities, can be expected to give similar although less definitive results, in view of the analytic similarities between the tests, and experience with other quasar groups.

The chronometric predictions fit extremely well, if the reasonable assumption is made that the optical sample suffers quite materially from luminosity selection when taken out to redshift 2; this assumption is indicated by the good fit for the subsample out to redshift 0.5. As in a number of earlier samples, the strong degree of spatial homogeneity the results indicate, on the chronometric hypothesis, naturally raises a question, if the hypothesis is accepted, as to the possible existence of gravitational or other dynamical effects which tend to enhance spatial homogeneity, or at least to maintain it. On the other hand, the Friedmann model predictions are rejected at conservative probability levels, indicating once again that the spatial distribution of quasars can be reconciled with the expanding-universe theory only on the assumption of very strong evolution.

The Q_F data are accepted by both the chronometric and expanding-universe theories, but they are less appropriate than the other data as a check on theoretical predictions. This is due to the relatively small Q_F sample size, and to the possible model-dependence of the type, whose criterion involves a restriction on angular diameter in fixed angular measure, of which the metric implications are theory and z -dependent.

c. Discussion

The results are similar to those earlier presented for less homogeneous quasar samples. It is also possible to analyze in a similar way the $\theta-z$ relations, but again as earlier the large dispersion in $\log \theta$ in the vicinity of

fixed z precludes any strongly indicative comparison between the chronometric and expansion theories on this basis.

The hypothesis that the quasar $m-z$ and $\theta-z$ relations are purely stochastic is a specific form of the "local" hypothesis which can be rejected on a definitive statistical basis by tests of trend in the $m-z$ and $\theta-z$ relations of the Q_s , confirming earlier more informal analyses by Miley (1971) and Setti and Woltjer. In particular, the Spearman rank-correlation test gives a probability $\sim 10^{-5}$ of obtaining a value of the Spearman coefficient as large as that observed, between m and z , if these variates are stochastically independent. This test is entirely independent of any assumption as to the distribution of m or z ; it is also model-independent. The same test can be conducted with the Q_s sample replaced by the DeVeny sample of 158 quasars earlier described; it is interesting that the results are of the same order of definitiveness, due to the lesser homogeneity of the sample. The Q_s thus appear as one of the purest and statistically useful classes of quasars yet identified.

19. Other observational considerations

Finally we turn to a number of phenomena, or anomalies from the expansion-theoretic standpoint, which do not primarily involve statistical testing.

a. *The energy requirements of quasars vis-à-vis bright galaxies*

Many authors have cited the unprecedented energy requirements of quasars on the expansion-theoretic hypothesis as the major anomaly associated with them. Many new, largely quite speculative, hypotheses have been proposed to explain the mechanism of the energy output. Most of these hypotheses are of a partial or qualitative nature which renders them immune from direct statistical testing.

There is no difficulty whatever regarding the energy production of quasars on the chronometric hypothesis. A straightforward analysis indicates that they are within ~ 1 mag of nearby bright galaxies, brightest cluster galaxies, Seyfert or Seyfert-like Markarian galaxies, and N-galaxies; cf. Table 25. Possible intergalactic absorption is too small to be important in the present connection, as shown by the consistently small chronometric dispersion for the bright quasar $m-z$ relation. More concretely, the relative intrinsic luminosities of galaxies and quasars are compatible with the hypothesis that quasars are the nuclei of certain relatively luminous galaxies, whose outer portions are invisible at larger redshifts. There is other evidence

TABLE 25

Luminosities of bright extragalactic objects: averages \pm standard errors

Data source	Sample and size	Absolute chronometric magnitude	Apparent magnitude	Absolute expansion ($q_0 = 1$) magnitude
de Vaucouleurs tape (1964)	15 galaxies of redshift nearest 250 km sec^{-1}	18.72 ± 1.21	11.02 ± 1.18	26.43 ± 1.26
de Vaucouleurs	15 galaxies of redshift nearest 500 km sec^{-1}	18.55 ± 1.09	11.60 ± 1.06	25.51 ± 1.13
de Vaucouleurs	15 galaxies of redshift nearest 1000 km sec^{-1}	17.86 ± 0.87	11.66 ± 0.86	24.05 ± 0.87
de Vaucouleurs	15 galaxies of redshift nearest 2000 km sec^{-1}	18.04 ± 0.60	12.59 ± 0.60	23.47 ± 0.60
de Vaucouleurs	15 galaxies of redshift nearest 4000 km sec^{-1}	18.20 ± 0.80	13.49 ± 0.80	22.87 ± 0.81
Peterson* (1970a)	44 bright cluster galaxies, complete to 15^m	17.47 ± 0.48	13.71 ± 0.82	21.16 ± 0.33
Sandage* (1972b)	41 bright cluster galaxies	17.78 ± 1.37	14.75 ± 2.50	20.58 ± 0.31
Sargent (1972)	24 Seyfert-like Markarian galaxies	19.01 ± 0.77	15.43 ± 0.89	
Burbridge and Burbridge (1967)	All 74 galaxies with data in list	18.27 ± 0.91	17.32 ± 1.09	17.83 ± 1.29
Lynds and Wills (1972)	All 30 quasars with data in list	18.69 ± 0.89	17.84 ± 0.99	18.03 ± 1.32
Sandage (1972b)	All 109 radio-noisy quasars with data in list	18.20 ± 0.89	17.26 ± 1.03	17.75 ± 1.30
DeVeny <i>et al.</i> (1971)	All 157 with unexceptionable data	18.42 ± 0.93	17.39 ± 1.02	18.11 ± 1.59
Wampler <i>et al.</i> (1973)	OQ 172 (redshift 3.53)	17.77	17.5	14.76
Sandage (1972b)	15 radio-quiet quasars	19.20 ± 1.08	17.74 ± 0.98	19.56 ± 2.52

* Magnitudes uncorrected for difference between expansion-theoretic apertures reported and chronometrically correct apertures.

for this hypothesis, and no significant evidence from the chronometric standpoint against it; thus from this standpoint, quasars are not significantly more exotic than galactic nuclei in which apparently violent activity is present. It is the qualitative nature of these activities, rather than the average energy output of the galaxies in question, which may suggest an unconventional explanation of their energy source.

More specifically, the best-fitting chronometric redshift-magnitude curve to the quasars listed by DeVeny *et al.* takes the form (assuming spectral index ~ 1)

$$m = 2.5 \log z - 2.5 \log(1 + z) + 18.4.$$

We define the "chronometric intrinsic magnitude" of an object of magnitude m and redshift z as the number c such that

$$m = 2.5 \log z - 2.5 \log(1 + z) + c.$$

This number is not necessarily independent of the location of the object due to possible deviation of the spectral index from 1, possible intergalactic absorption, etc. The advantage of this measure of intrinsic luminosity is that it is independent of the assumed value of the Hubble parameter; it should be borne in mind that only relative intrinsic luminosities are meaningful in the present sense. Table 25 details the relative intrinsic luminosities of various types of quasars and galaxies.

b. The sharp decrease in the number of quasars in the range 2.2–2.9 and apparent near cutoff beyond 2.9

This phenomenon is too well known observationally to require description. A variety of explanations has been proposed from the expansion-theoretic standpoint, all involving a greater or lesser degree of ad hoc assumption, and the introduction of one or more new parameters. There seems no reason to doubt that spectroscopic selection effects play a partial role; also, it becomes progressively more difficult to establish the larger redshifts, and it is reasonable to anticipate that intergalactic absorption or obscuration will increase with distance, and so with redshift in either the chronometric or the expansion theory. While these effects may largely explain the near cutoff above redshift 2.9, the order of magnitude of the attrition in the region 2.2–2.9 of demonstrated accessibility is more difficult to understand on the expansion-theoretic hypothesis.

To make a simple order-of-magnitude estimate, suppose to begin with that the quasars are approximately of the same intrinsic luminosity, and are uniformly distributed in space. The ratio $N(2.2 < z < 2.9)/N(z < 2.2)$ for quasars is then 1.29 on the Hubble theory, ≥ 0.33 for a Friedmann model with $|q_0| \leq 1$, and 0.09 on the chronometric theory. In the DeVeny list there are 200 quasars in the range $z < 2.2$ and 5 in the range $2.2 < z < 2.9$. The expansion-theoretic expected number in the latter range is 66–258, on the basis of the 200 observed in the former range. This is a discrepancy too great to be eliminated by reasonable modification of the luminosity function, or the spatial distribution, or to be explicable by spectroscopic selection of any known type. It is also perhaps beyond the need for formal statistical analysis; but on the hypothesis of approximately random selection of 205 quasars from all those of redshift < 2.9 , and those indicated regarding the luminosity function and spatial distribution, the equivalent Gaussian variate represented by the standard approximation to the Bernoulli distribution is 15.5 on the Hubble theory, and ≥ 9.9 for a Friedmann model with $0 \leq q_0 \leq 1$, corresponding to probabilities $< 10^{-53}$ and 10^{-23} , respectively. Clearly drastic supplementary hypotheses are required to explain the cutoff on the expansion theory, and the proposed explanations are of this nature.

In the chronometric theory, the expected number of quasars is 17.6. The

discrepancy from the observed value of 5 is 12.6, a number of quasars which might well arise from random fluctuations combined with possible sharp drops in the spectral function of quasars shortward of the Lyman α line, tendencies toward spectroscopic selection, and intergalactic absorption and/or obscuration. The formal Gaussian variate is here 3.1, just beyond the conventional significance level, the corresponding probability being 0.002. The discovery of just five additional quasars in the range $2.2 < z < 2.9$ would render the deviation insignificant by conventional standards (probability > 0.05). As indicated by the subtlety of the identification of 4C 05.34 as a quasar by Lynds and Wills (1972), confirmation that suspected quasars in this range are indeed such is relatively difficult to supply, and is in part anticipated on the chronometric theory according to which there should be relatively few other quasars at nearby redshifts available for comparison purposes. The difficulty of supplying this confirmation may well be partly responsible for the apparent slight deficiency in the number of quasars observed in the range in question on the chronometric hypothesis.

It may be noted finally that the preceding section was written prior to the discoveries of two quasars at redshifts ~ 3.5 . These discoveries and the attendant circumstances regarding colors are consistent with and indeed support the foregoing, but they exacerbate the discrepancy between a priori expansion-theoretic indications and actual observation.

c. Superlight velocities

It is evident that these apparent velocities are highly sensitive to the estimate of distance, and so to the redshift-distance relation. With the chronometric relation, all published apparent superluminal velocities are reduced to well below the velocity of light. Even if H were as low as $40 \text{ km sec}^{-1} \text{ Mpc}^{-1}$ at Virgo, instead of the larger value taken in the bulk of this paper, the largest apparent superluminal velocity, that of 3C 279 would be reduced to less than c . With $H = 80$ at 10 Mpc, its velocity would appear as $(0.57 \pm 0.17)c$. On the basis of the conventional expansion theory, its apparent velocity is $\sim (10 \pm 3)c$; see Whitney *et al.* (1971). While other explanations of superluminal velocities have been given (cf. Cavalieri *et al.*, 1971), the present one appears to be the scientifically most economical, in requiring no assumptions beyond the fundamental one of the chronometric model itself.

d. The relative absence of quasar identification for radio sources at faint magnitudes

Bolton (1969), Braccesi *et al.* (1970), and Fanti *et al.* (1973) have independently found that quasar identifications are relatively rare for radio sources on plates which are sufficiently sensitive to record objects of visual

magnitude in the vicinity of ~ 20.5 . Galaxy identifications have been made in this way, and on the expansion-theoretic hypothesis, there is no apparent reason why significant numbers of quasars should not appear on such plates. Such relative lack of quasars is, however, predicted by the chronometric theory, augmented by the earlier validated hypothesis that quasars form approximately a single luminosity class on which is superimposed a Gaussian variate of dispersion $\lesssim 1$ mag. Compare Figure 17, in which the small and decreasing slope of the chronometric $N(m)$ curve at $m = 19.5$ is indicative of the cutoff.

e. Apparent distance-dependence of and variation in the Hubble parameter

The persistent anomaly in the determination of the Hubble parameter by different observations is largely removed by the chronometric theory, as detailed in Section 8 of this chapter.

f. The cosmic microwave background radiation

As earlier noted, virtually any strictly temporally homogeneous theory of the cosmos will predict a blackbody background radiation, as the equilibrium photon gas formed by the free radiation in the universe. Conservation of energy and maximization of the entropy dictate the blackbody form, in the presence of ergodicity (cf., e.g., Mayer 1968). The latter is implied by any significant degree of overall stochastic perturbation, which in the real Cosmos arises from the evolution and motions of galaxies, scattering, absorption, and reemission by intergalactic matter, possible gravitational deflections, etc.

Turning now to comparison with observation, it is natural to inquire how well the observed relative energy of the background radiation and starlight of $\sim 10^3$ conforms to the theoretical analysis earlier given, which yielded an upper bound and putative order-of-magnitude estimate for the background energy. This was based on the assumption that emission and absorption by bright galaxies are major factors in the establishment of the background equilibrium radiation. Defining "bright" as of magnitude ≤ 13 at a redshift $cz = 2000 \text{ km sec}^{-1}$, the catalog of de Vaucouleurs (1964) indicates ~ 250 bright spiral galaxies in this redshift region, indicating $\mu \sim 1.4 \times 10^5$ (using now units with $R = c = 1$). The angular diameters given in the catalog correspond to a metric diameter of $\sim 10 \text{ kpc}$ on the chronometric hypothesis, assuming $z = 0.005$ at a distance of 15 Mpc (which incidentally limits the age of pristine radiation to $\lesssim 10^9$ ly). The value $r = 5 \text{ kpc} = 1.2 \times 10^{-5}$ then is indicated if the absorption in the Galaxy, $\sim 0.3 \csc b$, is reasonably typical. The resulting theoretical prediction for the ratio of the energy of the microwave background to that of

starlight is 1.7×10^5 , an excess over observation corresponding to a black-body temperature of ~ 2 times that observed. This seems fully comparable in precision to the accuracy of the prediction based on the "big-bang" hypothesis in view of the hypothetical parameters, such as the entropy density of the original universe, involved in the latter prediction. Faint galaxies and/or unknown forms of intergalactic matter could account for the discrepancy, as could also in part the probable underestimation of r resulting from the existence of significant dust exterior to the observed optical diameters of the galaxies.

g. Cosmic time scales

The universal and relativistic scales are nonlinearly related, indeed an infinite relativistic time corresponds to a finite universal time. The ages derived by radioactive dating and other microscopic considerations are relativistic, on the chronometric assumption that local elementary particle interactions are effectively observed by a relativistic clock. This position represents the minimal departure from conventional theoretical practice, and follows from the unicity of this clock implied by Lorentz and scale covariance.

The coincidence of the orders of magnitude of the apparent ages of the earth, sun, galaxy, etc., is understandable on this basis in the following way. At a fixed point taken as the origin in space, the relation between the universal and relativistic time is $\tan t = x_0/(1 - x_0^2/4)$, in units of R , earlier estimated as ~ 106 Mpc. All observed ages correspond to values of t in the range $-\pi < t < 0$, since $x_0 = 0$ when $t = 0$ and $x_0 = -\infty$ when $t = -\pi$. If the universal age of discrete objects in the universe is uniformly distributed in this range (to which attention may be confined, since older discrete objects would not be observable as such, light from them going through an infinite redshift), the corresponding relativistic age will follow a nonuniform but calculable distribution in the range $-\infty < x_0 < 0$.

Specifically, the uniform distribution law for t in the range $-\pi/2 < t < \pi/2$ is found (by calculus) to correspond to the Cauchy distribution law whose element over the range $-\infty < x_0 < \infty$ is $(2\pi)^{-1}(1 + \frac{1}{4}x_0^2)^{-1} dx_0$. Restricting consideration to the observable range $x_0 < 0$, the integral $\pi^{-1} \int_0^\infty x(1 + \frac{1}{4}x^2)^{-1} dx$ expressing the expected age of a random object of any specified type is divergent. It follows that the arithmetic means of the ages of a sample of such objects (e.g., galaxies) should fluctuate widely. However, the percentile points should converge to the corresponding percentile points in the overall population. The 50, 95, 97.5, and 99 percentile ages (i.e., the ages such that the given percentage has a lesser age) are 2, 25.4, 50.9, and 127.3, in units of the time for light to travel a distance equal to the radius of the universe. With $R = 106$ Mpc as earlier, this means that half of the galaxies should have ages in the range $\sim 0.7 \times 10^9$ to 10^{10} yr. This value

of R corresponds to the value $H = 100$ at 15 Mpc; with the larger value $R \sim 150$ Mpc corresponding to the parameter $H = 50$ at 15 Mpc the corresponding range is simply $\sim 10^9\text{--}10^{10}$ yr. The result obtained here appears to be in good agreement with the limited number of independent estimates or bounds on galaxy ages, and serves to explain within the chronometric framework the coincidence of the order of magnitude of the apparently older astronomical objects.

h. Holmberg's systematic effect in galaxy clusters

One of the striking features of extragalactic redshifts which appears at variance with theoretical anticipation is the "extremely high internal redshift dispersion found for clusters of nebulae," in the words of Holmberg (1961), who first noted and analyzed this effect, most notably by a precise and detailed treatment of the Virgo cluster. Holmberg shows that relatively conventional explanations such as "short lifetimes or tremendous gas contents" are unrealistic, and that the results found would be implied by a systematic effect of magnitudes on redshifts. While such an effect is physically different from a nonlinear redshift-distance relation, it is mathematically closely related, in that a suitable such relation will lead to effects such as those analyzed by Holmberg.

Indeed, the chronometric prediction is in satisfactory agreement with the data listed by Holmberg. His principal data are for the Virgo cluster, and are given as his Table 1. The dispersion in intrinsic velocities varies as the dispersion in absolute magnitude. For the expansion theory, this is quite large, indeed significantly greater than that in apparent magnitude; but for the chronometric absolute magnitudes, the dispersion is only slightly greater than that in apparent magnitude. The quantitative results vary with the particular subsample involved, but the qualitative results do not. The respective dispersions are: (a) in apparent magnitude, (b) in deviations from the Hubble line, (c) in chronometric absolute magnitude: (1) for all 84 nonblueshifted galaxies which are listed, (a) 1.15, (b) 1.69, (c) 1.29; (2) for all 46 nonblueshifted So or E galaxies (which as indicated by Holmberg are of particular interest in relation to the question of estimation of the mass of the cluster), (a) 1.30, (b) 1.71, (c) 1.39.

Another apparent effect of a generally similar nature has been detailed for the Coma cluster by Tifft (1972). As in the case of the Virgo cluster, analysis of the data precisely as listed, but on the basis of the chronometric rather than expansion theory, leads to an acceptably small apparent cluster redshift dispersion. Again the qualitative results are independent of the particular morphological type. The respective dispersions are (1) for all 70 galaxies with data, (a) 0.57, (b) 0.67, (c) 0.59; (2) for all 28 ellipticals, (a) 0.56, (b) 0.72, (c) 0.61; (c) for the 42 nonellipticals, (a) 0.51, (b) 0.63, and (c) 0.54.